Enzymatic and applied studies on gut microbial metabolisms of bioactive compounds

Haruko Sakurama

2014

CONTENTS

ABBREVIATIONS

AA	Arachidonic acid
AfcA	1,2-α-L-Fucosidase
AfcB	1,3-1,4-α-L-Fucosidase
Baicalin	Baicalein 7-*O*-β-D-glucuronide
BOF	Bofu-Tsusho-San
CAD	Charged aerosol detector
COSY	^{1}H-^{1}H-Chemical shift correlation spectroscopy
DFJ	Deoxyfuconojirimycin
DHA	Docosahexaenoic acid
EPA	Eicosapentaenoic acid
ESI-MS	Electrospray ionization mass spectrometry
Estrone-GlcA	Estrone 3-(β-D-glucuronide)
FAB	Fast atom bombardment
F1-3Gn	3-Fucosyl-*N*-acetylglucosamine
F1-4Gn	4-Fucosyl-*N*-acetylglucosamine
F1-6Gn	6-Fucosyl-*N*-acetylglucosamine
2'-FL	2'-Fucosyllactose
3-FL	3-Fucosyllactose
FPLC	Fast protein liquid chromatography
FucF	β-L-Fucopyranosyl fluoride
$FucN_3$	β-L-Fucopyranosyl azide
GC	Gas-liquid chromatography
GDL	Glucaro-δ-lactam inhibitor
GH	Glycoside hydrolase
GlcCerase	Glucosylceramidase
GlcGlcNAc	2-Acetoamide-2-deoxy-4-*O*-(β-glucosyl)-glucose
GNB	Galacto-*N*-biose
GRAS	Generally recognized as safe
GUS	β-Glucuronidase
HEPES	4-(2-Hydroxyethyl)-1-piperazineethanesulfonic acid
HMO	Human milk oligosaccharide

^{1}H-NMR	Proton nuclear magnetic resonance
HPLC	High-performance liquid chromatography
HPAEC-PAD	High-performance anion-exchange chromatography with pulsed amperometric detection
IPTG	Isopropyl-β-D-1-thiogalactopyranoside
LA	Linoleic acid
LacdiNAc	*N*, *N*'-Diacetyllactosediamine
LacNAc	*N*-Acetyllactosamine
LB	lysogeny broth
LDFT	Lactodifucotetraose
LNDFH	Lacto-*N*-difucohexaose
LNB	Lacto-*N*-biose I
LNBase	Lacto-*N*-biosidase
LNFP	Lacto-*N*-fucopentaose
LNT	Lacto-*N*-tetraose
LST	Sialyllacto-*N*-tetraose
MES	2-(*N*-Morpholino)ethanesulfonic acid
MOPS	3-(*N*-Morpholino)propanesulfonic acid
MS	Mass spectroscopy
MU	4-Methylumbelliferone
MU-GlcA	4-Methylumbelliferyl-β-D-glucuronide hydrate
NMIFA	Non-methylene-interrupted fatty acids
NND	*N*-Nonyl-deoxynojirimycin
NOESY	Two-dimensional nuclear Overhauser effect spectroscopy
Phenolphthalein-GlcA	Phenolphthalein β-D-glucuronide
*p*NP	*p*-Nitrophenol
*p*NP-Fuc	*p*-Nitrophenyl-α-L-fucopyranoside
*p*NP-GlcA	4-Nitrophenyl β-D-glucuronide
PUFAs	Polyunsaturated fatty acids
TOCSY	^{1}H Clean-total correlation spectroscopy
Tris	Tris(hydroxymethyl)aminomethane
VA	Vaccenic acid
Wogonoside	Wogonin 7-*O*-β-D-glucuronide

GENERAL INTRODUCTION

The host intestine is inhabited by a large diverse microbiota (1,2). For example, in adult humans, the gut microbiota consists of approximately 10^{14} bacterial cells (3), which represent 500-1000 species (4). The host has a mutualistic relationship with the gut microbiota. The gut microbiota derives residence and nutrition from the host (5). The microbiota also provides many effects to the host that influence the host's metabolism, immune and organ development, and behavior (6). The composition of the gut microbiota is known to be remarkably stable. However, its alteration has been discovered to lead to chronic diseases, such as irritable bowel syndrome, inflammatory bowel disease, colorectal cancer, obesity, and type 2 diabetes (7). Therefore, the establishment and maintenance of the mutualistic relationship between the host and the gut microbiota are key factors for the health of the host.

The composition of the gut microbiota is influenced by various factors, such as the use of antibiotics, lifestyle, and diet (6). Among these factors, orally administered diets available to the gut microbiota are one of the major determinants for its composition. For example, non-digestible oligosaccharides, such as oligofructose, can selectively promote the growth of the health-promoting bacteria, such as *Bifidobacteria* and *Lactobacillus* (5,9). Therefore, these oligosaccharides are used as prebiotics. On the other hand, the gut microbiota can complement the physiology of the host through various metabolites, such as essential vitamins and short-chain fatty acids (5). The gut microbial metabolism can activate the prodrugs, such as the flavonoid glycosides, which is found as a component of traditional herbal medicines (10-13). Thus, these fermentable bioactive compounds that are available to the gut microbiota should not only change the gut microbiota composition, but also influence the physiology of the host through their metabolites. Therefore, the studies on the gut microbial metabolisms of bioactive compounds and their metabolites expand our knowledge of the molecular basis on the mutualistic relationship between the host and the gut microbiota. This can lead to the development of novel bioactive compounds, based on the knowledge obtained from the studies. In this thesis, the author isolated and characterized the bacteria and/or its enzyme that is responsible for the metabolisms of bioactive compounds. Furthermore, the author applies this information to the production of functional compounds.

CHAPTERS 1-3 focus on the host-derived oligosaccharides and glycans, which serve

as sources of energy for the gut bacteria (5). Oligosaccharides, excluding lactose in human milk (human milk oligosaccharides, HMOs), are one of the attractive targets for novel prebiotics, among the host-derived oligosaccharides. HMOs are composed of more than 130 different oligosaccharide structures; they are also thought to be responsible for the intestinal colonization of bifidobacteria in breast fed infants. Among them, lacto-*N*-tetraose (LNT; Galβ1,3GlcNAcβ1,3Galβ1,4Glc) is one of main components of HMOs, which are specific features to humans (14,15). Furthermore, the α-L-fucosyl residues are frequently found at the non-reducing ends of the host-derived oligosaccharides and glycan, such as HMO and histo-blood group antigens Lewis (14,16). Therefore, the author isolated and characterized the glycoside hydrolases required for the host-derived glycans catabolism in CHAPTER 1, lacto-*N*-biosidase (LNBase); in CHAPTER 2, α-L-fucosidase. In addition, in CHAPTER 3, the author generated a 1,3-1,4-α-L-fucosynthase with exceptionally strict regio- and acceptor specificity, using glycosynthase technology.

CHAPTER 4 focuses on the metabolism of the flavonoid and steroid glucuronides, which have bioactivities that are normally masked or altered by glucuronidation. Baicalin (baicalein 7-*O*-β-D-glucuronide) is one of the major flavonoid glucuronides that are found in traditional herbal medicines. Orally administered baicalin are degraded into glucuronic acid and baicalein, and show an efficient drug action (10,12). Therefore, the bioconversion and bioavailability of baicalin depends on the gut microbiota, which varies from person to person. To show the effect of a drug, regardless of the gut microbiota, the author aimed to identify and characterize the baicalin-converting enzyme, β-glucuronidase, from *Lactobacillus brevis* subsp. *coagulans*; the author also discussed the ability of the enzyme to metabolize drugs and endogenous steroid hormones in the host.

CHAPTER 5 focuses on the biohydrogenation reaction of polyunsaturated fatty acids (PUFAs) by gut anaerobic bacteria. This is an area of desired research from the viewpoint of the development of novel bioactive lipids (17,18) and the modulation of the fatty acid composition of the host (19). The author isolated the bacterium hydrogenating C_{20} PUFAs and their metabolites, of which there is little information, unlike C_{18} PUFAs.

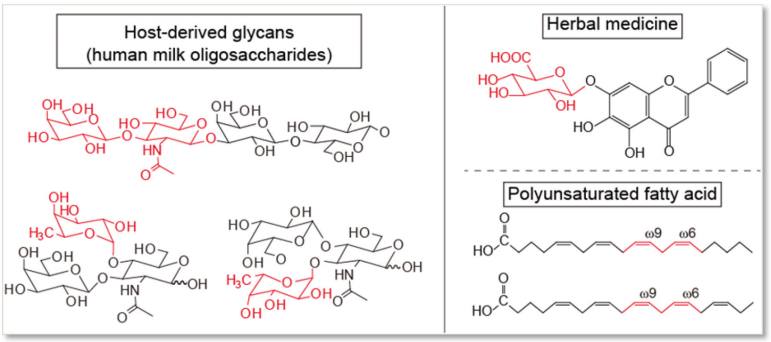

REFERENCES

1. Qin, J., Li, R., Raes, J., Arumugam, M., Burgdorf, K.S., Manichanh, C., Nielsen, T., Pons, N., Levenez, F., Yamada, T., Mende, D.R., Li, J., Xu, J., Li, S., Li, D., Cao, J., Wang, B., Liang, H., Zheng, H., Xie, Y., Tap, J., Lepage, P., Bertalan, M., Batto, J.M., Hansen, T., Le Paslier, D., Linneberg, A., Nielsen, H.B., Pelletier, E., Renault, P., Sicheritz-Ponten, T., Turner, K., Zhu, H., Yu, C., Li, S., Jian, M., Zhou, Y., Li, Y., Zhang, X., Li, S., Qin, N., Yang, H., Wang, J., Brunak, S., Doré, J., Guarner, F., Kristiansen, K., Pedersen, O., Parkhill, J., Weissenbach, J., MetaHIT Consortium, Bork, P., Ehrlich, S.D., and Wang, J. (2010) A human gut microbial gene catalogue established by metagenomic sequencing. *Nature* **464,** 59-65
2. Young, V.B. and Schmidt, T.M. (2008) Overview of the gastrointestinal microbiota. *Adv Exp Med Biol.* **635**, 29-40
3. Sekirov, I., Russell, S.L., Antunes, L.C., and Finlay, B.B. (2010) Gut microbiota in health and disease. *Physiol Rev.* **90**, 859-904
4. Xu, J. and Gordon, J.I. (2003) Honor thy symbionts. *Proc Natl Acad Sci USA*. **100**, 10452-10459
5. Hooper, L.V., Midtvedt, T., and Gordon, J.I. (2002) How host-microbial interactions shape the nutrient environment of the mammalian intestine. *Annu Rev Nutr*. **22**, 283-307
6. Sommer, F. and Bäckhed, F. (2013) The gut microbiota—masters of host development and physiology. *Nat Rev Microbiol.* **11**, 227-238.
7. Guinane, C.M. and Cotter, P.D. (2013) Role of the gut microbiota in health and chronic gastrointestinal disease: understanding a hidden metabolic organ. *Therap Adv Gastroenterol.* **6**, 295-308
8. Zoetendal, E.G., Akkermans, A.D., and De Vos, W.M. (1998) Temperature gradient gel electrophoresis analysis of 16S rRNA from human fecal samples reveals stable and host-specific communities of active bacteria. *Appl Environ Microbiol.* **64**, 3854-3859
9. Gibson, G.R. (1999) Dietary modulation of the human gut microflora using the prebiotics oligofructose and inulin. *J Nutr.* **129**, 1438S-1441S
10. Kobashi, K. and Akao, T. (1997) Relation of intestinal bacteria to pharmacological effect of glycosides. *Biosci Microflora* **16**, 1-7
11. Walle, T. (2004) Absorption and metabolism of flavonoids. *Free Radical Biology and*

Medicine **36**, 829–837

12. Yim, J.S., Kim, Y.S., Moon, S.K., Cho, K.H., Bae, H.S., Kim, J.J., Park, E.K., and Kim, D.H. (2004) Metabolic activities of ginsenoside Rb1, baicalin, glycyrrhizin and geniposide to their bioactive compounds by human intestinal microflora. *Biol Pharm Bull*. **27**, 1580-1593
13. Simons, A.L., Renouf, M., Hendrich, S., and Murphy, P.A. (2005) Human gut microbial degradation of flavonoids: structure-function relationships. *J Agric Food Chem*. **53**, 4258-4263
14. Urashima, T., Kitaoka, M., Terabayashi, T., Fukuda, K., Ohnishi, M., and Kobata, A. (2011) Milk oligosaccharides. in *Oligosaccharides: Sources, properties and applications* (Gordon, N.G., ed) pp 1-58, Nova Science Publishers, New York
15. Kobata, A. (2010) Structures and application of oligosaccharides in human milk. *Proc Jpn Acad Ser.* B**86,** 731-747
16. Becker, D.J. and Lowe, J.B. (2003) Fucose: biosynthesis and biological function in mammals. *Glycobiology* **13**, 41R-53R
17. Kishino, S., Ogawa, J., Yokozeki, K., and Shimizu, S. (2009) Metabolic diversity in biohydrogenation of polyunsaturated fatty acids by lactic acid bacteria involving conjugated fatty acid production. *Appl Microbiol Biotechnol*. **84**, 87-97
18. Kishino, S., Ogawa, J., Ando, A., Yokozeki, K., and Shimizu, S. (2010) Microbial production of conjugated gamma-linolenic acid from gamma-linolenic acid by *Lactobacillus plantarum* AKU 1009a. *J Appl Microbiol*. **108**, 2012-2018
19. Kishino, S., Takeuchi, M., Park, S.B., Hirata, A., Kitamura, N., Kunisawa, J., Kiyono, H., Iwamoto, R., Isobe, Y., Arita, M., Arai, H., Ueda, K., Shima, J., Takahashi, S., Yokozeki, K., Shimizu, S., and Ogawa, J. (2013) Polyunsaturated fatty acid saturation by gut lactic acid bacteria affecting host lipid composition. *Proc Natl Acad Sci USA*. **110**, 17808-17813

CHAPTER 1

Lacto-*N*-biosidase from *Bifidobacterium longum* subsp. *longum*

Infant intestinal microflora develops from a tripartite relationship between mother's milk, infant, and bacteria, and it is generally accepted that the microbiota in the intestines of breast-fed infants are rich in particular bifidobacterial species such as *Bifidobacterium breve*, *B. bifidum*, and *B. longum* subsp. *longum*/*infantis* (collectively termed infant gut-associated bifidobacteria) (1,2). These species/subspecies dominate in the gut ecosystem within a week after birth, and continue their predominance until weaning, when the gut microflora become adult-like (1). For this reason, human milk has long been considered to contain bifidogenic compounds (3-6).

Recent research indicates that oligosaccharides (human milk oligosaccharides, HMOs) are responsible for the bifidogenic effect of human milk. Present at concentrations between 10 and 20 g/L, HMOs constitute the third most abundant solid component in breast milk after lactose (Lac) and lipids, but have apparently no-nutritional value for infants (7-9). HMOs are characterized by their complex structures. To date, 115 HMO structures, classified into 13 core structures, have been determined (9). The core structures consist of Lac, at the reducing end, elongated by β1-3- linked lacto-*N*-biose I (Galβ1-3GlcNAc, LNB, type-1 chain) and/or β1-3/6-linked *N*-acetyllactosamine (Galβ1-4GlcNAc, LacNAc, type-2 chain) (10), and are frequently modified by fucose and sialic acid residues via α1-2/3/4 and α2-3/6 linkages, respectively (3,9). Among the different HMO structures, four molecular species, namely 2'-fucosyllactose (Fucα1-2Galβ1-4Glc), lacto-*N*-tetraose (LNT, Galβ1-3GlcNAcβ1-3Galβ1-4Glc), lacto-*N*-fucopentaose I (LNFP I, Fucα1-2Galβ1-3GlcNAcβ1-3Galβ1-4Glc), and lacto-*N*-difucohexaose I [LNDFH I, Fucα1-2Galβ1-3(Fucα1-4)GlcNAcβ1-3Galβ1-4Glc], are most abundantly present and comprise more than 50% of the total oligosaccharides, unless the milk is derived from non-secretor or Lewis-negative subjects (9,10). The latter three structures reveal an abundance of type-1 chains in the HMOs (see Supplemental Fig. S1). This composition is unique to HMOs and has not been observed in other mammalian milk oligosaccharides, including those of anthropoids (9). This uniqueness may explain why infant gut-associated bifidobacteria are equipped with specific enzymatic sets that are specifically involved in assimilation of type-1 HMOs (as described below).

Among the infant gut-associated bifidobacteria, *B. bifidum* and *B. longum* subsp. *infantis* (simply designated *B. infantis* in this chapter) have been thoroughly studied because they grow substantially on medium containing HMOs as sole carbon source (OD_{600}> 1.5) (11,12). *B. bifidum* produces a repertoire of secretory enzymes for HMOs degradation (Supplemental Fig. S1). 1,2-α-L-Fucosidase, 1,3-1,4-α-L-fucosidase, and sialidase act initially to uncover the core structure of HMOs (13-16). The type-1 chain is then digested by lacto-*N*-biosidase (LNBase) to liberate LNB, while the type-2 chain is degraded sequentially by β-galactosidase and β-*N*-acetylglucosaminidase to liberate Gal and GlcNAc, respectively (17,18). Subsequently, LNB is preferentially imported into the bifidobacterial cells via the GNB (galacto-*N*-biose)/LNB transporter for further degradation (19-21). Lac and monosaccharides are also utilized, although some remain unconsumed during growth in HMOs-containing medium (12). The GNB/LNB transporter is found solely in infant gut-associated bifidobacteria (Supplemental Fig. S1). Since LNB selectively stimulates these species among the different gut microbes, it is considered a key instigator of bifidogenic effect (22). *B. infantis* also possesses the GNB/LNB pathway, but has evolved a different strategy for HMOs assimilation (11). This organism apparently imports all classes of HMOs in their intact forms and degrades them by *exo*-glycosidases in the cytoplasm (23, 24, 25). Therefore, *B. infantis* shows no preference for type-1 chain, although cytoplasmic digestion inevitably involves LNTβ-1,3-galactosidase (type-1 specific) which is exclusively found in infant gut-associated bifidobacteria (23). It should be mentioned that most β-galactosidases are incapable of hydrolyzing type-1 chains.

In contrast to above-mentioned two species, the other infant gut-associated bifidobacteria, *B. longum* subsp. *longum* (referred to as *B. longum*) and *B. breve* have received far less attention, perhaps because they grow poorly on HMOs-containing medium (OD_{600}< 0.3) (12,26). Since more than 70% of HMOs are fucosylated (i.e. derived from secretor and Lewis-positive donors), the poor growth ability of the two species may be attributable to lack of 1,2-α-L-fucosidase and 1,3-1,4-α-L-fucosidase (5). Accordingly, when *B. breve* JCM1192^T and *B. longum* JCM1217^T are inoculated in HMOs-containing media, they consume LNT only (12). In the spent medium of *B. breve* JCM1192 cultures, no degradation products (mono-, di-, and trisaccharides) of LNT have been detected, while in the culture supernatant of *B. longum* JCM1217, Lac appears transiently as LNT decreases. Thus, while *B. breve* JCM1192 imports intact LNT as does *B. infantis*, LNT consumption by *B. longum* JCM1217 should involve

secretory LNBase and the subsequent GNB/LNB pathway (Supplemental Fig. S1). Indeed, LNBase activity has been previously detected in *B. longum* strains JCM1217 and JCM7054 (17).

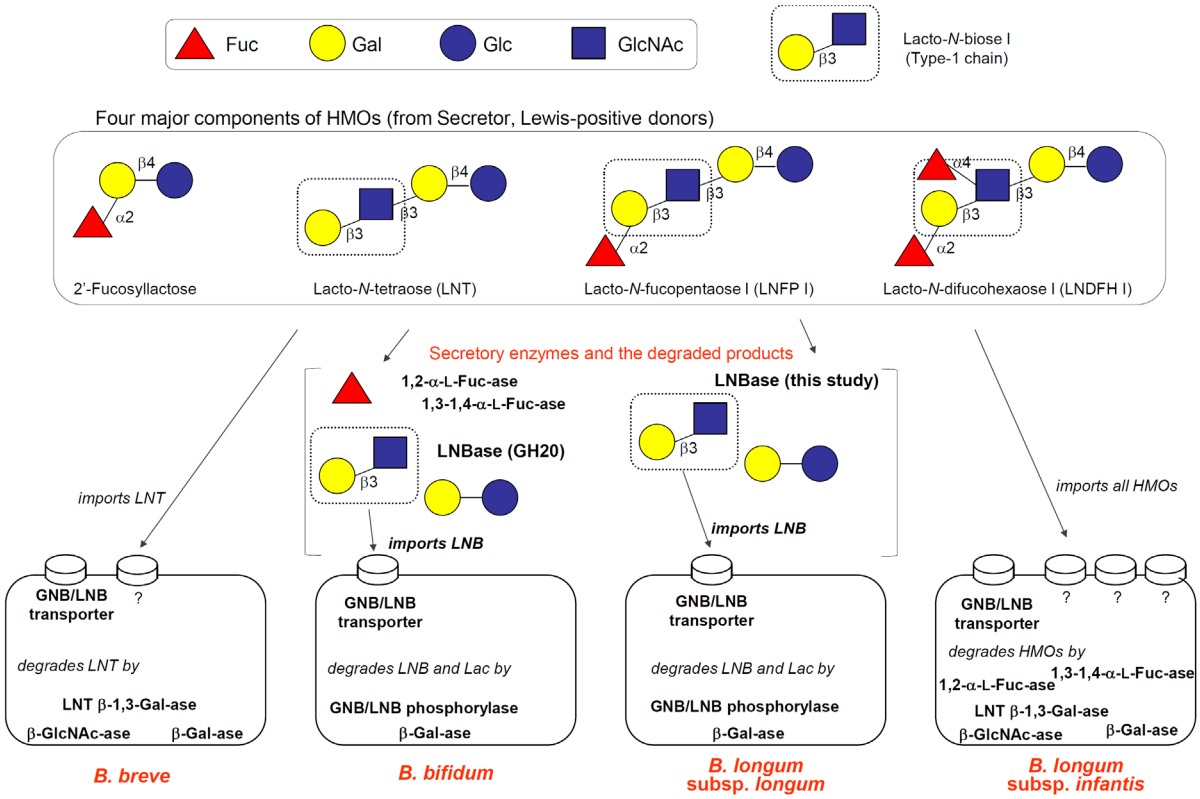

Supplemental Figure S1. Infant gut-associated bifidobacteria possess species/subspecies-specific enzymatic sets dedicated to the assimilation of HMOs. See text for the detailed description. Four major components of HMOs (Secretor, Lewis-postive donors) are also shown.

The genomic sequence of *B. longum* JCM1217 was made publicly available by Fukuda *et al*. in 2011 (27). Interestingly, Wada *et al*. found that this strain possesses no gene homologous to the previously identified LNBase (glycoside hydrolase family 20, GH20) from *B. bifidum* (17). Although the *B. longum* JCM1217 genome encodes a GH20 enzyme, the protein obviously lacks the sequence motifs to distinguish LNBase from β-*N*-acetylhexosaminidase (another GH20 member) (28). Actually, the GH20 enzyme of *B. longum* JCM1217 was recently found to be β-*N*-acetylglucosaminidase active on lacto-*N*-triose II (GlcNAcβ1-3Galβ1-4Glc) and on chitin oligosaccharides, but not on LNT (29). These findings prompted the author to identify a potentially novel LNBase gene encoded in the genome of *B. longum*.

Here, the author found that the locus_tag BLLJ_1505 and BLLJ_1506, neither of which has been functionally annotated, constitute LNBase. The enzyme body is the product of BLLJ_1505, while the product of BLLJ_1506 acts as a designated chaperon for the

BLLJ_1505 protein (LNBase). The substrate specificity of this novel LNBase was found to be quite different from that of GH20 LNBase. Interestingly, it liberated GalNAcβ1-3GlcNAc from the *p*-nitrophenyl sugar. The disaccharide structure is present in the *O*-glycans of α-dystroglycan (30). BLLJ_1505 and BLLJ_1506 homologs were found in the genomes of *B. longum*, *B. bifidum*, and a few gut microbes, suggesting that this LNBase has uniquely evolved in particular species.

EXPERIMENTAL PROCEDURES

Chemicals−Lacto-*N*-tetraose (LNT, Galβ1-3GlcNAcβ1-3Galβ1-4Glc), lacto-*N*-*neo*tetraose (LN*n*T, Galβ1-4GlcNAcβ1-3Galβ1-4Glc), lacto-*N*-fucopentaose (LNFP) I (Fucα1-2Galβ1-3GlcNAcβ1-3Galβ1-4Glc), LNFP II [Galβ1-3(Fucα1-4)GlcNAcβ1-3Galβ1-4Glc], sialyllacto-*N*-tetraose (LST) a (Neu5Acα2-3Galβ1-3GlcNAcβ1-3Galβ1-4Glc), and LST b [Galβ1-3(Neu5Acα2-6)GlcNAcβ1-3Galβ1-4Glc] were purchased from IsoSep (Tullinge, Sweden). Lacto-*N*-hexaose [LNH, Galβ1-3GlcNAcβ1-3(Galβ1-4GlcNAcβ1-6)Galβ1-4Glc] was obtained from Dextra Laboratories (Reading, UK). Lacto-*N*-biose I (Galβ1-3GlcNAc, LNB) and lacto-*N*-triose II (GlcNAcβ1-3Galβ1-4Glc) were prepared as described previously (18,31). *p*-Nitrophenyl (*p*NP)-β-lacto-*N*-bioside I (LNB-β-*p*NP) was obtained from Sigma-Aldrich (MO) or synthesized essentially as described previously (32). Briefly, hepta-*O*-acetyl-LNB was prepared by treating LNB with acetic anhydride and pyridine. Following chlorination with hydrogen chloride in acetic acid, *p*-nitrophenol was glycosydated in dimethylformamide. *O*-Deacetylation was carried out using sodium methoxide in methanol. The synthesized LNB-β-*p*NP was used for screening a genomic library of *B. longum* subsp. *longum* JCM1217 (described later). GalNAcβ1-3GlcNAc-β-*p*NP and GalNAcβ1-4GlcNAc (LacdiNAc)-β-*p*NP were purchased from Tokyo Chemical Industry (Tokyo, Japan). Other reagents of analytical grade were obtained from commercial sources. The oligonucleotides used in the plasmid- and strain constructions are listed in Supplemental Table S1.

Bacterial strains and media−The strains used in this chapter were *Bifidobacterium longum* subsp. *longum* JCM1217^{T} and 105-A (33) and *Escherichia coli* DH5α and BL21 Δ*lacZ* (DE3) / pRERE2 (23). Bifidobacteria were grown in GAM broth (Nissui

Pharmaceutical, Tokyo, Japan) or basal medium (17) at 37°C under anaerobic conditions. Chloramphenicol and spectinomycin were added at final concentrations of 4 and 30 μg/ml, respectively, as required. *E. coli* strains were grown in lysogeny broth (LB) broth, and when necessary, ampicillin, chloramphenicol, and spectinomycin were added at concentrations of 100, 30, and 30 μg/ml, respectively.

Supplemental Table S1 Primers used for plasmid construction

For *lnbX* disruption	
forward primer (BamHI)	5'-gc*ggatcc*TCGCTGATGATCTGCAACTGGT-3'
reverse primer (BamHI)	5'-gc*ggatcc*AGCGACAATGTGACCTTCTTGC-3'
For constructing shuttle vector pTK2064 (pSC101*ori* pTB4*ori* Cam^R)	
forward primer for pSC101 *ori* amplification [pMW118 (Nippon gene, Tokyo, Japan) as a template]	5'-GACAGTAAGACGGGTAAGCCTG-3'
reverse primer for pSC101 *ori* amplification [pMW118 (Nippon gene, Tokyo, Japan) as a template]	5'-GTGCATATGGACAGTTTTCCCT-3'
forward primer for pTB4 *ori* and Cam^R gene amplification [pBS423 as a template]	5'- GAGGCCCTTTCGTCTTCAAGAA-3'
reverse primer for pTB4 *ori* and Cam^R gene amplification [pBS423 as a template]	5'-GTGATGCCGGCCACGATGCGT-3'
For complementation analysis	
forward primer for *lnbXY* amplification (In-Fusion at the NdeI site of pTK2064)	5'-ggaaaactgtccataGGGAGTGACCATGAACGGTATCGT-3'
reverse primer for *lnbXY* amplification (In-Fusion at the NdeI site of pTK2064)	5'-agggcctcgtgcataCGGGACACCCGCCTTATTCGTTCT-3'
forward primer for *lnbX* amplification (In-Fusion at the NdeI site of pTK2064)	same as the primer used for *lnbXY* amplification
reverse primer for *lnbX* amplification (In-Fusion at the NdeI site of pTK2064)	5'-agggcctcgtgcataGCAGGACCGCCGCCACCGCGACT-3'
forward primer for placing *lnbY* under the control of the *lnbX* promoter (inverse PCR, pTK2174 as a template)	5'-ATGCCACGTAGGCACCGGTTCG-3'
reverse primer for placing *lnbY* under the control of the *lnbX* promoter (inverse PCR, pTK2174 as a template)	5'-GCCGCTTTCCTTCCTTTCGATTGT-3'
For recombinant LnbX and LnbY expression	
forward primer for non-tagged LnbX (In-Fusion)	5'-aaggagatatacat*aTG*CAGTCAGCAACGCAAGGAAAG-3'
reverse primer for non-tagged LnbX (In-Fusion)	5'-gttagcagccggatc*TTA*GTCGGCGCCGGTGGCGGTCA-3'
forward primer for His-tagged LnbX (In-Fusion)	same as the primer used for non-tagged LnbX amplification
reverse primer for His-tagged LnbX (In-Fusion)	5'-tgctcgagtgcggccGCGTCGGCGCCGGTGGCGGTCA-3'
forward primer for non-tagged LnbY (NdeI)	5'-gg*catATG*ACGCACGGCGACGGCGCCTTCG-3'
reverse primer for non-tagged LnbY (BamHI)	5'-gc*ggatcc**TA***CCCGAGCCTGCCTGCCGTGA-3'
forward primer for His-tagged LnbY (NdeI)	5'-gc*catATG*GCGGCGCACCACCACCACCACCACACGCACGGCGACGG CGCCTTCGC-3'
reverse primer for His-tagged LnbY (BamHI)	same as the primer used for non-tagged LnbY amplification
For constructing ColE1-compatible, LnbY-expressing plasmid	
forward primer for amplification of pCDF *ori* and Sp^R gene (pCDF Duet-1 as a template)	5'-TTGAGAAGCACACGGTCACACT-3'
reverse primer for amplification of pCDF *ori* and Sp^R gene (pCDF Duet-1 as a template)	5'-GAGAGCCTTCAACCCAGTCAGCT-3'
forward primer for amplification of T7-*lnbY* cassette (pET3a-*lnbY* or pET3a-(*His*)*lnbY* as a template)	5'-CTCTCCCTTATGCGACTCCTGC-3'
reverse primer for amplification of T7-*lnbY* cassette (pET3a-*lnbY* or pET3a-(*His*)*lnbY* as a template)	5'-ACTTGGAGCCACTATCGACTAC-3'

Construction of a genomic library of* B. longum *JCM1217−The genome of strain JCM1217 was extracted as described previously (13), and partially digested with *Sau*3AI. The 8−10 kbp DNA fragments were recovered and ligated with the *Bam*HI-digested pBR322. The resulting reaction mixture was used to transform *E. coli* DH5α to obtain the genomic library, which was then screened for LNB-β-*p*NP hydrolysis. Note that *E. coli* DH5α exhibits neither β-1,3-galactosidase nor LNBase activity.

***Gene disruption and complementation analysis of* B. longum**−A targeted gene disruption in *B. longum* was carried out as follows. The region corresponding to nucleotide numbers 1794468−1795807 (see Fig. 1) was amplified by high-fidelity PCR using PrimeStar MAX DNA polymerase (Takara Shuzo, Shiga, Japan). *Bam*HI sites were attached at both ends (Supplemental Table S1). The amplified fragment (a partial *lnbX* gene) was ligated with the 1.9-kbp *Bam*HI fragment (carrying ColE1 *ori* and the spectinomycin-resistance gene) of pBS423 (34) to generate a suicide plasmid. The resulting plasmid was introduced into *B. longum* 105-A by electroporation and integrated into the genome by a single cross over event at the *lnbX* locus. Spectinomycin-resistant colonies were isolated, and the disruption of the *lnbX* gene was confirmed by genomic PCR analysis (data not shown).

Complementation analysis was performed using *E. coli*-bifidobacteria shuttle vector pTK2064, in which ColE1 *ori* (high copy) of plasmid pBS423 (34) was replaced with pSC101 *ori* (low copy) (Supplemental Table S1). Exchanging the *ori* ensured stable maintenance of the target genes (~6.3 kbp, GC-content 66%) in cells. The *lnbX* and *lnbXY* genes (1792583−1798023 and 1792583−1798862 nt, respectively, in Fig. 1) were amplified by high-fidelity PCR and inserted into the *Nde*I site of pTK2064 by In-Fusion methodology (Clontech Laboratories, CA) to generate pTK2193 ($lnbX^+$) and pTK2174 ($lnbX^+Y^+$), respectively. A plasmid (pTK2241) carrying the *lnbY* gene under the control of *lnbX* promoter was constructed by inverse-PCR using pTK2174 as a template, in which nucleotides 1793160−1797962 (Fig. 1) was eliminated (Supplemental Table S1). All of the PCR-amplified fragments were sequenced to ensure that no base changes other than those designed had occurred.

Expression and purification of recombinant proteins−Recombinant LnbX and LnbY were expressed in *E. coli* and purified as both non-tagged and hexahistidine (His)-tagged

forms. The expression vectors contained the DNAs coding for amino acid residues 31-1573 of LnbX and amino acid residues 30-280 of LnbY, following genetic removal of the signal peptide and membrane anchor of LnbX and the signal peptide of LnbY. The non-tagged and C-terminal His-tagged LnbX proteins were expressed using pET3a and pET23b (Novagen, Darmstadt, Germany), respectively (Supplemental Table S1). The PCR-generated fragments were inserted into the *Nde*I−*Bam*HI and *Nde*I-*Not*I sites of pET3a and pET23b, respectively, by In-Fusion methodology. To express the non-tagged and N-terminal His-tagged LnbY, the amplified genes were first inserted into the *Nde*I−*Bam*HI site of pET3a and the resulting T7-expression cassettes were moved to a ColE1-compatible plasmid pCDF (Novagen) (Supplemental Table S1). The entire fragments used for later manipulation were sequenced.

The non-tagged LNBase (LnbX) was purified from the cell-free extract of *E. coli* cells co-expressing the *lnbX* and *lnbY* genes. The cells were grown in 2 liters of LB medium, and when the optical density at 600 nm reached 0.5, isopropyl-β-D-1-thiogalactopyranoside was added to induce protein expression. The cells were harvested, suspended in 20 mM tris(hydroxymethyl)aminomethane-HCl (Tris-HCl) buffer (pH 8.0), and disrupted by sonication. The supernatant was applied to DEAE-Sepharose fast flow column (GE Healthcare Life Sciences, Uppsala, Sweden), and proteins were eluted by a linear gradient of 1 M NaCl. Each fraction was tested for LNB-β-*p*NP-hydrolyzing ability. Active fractions were combined, dialyzed to 50 mM sodium phosphate buffer (pH 7.0) containing 0.8 M ammonium sulfate, and applied to a Butyl-Sepharose 4 column (GE Healthcare Life Sciences). Elution was performed by decreasing the concentration of ammonium sulfate to 0 M. The protein was further purified by MonoQ 5/50 GL [0−1 M NaCl in 20 mM Tris-HCl buffer (pH 8.0)] (GE Healthcare Life Sciences), Poros HP [0.8−0 M ammonium sulfate in 50 mM sodium phosphate buffer (pH 7.0)] (PerSeptive Biosystems, MA), and Superdex 200 10/300 GL [20 mM Tris-HCl buffer (pH 8.0) containing 150 mM NaCl] (GE Healthcare Life Sciences) column chromatography. The purified protein was concentrated using Amicon Ultra 100K (Millipore, MA). His-tagged LnbX was similarly expressed and purified by Ni-NTA agarose (Qiagen, Hilden, Germany), MonoQ 5/50 GL, and Superdex 200 10/300 GL column chromatography.

Non-tagged LnbY was purified similarly, using the same columns. The purity of LnbY was assessed by SDS-polyacrylamide gel electrophoresis of each fraction. His-tagged LnbY was purified by Ni-NTA agarose and Superdex 75 10/300 GL column chromatography. The

purified protein was concentrated using Amicon Ultra 10K.

Protein concentrations were determinedusing a Bradford protein assay kit (Bio-Rad Laboratories, CA). Bovine serum albumin was used as a standard.

Inductively coupled plasma emission spectroscopy−Prior to the analysis, the purified, non-tagged LnbX and LnbY were extensively dialyzed against 5 mM Tris-HCl (pH 8.0) in the presence and absence of 0.2 mM EDTA. The content and concentration of metal ions in the proteins were determined by inductively coupled plasma emission spectroscopy using ICPS-8100 (Shimadzu, Kyoto, Japan), with dialysis buffer as a control. The standard was ICP multielement standard solution IV.

Edman-degradation analysis−The N-terminal amino acid sequence of the non-tagged LnbX was determined by Edman-degradation using a PPSQ-33A protein sequencer (Shimadzu).

Assay−The standard reaction mixture contained 50 mM 2-(*N*-morpholino)ethanesulfonic acid (MES) buffer (pH 5.4). *p*NP-Sugars and oligosaccharides were used as the substrates. The reaction was initiated by adding the enzyme, and the reaction mixture was incubated at 25°C for an appropriate time, in which the linearity of the reaction rate was observed. The enzyme concentrations used in the kinetic analysis were 0.90 nM (LNB-β-*p*NP), 1.8 nM (GalNAcβ1-3GlcNAcβ-*p*NP and LNT), and 140 nM (LNFP I). The substrate concentrations were varied from 0.3–2 times the respective K_m values. The reaction was terminated by adding 1 M sodium carbonate (for *p*NP-sugars) or by heating (for oligosaccharides). The amount of liberated *p*-nitrophenol was determined from the absorbance at 400 nm. Oligosaccharide hydrolysis was monitored by high-performance anion-exchange chromatography with pulsed amperometric detection (HPAEC-PAD) using a Dionex ICS 3000 system, equipped with a CarboPac PA-1 column (Dionex, Sunnyvale, CA). The elution was performed under constant flow (0.25 ml/min) with a linear gradient of 0−330 mM sodium acetate in 125 mM NaOH at 30°C for 20 min. Standard curve was constructed from known concentrations of Lac. The reaction products of the LNFP I hydrolysis were treated with 1,2-α-L-fucosidase (13) prior to HPAEC-PAD analysis to remove fucosyl residue from the 2'-fucosyl-LNB (Fucα1-2Galβ1-3GlcNAc) (reaction product), which co-elutes with Lac.

The kinetic parameters were calculated by curve fitting the experimental data to the Michaelis-Menten equation, using KaleidaGraph 4.0 (Synergy Software, PA). One unit of enzyme activity was determined as the amount of enzyme required to produce 1 μmol of *p*-nitrophenol or Lac under the specified conditions.

The physicochemical properties of the enzyme were determined using 1 mM LNB-β-*p*NP as a substrate. To estimate the optimal temperature, the reaction mixture was incubated at various temperatures for a short period (<1 min). The optimal pH was determined using the following buffers (100 mM): citrate-NaOH (pH 4.0–5.0), MES (pH 5.0–6.5), 3-(*N*-morpholino)propanesulfonic acid (MOPS) (pH 6.5–8.0) and Tris-HCl (pH 8.0-9.0). The temperature and pH stabilities were determined from the residual activities following enzyme incubation in 50 mM MES (pH 5.4) for 30 min at various temperatures and overnight dialysis against various 10 mM buffers at 4°C, respectively.

The native molecular mass of the proteins was determined by size exclusion chromatographyusing Superdex 200 10/300 GL (for LnbX) and Superdex 75 10/300 GL (for LnbY). Thyroglobulin (669 kDa), ferritin (440 kDa), aldolase (158 kDa), conalbumin (75 kDa), ovalbumin (43 kDa), ribonuclease A (13.7 kDa), and aprotinin (6.5 kDa) were used as standards. Void volume was determined by Blue Dextran 2000.

Determination of stereochemical course of hydrolysis−The reaction mixture containing 50 mM MES buffer (pH 5.4), 2 mM LNB-β-*p*NP, and the enzyme (7 mU) was incubated at 30°C in a total volume of 60 μl. The mixture was sampled at specified times and immediately injected into a high-performance liquid chromatography (HPLC) system equipped with TSKgel Amide-80 (4.6 × 250 mm) (Tosoh, Tokyo, Japan). Elution was carried out using a solvent system of acetonitrile/water of 65/35 at a flow rate of 1 mL/min, and was monitored at 214 nm.

Electrospray ionization-mass spectrometry (ESI-MS)−For oligosaccharide analysis, mass spectra were obtained on a LCMS-2020 system (Shimadzu) in positive ion mode. The samples were dissolved in 0.1% formic acid/acetonitrile (1/1, by volume) and injected at 3 μl/min with a micro syringe pump.

Western blot analysis using anti-His-tag antibodies−Cell-free extracts (0.6 mg) of *E.*

coli cells expressing His-tagged LnbX in the presence and absence of co-expression of non-tagged LnbY were separated by size exclusion chromatography (Superdex 200 10/300 GL). Each fraction (0.5 ml) was assayed for protein concentration, LNBase activity, and LnbX content. LnbX was detected using anti-His-tag antibodies conjugated with horse radish peroxidase (Qiagen), following SDS-polyacrylamide gel electrophoresis and membrane transfer (Immobilon-P, Millipore). Chemiluminescence was detected using ECL western blotting detection reagents (GE Healthcare Life Sciences) and a LAS-3000 (Fuji Film, Tokyo, Japan).

In vitro *refolding of LnbX*−Denatured LnbX was refolded in the presence and absence of LnbY and metals (Ca^{2+} and Mg^{2+}). This experiment was carried out on C-terminal His-tagged LnbX and N-terminal His-tagged LnbY. The purified LnbX (final concentration 1 μM) denatured in 6 M guanidine-HCl was diluted 100-fold by adding 50 mM 4-(2-hydroxyethyl)-1-piperazineethanesulfonic acid (HEPES) buffer (pH 7.0) containing various concentrations of LnbY (0, 1, 5, 20, 50 μM) and metal ions (0, 0.01, 0.1, 1, and 5 mM of $CaCl_2$ and $MgCl_2$) in a total volume of 500 μl. The mixture was immediately placed in the dialysis cassette (Slide-A-Lyzer G2, Thermo Scientific, MA), and dialyzed against HEPES buffer containing or not containing metal ions. The samples were removed from the dialysis cassettes at specified times and monitored for hydrolytic activity toward LNB-β-*p*NP. Enzymes were assayed within 2 min of incubation to avoid refolding during activity determination.

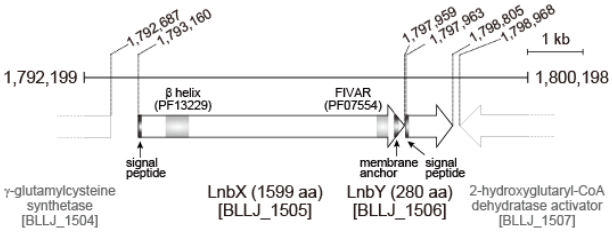

Figure 1. Genetic organization of the *lnbXY* locus in the genome of *B. longum* subsp. *longum* JCM1217. Shown is the shortest region contained within the LNBase$^+$-*E. coli* transformants. The locus_tag, the annotated functions, and the Pfam motifs are indicated. The numbering is based on GenBank accession number NC_015067.

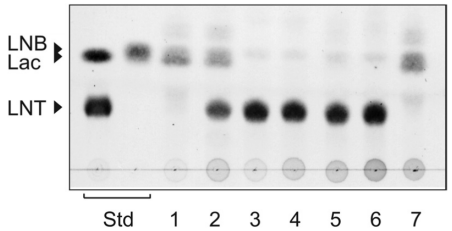

Figure 2. Complementation analysis of *lnbX*-deficient *B. longum* subsp. *longum*. The strain carrying a disrupted *lnbX* gene was transformed with a plasmid carrying *lnbX*, *lnbY*, or *lnbXY*. Note that *lnbY* was expressed under the control of the *lnbX* promoter. The cells were grown in GAM medium overnight, harvested, and then suspended in basal medium (17) containing 5 mM LNT. The suspensions were incubated anaerobically for 1 h and the supernatants were analyzed by thin-layer chromatography using a solvent system of 1-butanol/acetic acid/water (2:1:1, by volume). The sugars were visualized by diphenylamine-phosphoric acid (45). Lane 1: JCM1217; lane 2: 105-A; lane 3: 105-A *lnbX*::Sp^R; lane 4: pTK2064 (empty vector) / *lnbX*::Sp^R; lane 5: pTK2064-*lnbX*$^+$ / *lnbX*::Sp^R; lane 6: pTK2064-*lnbY*$^+$(*lnbX*p) / *lnbX*::Sp^R; lane 7: pTK2064-*lnbX*$^+$*Y*$^+$/ *lnbX*::Sp^R. Standards used were LNT, lactose (Lac), and lacto-*N*-biose I (LNB).

RESULTS

***Identification of BLLJ_1505 and BLLJ_1506 as the constituents of LNBase from* B. longum**−A genomic library of *B. longum* JCM1217 was constructed using *E. coli* DH5α, and the transformants were screened for their ability to liberate *p*-nitrophenol from LNB-β-*p*NP. Five out of 1,920 transformants tested positive for the activity. Sequence analysis revealed that DNA fragment in the plasmid isolated from the clones covers a particular genomic locus. The shortest fragment comprises genomic nucleotides 1792199−1800198 (Fig. 1). This region includes two complete open reading frames (ORFs) designated BLLJ_1505 (1599 aa) and BLLJ_1506 (280 aa). Neither ORF had been functionally annotated, nor did they share sequence similarities with any characterized proteins. The insert also contained two truncated ORFs (BLLJ_1504 and BLLJ_1507), which were close homologs of bacterial γ-glutamylcysteine synthetase and 2-hydroxyglutaryl-CoA dehydratase activator, respectively. Pfam analysis (http://pfam.sanger.ac.uk/) indicated a right-handed β helix region (β helix, PF13229) at amino acid residues 158−315 of BLLJ_1505 and an uncharacterized sugar-binding domain (FIVAR, PF07554) at residues 1435−1487, while BLLJ_1506 lacks any functional motifs (35). SignalP 4.1 (http://www.cbs.dtu.dk/services/SignalP/) and PSORT (http://psort.hgc.jp/) servers predicted the presence of a signal peptide (1−30 aa) and a membrane anchor (1577−1593 aa) in BLLJ_1505 and a signal peptide (1−29 aa) in BLLJ_1506 (36). BLLJ_1505 and BLLJ_1506 were separated by 3-bp, and an inverted repeat was found immediately downstream of BLLJ_1506 (1798848−1798889 nt). Homologs of these proteins in database are introduced later.

The author first disrupted locus-tag BLLJ_1505 by homologous recombination event. This manipulation was performed on *B. longum* strain 105-A (LNBase^{+}) rather than JCM1217, because the latter is not amenable to standard genetic manipulation (33). Sequence identity of 99% was observed between the genes from both strains (data not shown). Disruption of the corresponding gene in strain 105-A resulted in complete loss of LNT-hydrolyzing ability, as revealed by TLC analysis (Fig. 2, lane 3). Activity was not restored by introducing BLLJ_1505 via a shuttle vector (Fig. 2, lane 5). BLLJ_1506 alone similarly failed to rescue the LNBase^{-}-phenotype (Fig. 2, lane 6); however, when both BLLJ_1505 and BLLJ_1506 were introduced, the activity resumed (Fig. 2, lane 7). These results indicate that LNBase of *B.*

longum JCM1217 consists of BLLJ_1505 and BLLJ_1506 (hereafter referred to as *lnbX* and *lnbY*, respectively).

Besides *B. longum*, both *lnbX* and *lnbY* were required for the active LNBase expression in *E. coli*. In this experiment, the signal peptide and membrane anchor of LnbX and the signal peptide of LnbY were genetically removed and the corresponding genes were expressed in separate plasmids (see EXPERIMENTAL PROCEDURES). The cell-free extract of the *E. coli* strain carrying both *lnbX* and *lnbY* showed LNB-β-*p*NP-hydrolyzing activity (9.5 U/mg), whereas strains expressing either *lnbX* or *lnbY* did not (Table 1). Interestingly, mixing the cell-free extracts of *E. coli* strains individually expressing *lnbX* and *lnbY* induced low-level activity (0.38 U/mg). When added prior to mixing, EDTA completely quenched the activity, while after mixing, it produced no effect on activity (0.34 U/mg). Similarly, EDTA did not alter the activity in the cell-free extract of *E. coli* cells co-expressing *lnbX* and *lnbY* (9.5 vs. 9.6 U/mg).

Table 1 LNBase activity of LnbX-, LnbY-, and LnbXY expressing *E. coli* cells.

Cell-free extracts of *E. coli* cells expressing	Specific activity
	units/mg
LnbX	ND[a]
LnbY	ND
LnbXY	9.5
LnbXY + EDTA	9.6
LnbX + LnbY[b]	0.38
LnbX + LnbY + EDTA	
LnbX + LnbY before mixing[c]	ND
LnbX + LnbY after mixing[d]	0.34

The reaction was carried out in 50 mM MES buffer (pH 5.4) containing 1 mM LNB-β-*p*NP at 30°C. EDTA (final concentration 1 mM) was added where indicated.

[a]nd, not detected.

[b]Prior to enzyme assay, the cell-free extracts of *E. coli* cells individually expressing LnbX and LnbY were mixed and incubated for 30 min at 30°C.

[c]EDTA was added before mixing.

[d]EDTA was added after mixing.

Table 2 Summary of purification of recombinant non-tagged LNBase (LnbX)

Purification step[a]	Total protein	Total units	Specific activity	-Fold	Yield
	mg	*units*	*units/mg*	*-fold*	*%*
Cell-free extract	591	6020	10.2	1	100
DEAE-Sepharose fast flow	262	5120	19.5	1.9	85
Butyl-Sepharose 4	113	3410	30.2	3.0	57
Mono Q 5/50 GL	61.8	2150	34.8	3.4	36
Poros HP 4.6/100	30.9	1130	36.6	3.6	19
Superdex 200 10/300 GL	18.0	670	37.2	3.6	11

[a]LNBase was purified from the cell-free extracts of *E. coli* cells co-expressing non-tagged LnbX and LnbY proteins. Purification was carried out by monitoring LNB-β-*p*NP-hydrolyzing activity, as described under EXPERIMENTAL PROCEDURES. See also Fig. 3.

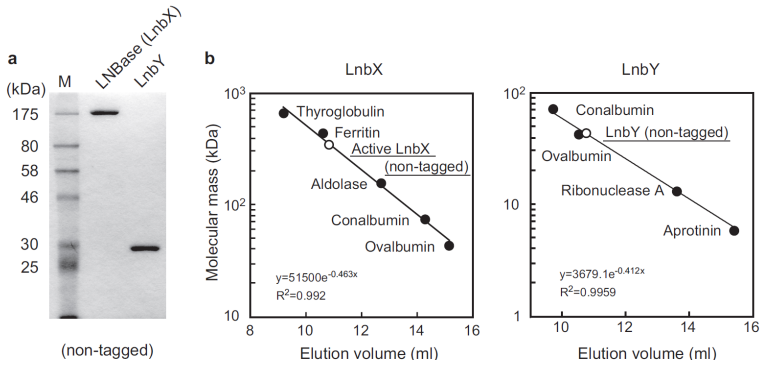

Figure 3. Purification of non-tagged, recombinant LnbX and LnbY proteins. (a) The results of SDS-polyacrylamide gel electrophoresis. LNBase (LnbX) was purified by monitoring LNB-β-*p*NP-hydrolyzing activity. The N-terminal five amino acid residues of LnbX are MQSAT, determined by Edman-degradation. The purified proteins were examined for their metal content (see text). (b) The native molecular weights of LnbX and LnbY were determined by size-exclusion chromatography using Superdex 200 10/300 GL (for LnbX) and Superdex 75 10/300 GL (for LnbY) columns. Thyroglobulin (669 kDa), ferritin (440 kDa), aldolase (158 kDa), conalbumin (75 kDa), ovalbumin (43 kDa), ribonuclease A (13.7 kDa), and aprotinin (6.5 kDa) were used as standards.

Purification and physicochemical characterization−The author first purified non-tagged recombinant LNBase from *E. coli* cells co-expressing LnbX and LnbY. Purification was carried out by monitoring the LNB-β-*p*NP-hydrolyzing activity. The purification process is summarized in Table 2. The purified protein yielded a single band on SDS-polyacrylamide gel electrophoresis with an apparent molecular mass of 161 kDa, which agrees with the calculated mass of LnbX (164 kDa) (Fig. 3a). Edman-degradation analysis revealed the N-terminal amino acid sequence as MQSAT, consistent with the designed construct for expressing LnbX (31−1573 residues). Addition of His-tag to the C-terminus of the protein did not alter the enzymatic properties of LnbX (discussed later) and the tagged protein was easily purified by Ni^{2+}-affinity chromatography. Moreover, LnbX migrated to a virtually identical position in the SDS-polyacrylamide gel electrophoresis regardless of whether LnbY was co-expressed or not (see Fig. 7a). Addition of purified LnbY to purified LnbX (correctly folded form, described later) produced no effect on LNBase activity (data not shown). These results indicated that the active LNBase molecule from *B. longum* is a single gene product (that of *lnbX*). The native molecular mass of LNBase (LnbX) deduced from size exclusion chromatography was 356 kDa, indicating that the enzyme forms a dimer in solution (Fig. 3b).

Inductively coupled plasma emission spectroscopy revealed that LnbX contains 1 ± 0.1 molecule of magnesium, 3 ± 0.6 molecules of calcium, and 0.4 ± 0.1 molecule of zinc. Magnesium and calcium ions are probably tightly bound to or buried in the protein because the addition of EDTA to the dialysis buffer did not alter the metal contents; however, zinc ion was deprived from the protein by adding EDTA. Recall that EDTA does not affect the specific activity of the purified enzyme.

The optimal pH and temperature of the enzyme for LNB-β-*p*NP hydrolysis was 5.4 (MES buffer) and 60°C, respectively. The enzyme was stable in the pH range 4.5−9.5 and below 45°C for 30 min. The purified recombinant enzyme maintained its activity at least for 3 weeks (data not shown).

The author also purified non-tagged LnbY (Fig. 3a). The molecular mass of recombinant LnbY (30-280 aa) was estimated to be 28.2 kDa (calculated, 27.4 kDa) on SDS-polyacrylamide gel electrophoresis and 48.5 kDa on gel filtration analysis, indicating a dimer formation (Fig. 3b). LnbY appeared to contain no metal ions.

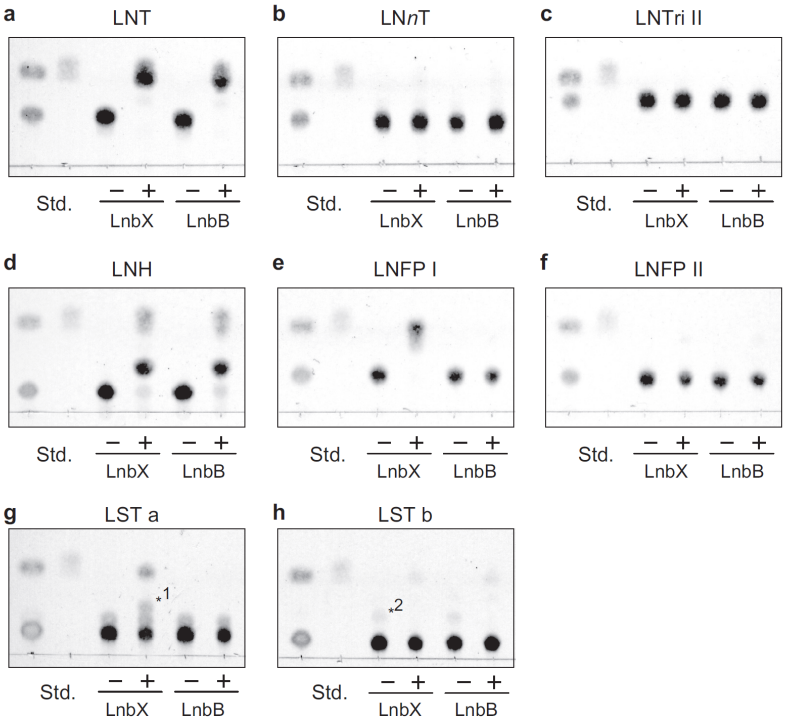

Figure 4. Substrate specificity of LNBases from *B. longum* subsp. *longum* (LnbX) and from *B. bifidum* (LnbB, a GH20 enzyme). The reactions were carried out in 50 mM MES (pH 5.4) (for LnbX) and citrate-phosphate (pH 4.5) (for LnbB) buffers containing 5 mM substrates in the presence and absence of the enzyme (6 mU towards LNB-β-*p*NP). The reaction products were analyzed by a thin-layer chromatography using a solvent system of 1-butanol/acetic acid/water (2:1:1, by volume). The sugars were visualized by diphenylamine-phosphoric acid (45). The substrates used were: lacto-*N*-tetraose (LNT) (a); lacto-*N*-*neo*tetraose (LN*n*T) (b); lacto-*N*-triose II (LNTri II) (c); lacto-*N*-hexaose (LNH) (d); lacto-*N*-fucopentaose I (LNFP I) (*e*);LNFP II (f); sialyllacto-*N*-tetraose a (LST a) (g); and LST b (h). *1 and *2 indicate 3'-sialyl-lacto-*N*-biose I (hydrolysis product, see Fig. 5c) and LNT (contaminant of LST b), respectively. Standards used are lactose and each substrate (far left lane) and lacto-*N*-biose I (near left lane). See also Table 3.

Table 3 Substrate specificity of LNBases from *B. longum* subsp. *longum* (LnbX) and *B.bifidum* (LnbB)

Substrate	Hydrolysis[a]		Kinetic parameter					
			LnbX			LnbB[b]		
	LnbX	LnbB	K_m	k_{cat}	k_{cat}/K_m	K_m	k_{cat}	k_{cat}/K_m
			mM	s^{-1}	$mM^{-1}s^{-1}$	mM	s^{-1}	$mM^{-1}s^{-1}$
LNB-β-*p*NP Galβ1−3GlcNAcβ-*p*NP	+++	+++	0.119 ± 0.022	96.1 ± 4.1	806 ± 123	0.099 ± 0.011	15.4 ± 0.7	156 ± 11
GalNAcGlcNAc-β-*p*NP GalNAcβ1−3GlcNAcβ-*p*NP	+++	−	0.186 ± 0.010	39.4 ± 0.6	211 ± 8			
Lacto-*N*-tetraose Galβ1−3GlcNAcβ1−3Galβ1−4Glc	+++	+++	0.401 ± 0.015	113 ± 2	282 ± 7	0.626 ± 0.029	42.1 ± 0.9	67.2 ± 1.9
Lacto-*N*-*neo*tetraose Galβ1−4GlcNAcβ1−3Galβ1−4Glc	−	−						
Lacto-*N*-triose II GlcNAcβ1−3Galβ1−4Glc	−	−						
Lacto-*N*-hexaose Galβ1−3GlcNAcβ1−3(Galβ1−4GlcNAcβ1−6)Galβ1−4Glc	++	++	ND[c]	ND	ND	ND	ND	ND
Lacto-*N*-fucopentaose I Fucα1−2Galβ1−3GlcNAcβ1−3Galβ1−4Glc	+++	−	14.6 ± 4.3	13.5 ± 1.5	0.923 ± 0.179			
Lacto-*N*-fucopentaose II Galβ1−3(Fucα1−4)GlcNAcβ1−3Galβ1−4Glc	−	−						
Sialyllacto-*N*-tetraose a Neu5Acα2−3Galβ1−3GlcNAcβ1−3Galβ1−4Glc	+	−	ND	ND	ND			
Sialyllacto-*N*-tetraose b Galβ1−3(Neu5Acα2−6)GlcNAcβ1−3Galβ1−4Glc	−	−						

[a]:The reactions were carried out in 50 mM MES buffer (pH 5.4) (for LnbX) and citrate-phosphate buffer (pH 4.5) (for LnbB) containing 1 mM (for *p*NP-sugars) and 5 mM (for oligosaccharides) substrates. Mixtures were incubated overnight at 25°C in the presence and absence of the enzyme (6 mU towards *p*NP-LNB). The reaction products were analyzed by thin-layer chromatography (TLC) (see Fig. 4). Neither LnbX nor LnbB acted on *p*NP-monosaccharides (L-Ara*pα*-*p*NP, Galβ-, GalNAcβ-, Glcβ-, GlcNAβ-, GlcUAβ-, Manβ-, Xylβ-), Lacβ-*p*NP, and LacdiNAcβ-*p*NP. +++: complete hydrolysis (100%), ++: significant hydrolysis (>50%), +: partial hydrolysis (<50%), −: no hydrolysis.
[b]: The kinetic parameters of LnbB are taken from our recent report (28).
[c]: Not determined.

Substrate specificity−Substrate specificity was determined using C-terminal His-tagged LnbX. The specific activity on LNB-β-*p*NP was essentially the same for the His-tagged- (34.1 U/mg) and non-tagged (37.2 U/mg) enzymes. Hydrolytic activity was evaluated by overnight incubation of the enzyme (6 mU towards LNB-β-*p*NP) with various *p*NP-sugars (1 mM) and oligosaccharides (5 mM) (Table 3 and Fig. 4). The activity of GH20 LNBase from *B. bifidum* (LnbB) was also evaluated for comparison (17,28). LnbX hydrolyzed both LNB-β-*p*NP and GalNAcβ1-3GlcNAcβ-*p*NP, while LnbB was inactive towards GalNAcβ1-3GlcNAcβ-*p*NP (Table 3). LnbX was able to act on LNT, LNH, LNFP I, and LST a, whereas LnbB acted only on LNT and LNH (Fig. 4a,d,e,g). The hydrolysis of LNT, LNFP I and LST a by LnbX at the Galβ1-3GlcNAc linkage was confirmed by ESI-MS analysis. The reaction products of LNT hydrolysis yielded molecular ion peaks corresponding to sodium adducts of Lac (calculated for $[M + Na]^+$, 365.11; observed, 365.05) and LNB (calculated for $[M + Na]^+$, 406.13; observed, 406.05) (Fig. 5a), while the LNFP I hydrolysis gave rise to sodium adducts of Lac (observed, 365.05) and 2'-fucosyl-LNB (calculated for $[M + Na]^+$, 552.19; observed, 552.20) (Fig. 5b). The spot corresponding to a trisaccharide in the TLC analysis of the LST a hydrolysate yielded molecular ion peaks matching sodium adduct (calculated for $[M + Na]^+$, 697.23; observed, 697.20) and deprotonated, disodium adduct (calculated for $[M - H +2Na]^+$, 719.21; observed 719.15) of 3'-sialyl-LNB (Fig. 5c). No corresponding peaks appeared in the control experiments without enzyme (data not shown).

Both LnbX and LnbB were inactive on LN*n*T, lacto-*N*-triose II, LNFP II, and LST b (Fig. 4b,c,f,h). Neither enzyme hydrolyzed *p*NP-monosaccharides (L-Ara*pα*-*p*NP, Galβ-*p*NP, GalNAcβ-*p*NP, Glcβ-*p*NP, GlcNAβ-*p*NP, GlcUAβ-*p*NP, Manβ-*p*NP, Xylβ-*p*NP), Lacβ-*p*NP, orGalNAcβ1-4GlcNAcβ (LacdiNAc)-*p*NP.

The activity of LnbX towards LNB-β-*p*NP (1 mM) was not inhibited by LacNAc (5 mM). The rate of hydrolysis of GalNAcβ1-3GlcNAcβ-*p*NP (1 mM) by LnbX was not affected in the presence of 5 mM LacdiNAcβ-*p*NP (data not shown).

Kinetic analysis revealed that the catalytic efficiency of LnbX towards LNB-β-*p*NP and LNT is 5- and 4-fold higher, respectively, than that of LnbB (806 vs. 156 mM^{-1} s^{-1} for LNB-β-*p*NP; 282 vs. 67.2 mM^{-1} s^{-1} for LNT) (Table 3). This difference is mostly due to the higher k_{cat} values of LnbX (96.1 s^{-1} for LNB-β-*p*NP and 113 s^{-1} for LNT) than those of LnbB (15.4 s^{-1} for LNB-β-*p*NP and 42.1 s^{-1} for LNT) towards these substrates. The kinetic analysis also revealed

that activity of LnbX on GalNAcβ1-3GlcNAcβ-*p*NP (k_{cat}/K_m value of 211 mM^{-1} s^{-1}) is significant and comparable to that on LNB-β-*p*NP. Relative to LNT, LnbX showed 40-fold higher K_m value (14.6 vs. 0.401 mM) and 8-fold lower k_{cat} value (13.5 vs. 113 s^{-1}) for LNFP I, implying that the enzyme is less effective towards LNFP I (nonetheless significant; see Fig. 4e). The activity of the enzyme on LST a was too low to determine the kinetic parameters.

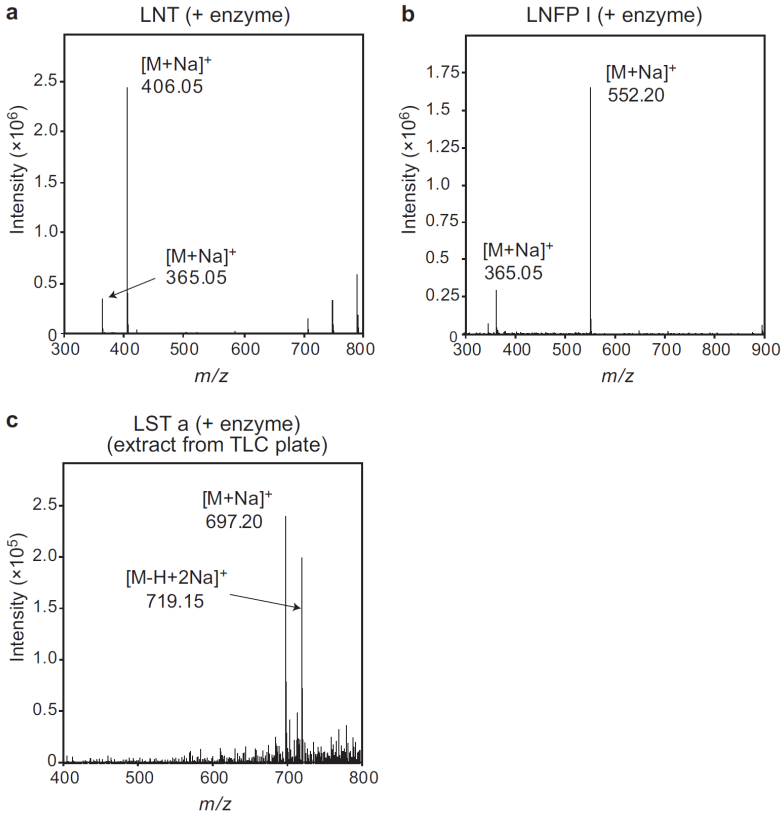

Figure 5. ESI-MS analysis of the reaction products catalyzed by LnbX.The reactions were carried out in 50 mM MES (pH 5.4) buffer containing 5 mM lacto-*N*-tetraose (LNT) (a), lacto-*N*-fucopentaose I (LNFP I) (b), and sialyllacto-*N*-tetraose a (LST a) (c) in the presence of the enzyme. When LNT and LNFP I were used as substrates, the reaction products were deionized by Amberlite MB-3 (Millipore, MA) and lyophilized prior to the analysis. In LST a hydrolysis, the reaction products were first separated by thin-layer chromatography and the spot corresponding to a trisaccharide was extracted and purified by Sep-Pak C18 Plus (Waters, MA). Control experiments were performed without the enzyme (data not shown).

Stereochemistry of hydrolysis−Stereochemical course of the reaction was determined by monitoring the anomeric configuration of LNB released from the *p*NP-substrate (Fig. 6). A normal-phase HPLC was employed for this purpose. LNB appeared with the ratio of α-anomer to β-anomer of 25/75 and 35/65 after 1-min and 10-min incubation, respectively. The peak area for LNB-β-*p*NP decreased while those of *p*-nitrophenol and LNB increased as the reaction proceeded (10 and 30 min), and the α/β-ratio of LNB had almost reached the equilibration of mutarotation (60/40) at 120 min. These results showed that LnbX is a retaining enzyme.

Role of LnbY in the folding process of LnbX−To examine the folding state of LnbX, the author performed gel filtration analysis using the cell-free extracts of *E. coli* cells expressing His-tagged LnbX with and without LnbY (non-tagged), followed by SDS-polyacrylamide gel electrophoresis and western blot analysis using anti-His tag antibodies (Fig. 7a,b). The protein concentration and specific activity (from 7.5 to 13 mL elution volume) were also determined for each fraction. The quantity of His-tagged LnbX obtained in a soluble fraction was consistent and independent of LnbY co-expression (Fig. 7a). LnbX eluted in a void volume in the absence of LnbY whereas it eluted at 10.5−11.0 mL (molecular mass 399−316 kDa) in the presence of LnbY. No LNBase activity was detected in any fractions of cell-free extract of the strain expressing LnbX alone, whereas the activity exactly coincided with the LnbX protein peak of the cell-free extract of the strain co-expressing LnbY in the chromatography.

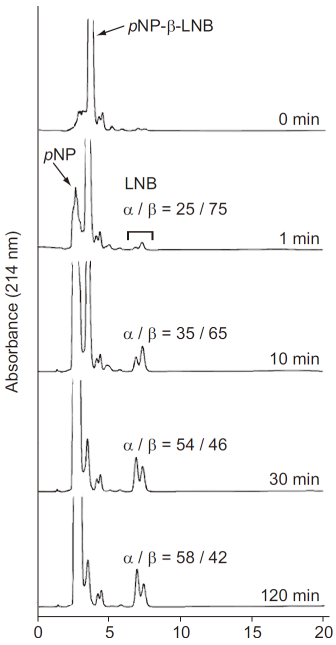

Figure 6. Stereochemical course of the hydrolysis catalyzed by LnbX. The reaction mixture containing 50 mM MES buffer (pH 5.4), 2 mM LNB-β-*p*NP, and the enzyme (7 mU) was incubated at 30°C, and sampled at the indicated times to be analyzed by a HPLC system equipped with TSKgel Amide-80 (4.6 × 250 mm). Elution was carried out at room temperature using acetonitrile/water (65/35) flowing at 1 ml/min, and was monitored by measuring the absorbance at 214 nm.

In vitro refolding experiment of LnbX was also performed, in which the renaturation process was represented by the enzymatic activity on LNB-β-*p*NP (see EXPERIMENTAL PROCEDURES). When the denatured LnbX was incubated and dialyzed alone, no detectable activity was observed throughout the incubation periods (Fig. 7c). No precipitation occurred during dialysis to reflect that the protein formed a soluble aggregate in the cell-free extracts of *E. coli* cells expressing LnbX alone (Fig. 7b, left panel). In contrast, when the refolding solution contained LnbY (non-denatured), activity gradually recovered. Efficient refolding occurred when Ca^{2+} and Mg^{2+} were supplemented together with LnbY. As mentioned above, both metal ions are contained in the native enzyme. Magnesium ions were found to be more important than calcium ions in the refolding process. When Mg^{2+} alone was added, the activity was over 90% of that obtained in the presence of the two metal ions, while Ca^{2+} alone failed to attain 70% activity (data not shown). Refolding also depended on the concentration of the metal ions; 0.1 mM was found to optimize refolding within the tested range (10 μM,

0.1 mM, 1 mM and 5 mM; data not shown). Interestingly, the metal ions by themselves could slightly stimulate the refolding of denatured LnbX, and very low but non-negligible activity was detected as the incubation continued (Fig. 7c). Refolding efficiency varied with the molar ratio of LnbY added to denatured LnbX. When the ratios were increased to 5 and 20 from equimolar, LNB-β-*p*NP-hydrolyzing activity was elevated by 1.2- and 1.5-fold, respectively; however, a ratio of 50 caused a decline in the activity (Fig. 7d). The highest activity attained in the refolding experiments (6.3 U/mg) was one-sixth that of the native recombinant enzyme (37.2 U/mg), indicating a renaturation efficiency of about 17%.

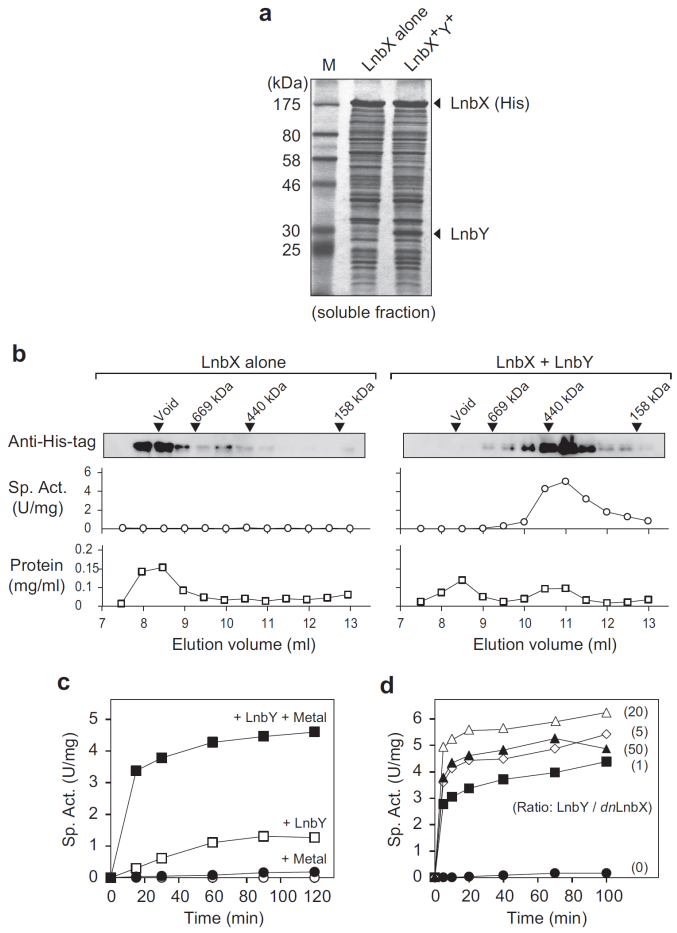

Figure 7. Requirement of LnbY for proper folding of LnbX. (a) The results of SDS- polyacrylamide gel electrophoresis of the soluble fraction of the cell-free extracts of *E. coli* cells expressing either LnbX(His) alone or LnbX(His) and LnbY. (b) The cell-free extracts were separated by size exclusion chromatography (Superdex 200 10/300 GL). Each fraction (0.5 ml) of the elution volume (7.5−13 mL) was subjected to SDS-polyacrylamide gel electrophoresis, followed by western blot analysis using anti-His-tag antibodies linked to horse radish peroxidase. The fractions were also assayed for protein (mg/ml) and enzyme activity (U/mg). The peak fractions of the marker proteins (thyroglobulin: 669 kDa; ferritin: 440 kDa; aldolase: 158 kDa) and the void fraction are indicated. (c) *In vitro* refolding of denatured LnbX (1 μM) was carried out in the presence and absence of LnbY (1 μM) and the metal ions (0.1 mM $CaCl_2$ and $MgCl_2$). The refolding mixture comprising denatured LnbX alone (open circles), denatured LnbX and metal ions (filled circles), denatured LnbX and non-denatured LnbY (open squares), or denatured LnbX, non-denatured LnbY, and metal ions (filled squares) was dialyzed against 50 mM HEPES buffer containing or not containing 0.1 mM metal ions. The samples were removed from the dialysis cassettes at the indicated times and assayed for activity content. (d) The refolding was carried out in varying concentrations of LnbY in the presence of 0.1 mM metal ions. The ratios of LnbY to denatured LnbX are: 0 (filled circles), 1 (filled squares), 5 (open diamonds), 20 (open triangles), and 50 (filled triangles).

DISCUSSION

The present study revealed a novel LNBase in *B. longum* that completely differs from hitherto identified GH families with respect to amino acid sequence, substrate specificity, maturation process, and possibly structure.

Physicochemical properties−Initially, the author considered that LNBase is a hetero-dimer comprising the LnbX and LnbY subunits, since LNB-β-*p*NP-hydrolyzing activity occurred when the cell-free extracts of *E. coli* strains individually expressing LnbX and LnbY were mixed and incubated (Table 1). However, the subsequent experiments revealed that the purified LNBase consists solely of the *lnbX* gene product. The C-terminus of the protein could be truncated to 1431 amino acid residues (immediately upstream of the FIVAR domain, Fig. 1) without loss of activity (data not shown).

Sequence feature−In the complementation analysis using *lnbX*-deficient *B. longum*, plasmid-mediated introduction of the *lnbX* gene failed to restore LNBase activity, even though the genome of the deficient strain contained an intact *lnbY*. Introduction of both *lnbX* and *lnbY* genes by plasmid recovered the LNBase^{+}-phenotype of the parental strain (Fig. 2). These results indicate that the *lnbX* and *lnbY* genes constitute an operon, and the failure of the phenotypic change in the strain carrying plasmid-borne *lnbX* is due to a polar effect. The two genes were separated by a mere 3-bp, and a promoter-like sequence was not found upstream of the ORF of *lnbY*; instead, a 42-bp inverted repeat was found immediately downstream of *lnbY*.

In the genomes of *B. longum* JCM1217 and *B. longum* BBMN68, the *lnbXY* gene is located between the γ-glutamylcysteine synthetase and 2-hydroxyglutaryl-CoA dehydratase activator genes (99% identity in nucleotide sequence over the region covering the four genes) (Supplemental Fig. S2). In the genomes of *B. longum* strains DJ010A, F8, JDM301, KACC91563, and NCC2705 (possibly LNBase^{-}), the γ-glutamylcysteine synthetase gene is located just downstream of the 2-hydroxyglutaryl-CoA dehydratase activator gene (KEGG database; http://www.genome.jp/kegg/). The author currently lacks knowledge of how strains JCM1217 and BBMN68 acquired the *lnbXY* gene at this locus. No insertion sequence was found at either end of the gene (IS Finder: https://www-is.biotoul.fr/). Interestingly, however,

the genomes of *B. bifidum* strains BGN4, PRL2010, and S17 contain *lnbX* and *lnbY* homologs with 50–60% amino acid sequence identity, which are also located near the γ-glutamylcysteine synthetase and 2-hydroxyglutaryl-CoA dehydratase activator genes (Supplemental Fig. S2). In these genomes, the *lnbX* and *lnbY* homologs are separated by the γ-glutamylcysteine synthetase gene and their sense strands are opposed. Note that in *B. bifidum* either the LnbX homolog or the LnbY homolog lacks a signal peptide; therefore, even though both proteins are expressed in the cells they cannot associate to assist the folding of LnbX.

The LnbX homologs have been found in the human gut microbial genomes of *Ruminococcus lactaris* ATCC29176 (RUMLAC_00599), *Clostridium nexile* DSM1787 (clonex_02958), and *C. celatum* DSM1785 (HMPRF0216_02974). The amino acid identity between these homologs and *B. longum* LnbX is about 40%. Among these bacteria, *R. lactaris* ATCC29176 alone possesses the LnbY homolog (27% identity, RUMLAC_00598), but the protein lacks a signal peptide. These results suggest that the gene(s) has specifically evolved within the gut niche. Given the length and sequence diversity among the few known occurrences, the gene(s) might still be evolving. Further elucidation requires characterization of each of these homologs.

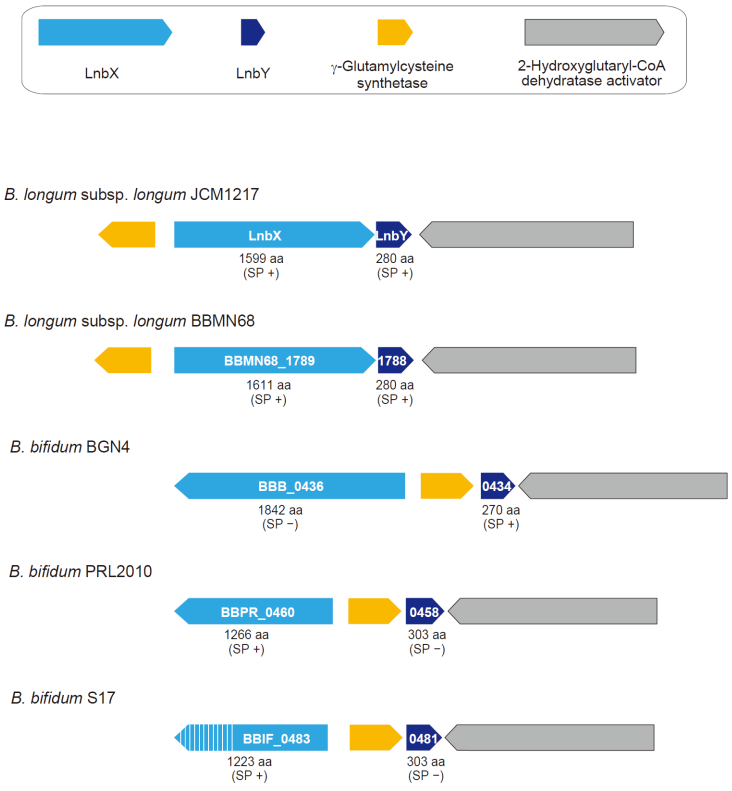

Supplemental Figure S2. The genetic landscape of the sequence-completed bifidobacterial genomes at the lnbXY locus. LnbX and LnbY (and their corresponding ORFs) were shown in cyan and navy blue, respectively, with their lengths (aa) and the presence (+) and absence (−) of signal peptides (predicted by SignalP4.1 server). The ORFs shown in orange and gray were the homologues of γ-glutamylcysteine synthetase and 2-hydroxyglutaryl-CoA dehydratase activator, respectively. Note that BBIF_0483 from *B. bifidum* S17 shows 60% identity with LnbX at the N-terminal half only (~700 aa), whereas the others share identity (>60%) at the whole region. It should also be mentioned that the direction of some ORFs in the *B. bifidum* genomes was opposite to that found in the *B. longum* subsp. *longum* genomes, even though the conserved occurrence of these genes at the same loci.

Substrate specificity−Besides sequence, the substrate specificity of LNBase from *B. longum* significantly differs from that of GH20 LNBase from *B. bifidum*. Whereas GH20 LNBase (including one from *Streptomyces* sp.) acts only on unmodified LNB structures (Fig. 4) (17, 37), the novel LNBase from *B. longum* was able to act on LNFP I and LST a, which have Fuc and Neu5Ac residues at the O2 and O3 positions of the distal Gal residue, respectively. Considering the high activity of LnbX on LNT, followed by LNFP I and LST a, and that the enzyme is inactive on GlcNAc-*p*NP, binding of the substrate at subsite (-2) might be indispensable for the enzyme to exert its activity. The subsite (-2) is slightly widened at the O2 position of (-2) Gal, enabling LnbX to efficiently hydrolyze GalNAcβ1-3GlcNAcβ-*p*NP (Table 3). GalNAcβ1-3GlcNAcβ disaccharide structure has been found in the *O*-mannosyl glycans of α-dystroglycan, and β1-3GalNAc transferase with acceptor specificity towards GlcNAc (*B3GALNT2*) has been identified in humans and mice (38). Recently, Stevens *et al*. reported that mutations in *B3GALNT2* cause congenital muscular dystrophy-dystroglycanopathy, characterized by brain and eye anomalies (39). GalNAcβ1-3GlcNAc is a linkage isomer of LacdiNAc (*N*, *N*'-diacetyllactosediamine, GalNAcβ1-4GlcNAc) found in the *N*-glycans of glycoproteins such as lutropin (a hormone produced by gonadotroph cells) and tenascin-R (an extracellular matrix exclusively expressed in the central nervous system) as well as in glycoproteins from parasites (40,41). The LacdiNAc structure in the leukemia inhibitory factor (LIF) receptor is known to influence self-renewal maintenance of mouse embryonic stem cells (42). Considering that LnbX does not act on LacdiNAcβ-*p*NP and that GalNAcβ1-3GlcNAcβ-*p*NP hydrolysis is not inhibited by the presence of LacdiNAcβ-*p*NP, the enzyme may serve as a new tool for examining the glycan structures of glycoconjugates and for distinguishing between GalNAcβ1-3GlcNAc and LacdiNAc structures. However, the author has not tested whether the enzyme can liberate GalNAcβ1-3GlcNAc from natural substrates.

With respect to the unique substrate specificity of *B. longum* LNBase, the author also emphasizes that *B. longum* JCM1217 grown in HMO medium induces a slight but continuous decrease of LNFP I (0.67 g/L to 0.24 g/L) (12). The author did not identify 2'-fucosyl LNB in that study because the author lacked a standard compound and the author had not elucidated the unique substrate specificity of LnbX. Interestingly, the HPLC profile in that paper displays a small peak between Lac and 2'-fucosyllactose (12).

LnbY as a designated chaperon for LnbX−In both bifidobacteria and *E. coli*, LnbY is required for active expression of LnbX, i.e. LNBase activity (Table 1 and Fig. 2). In the absence of LnbY co-expression, LnbX formed a soluble aggregate and eluted in the void fraction in the gel filtration analysis with no detectable activity (Fig. 7b, left panel). In the presence of LnbY, active LnbX was expressed and eluted at the anticipated fraction (Fig. 7b, right panel). Also, as mentioned above, no apparent post-translational modification occurred on LnbX. These results strongly suggest that the LnbY protein is involved in the folding process of LnbX. The denatured LnbX gained considerable activity during the incubation with LnbY and removal of guanidine-HCl by dialysis (Fig. 7c). The presence of two metal ions (Ca^{2+} and Mg^{2+}, especially Mg^{2+}) was important for efficient refolding (Fig. 7c). The addition of EDTA to mature LnbX had no effect on enzymatic activity (Table 1), nor sequestered the ions during dialysis, indicating that the two metal ions were tightly bound by the protein and stabilized the correct folding of LnbX. Indeed, the two metals slightly stimulated correct folding of LnbX even in the absence of LnbY (Fig. 7c). The results in Table 1 also indicate that LnbY can partially renature a soluble aggregate form of LnbX. To the author's knowledge, this is the first glycosidase that requires a designated chaperon for its active expression. Mucin type core 1 (T antigen)-synthesizing β1-3Gal transferase (C1βGal-T) is known to require its designated chaperon, Cosmc (43). Although the C1βGal-T and Cosmc genes are located on different chromosomes, Cosmc appears to be specialized for C1βGal-T folding, since the activity of other glycosyltransferases is normal in *Cosmc*-null Jurkat cells. Interestingly, both C1βGal-T and Cosmc are secretory proteins and form homo-dimers, and thus share a functional similarity with LnbX and LnbY. Another functional homolog is seen in the synthetic pathway of glycosylphosphatidylinositol (GPI)-anchor. PGI-X has been identified as an important component for active expression of PIG-M, the catalytic subunit of GPI mannosyltransferase I (44). Interestingly, these chaperon proteins are of similar size (Cosmc (318 aa), PGI-X (252 aa), and LnbY (280 aa)) despite their sequence dissimilarity.

Physiology in HMO assimilation−By identifying the *lnbXY* gene, the author unequivocally revealed that *B. longum* JCM1217 extracellularly decomposes LNT by this novel LNBase. The produced LNB and Lac should be imported into the bifidobacterial cells by the GNB/LNB transporter and the Lac transporter, respectively, for further degradation (19, 20, 21) (Supplemental Fig. S1). Among the infant gut-associated bifidobacteria, *B. bifidum*

and some strains of *B. longum* specifically degrade type-1 HMOs by LNBase (LnbB and LnbX, respectively). *B. longum* LNBase showed lower K_m and higher k_{cat} values for LNT than *B. bifidum* LNBase. Therefore, assuming that the LnbX homolog of *B. bifidum* does not function within cells (as described above), *B. longum* can exploit LNT over *B. bifidum*. This might be an important survival strategy for gut-dwelling *B. longum* since this subspecies essentially assimilates LNT only among HMOs due to the lack of α-L-fucosidase (12). *B. longum* might employ its highly active LNBase to sequester LNTs formed from LNFP I and LNDFH I (the main HMO species) by *B. bifidum* 1,2-, and 1,3/4-α-L-fucosidases in the gut (13,15). In this sense, it is interesting that *B. bifidum* grown in HMO medium ignores the degradation products of HMOs in the spent medium even during the exponential growth phase (12). *B. infantis* probably circumvents the interception by ingesting all HMOs as intact forms and digesting them intracellularly (23-25).

Concluding remarks−Hitherto uncharacterized protein sequences of unknown function, namely BLLJ_1505 and BLLJ_1506, are found to constitute LNBase, an enzyme exhibiting unique substrate specificity and maturation process. These findings are important not only for comprehensive understanding of HMOs assimilation by infant-gut bifidobacteria but also in functional glycomics research, since *B. longum* LNBase is the first reported enzyme to liberate GalNAcβ1-3GlcNAc.

REFERENCES

1. Mitsuoka, T. (1988) Intestinal flora and host. *Asian Med J.* **31**, 400-409
2. Penders, J., Thijs, C., Vink, C., Stelma, F.F., Snijders, B., Kummeling, I., van den Brandt, P.A., and Stobberingh, E.E. (2006) Factors influencing the composition of the intestinal microbiota in early infancy. *Pediatrics* **118,** 511-521
3. Kunz, C., Rudloff, S., Baier, W., Klein, N., and Strobel, S. (2000) Oligosaccharides in human milk: structural, functional, and metabolic aspects. *Annu Rev Nutr*. **20,** 699-722
4. Bode, L. (2006) Recent advances on structure, metabolism, and function of human milk oligosaccharides. *J Nutr*. **136,** 2127-2130
5. Newburg, D.S. and Neubauer, S.H. (1995) *Carbohydrates* in milk. in *Handbook of Milk Composition* (Jensen, R.G., ed) pp. 273-349, Academic Press

6. Kobata, A. (2013) Exo- and endoglycosidases revisited. *Proc Jpn Acad Ser. B***89,** 97-117
7. Brand-Miller, J.C., McVeagh, P., McNeil, Y., and Messer, M. (1998) Digestion of human milk oligosaccharides by healthy infants evaluated by the lactulose hydrogen breath test. *J Pediatr*. **133**, 95-98
8. Gnoth, M.J., Kunz, C., Kinne-Saffran, E., and Rudloff, S. (2000) Human milk oligosaccharides are minimally digested *in vitro*. *J Nutr*. **130,** 3014-3020
9. Urashima, T., Kitaoka, M., Terabayashi, T., Fukuda, K., Ohnishi, M., and Kobata, A. (2011) Milk oligosaccharides. in *Oligosaccharides: Sources, properties and applications* (Gordon, N.G., ed) pp 1-58, Nova Science Publishers, New York
10. Kobata, A. (2010) Structures and application of oligosaccharides in human milk. *Proc Jpn Acad Ser. B***86**, 731-747
11. Sela, D.A., Chapman, J., Adeuya, A., Kim, J.H., Chen, F., Whitehead, T.R., Lapidus, A., Rokhsar, D.S., Lebrilla, C.B., German, J.B., Price, N.P., Richardson, P.M., and Mills, D.A. (2008) The genome sequence of *Bifidobacterium longum* subsp. *infantis* reveals adaptations for milk utilization within the infant microbiome. *Proc Natl Acad Sci USA*. **105,** 18964-18969
12. Asakuma, S., Hatakeyama, E., Urashima, T., Yoshida, E., Katayama, T., Yamamoto, K., Kumagai, H., Ashida, H., Hirose, J., and Kitaoka, M. (2011) Physiology of consumption of human milk oligosaccharides by infant-gut associated bifidobacteria. *J Biol Chem*. **286**, 34583-34592
13. Katayama, T., Sakuma, A., Kimura, T., Makimura, Y., Hiratake, J., Sakata, K., Yamanoi, T., Kumagai, H., and Yamamoto, K. (2004) Molecular cloning and characterization of *Bifidobacterium bifidum* 1,2-α-L-fucosidase (AfcA), a novel inverting glycosidase (glycoside hydrolase family 95). *J Bacteriol*. **186**, 4885-4893
14. Nagae, M., Tsuchiya, A., Katayama, T., Yamamoto, K., Wakatsuki, S., and Kato, R. (2007) Structural basis on the catalytic reaction mechanism of novel 1,2-α-L-fucosidase (AfcA) from *Bifidobacterium bifidum*. *J Biol Chem.* **282**, 18497-18509
15. Ashida, H., Miyake, A., Kiyohara, M., Wada, J., Yoshida, E., Kumagai, H., Katayama, T., and Yamamoto, K. (2009) Two distinct α-L-fucosidases from *Bifidobacterium bifidum* are essential for the utilization of fucosylated milk oligosaccharides and glycoconjugates. *Glycobiology* **19**, 1010-1017
16. Kiyohara, M., Tanigawa, K., Chaiwangsri, T., Katayama, T., Ashida, H., and Yamamoto,

K. (2011) An exo-α-sialidase from bifidobacteria involved in the degradation of sialyloligosaccharides in human milk and intestinal glycoconjugates. *Glycobiology* **21**, 437-447

17. Wada, J., Ando, T., Kiyohara, M., Ashida, H., Kitaoka, M., Yamaguchi, M., Kumagai, H., Katayama, T., and Yamamoto, K. (2008) *Bifidobacterium bifidum* lacto-*N*-biosidase, a critical enzyme for the degradation of human milk oligosaccharides with a type-1 structure. *Appl Environ Microbiol*. **74**, 3996-4004
18. Miwa, M., Horimoto, T., Kiyohara, M., Katayama, T., Kitaoka, M., Ashida, H., and Yamamoto, K. (2010) Cooperation of β-galactosidase and β-*N*-acetylhexosaminidase from bifidobacteria in assimilation of human milk oligosaccharides with type 2 structure. *Glycobiology* **20**, 1402-1409
19. Kitaoka, M., Tian, J., and Nishimoto, M. (2005) Putative galactose operon involving lacto-*N*-biose phosphorylase in *Bifidobacterium longum*. *Appl Environ Microbiol*. **71**, 3158-3162
20. Nishimoto, M. and Kitaoka, M. (2007) Identification of *N*-acetylhexosamine 1-kinase in the complete lacto-*N*-biose I/galacto-*N*-biose metabolic pathway in *Bifidobacterium longum*. *Appl Environ Microbiol.* **73**, 6444-6449
21. Suzuki, R., Wada, J., Katayama, T., Fushinobu, S., Wakagi, T., Shoun, H., Sugimoto, H., Tanaka, A., Kumagai, H., Ashida, H., Kitaoka, M., and Yamamoto, K. (2008) Structural and thermodynamic analyses of solute-binding protein from *Bifidobacterium longum* specific for core 1 disaccharide and lacto-*N*-biose I. *J Biol Chem*. **283**, 13165-13173
22. Xiao, J.-Z., Takahashi, S., Nishimoto, M., Odamaki, T., Yaeshima, T., Iwatsuki, K., Kitaoka, M. (2009) Distribution of in vitro fermentation ability of lacto-*N*-biose I, a major building block of human milk oligosaccharides, in bifidobacterialstrains. *Appl Environ Microbiol.* **76**, 154-159
23. Yoshida, E., Sakurama, H., Kiyohara, M., Nakajima, M., Kitaoka, M., Ashida, H., Hirose, J., Katayama, T., Yamamoto, K., and Kumagai, H. (2012) *Bifidobacterium longum* subsp. *infantis* uses two different β-galactosidases for selectively degrading type-1 and type-2 human milk oligosaccharides. *Glycobiology* **22**, 361-368
24. Garrido, D., Ruiz-Moyano, S., and Mills, D.A. (2012) Release and utilization of *N*-acetyl-D-glucosamine from human milk oligosaccharides by *Bifidobacterium longum* subsp. *infantis*. *Anaerobe* **18**, 430-435

25. Sakurama, H., Fushinobu, S., Hidaka, M., Yoshida, E., Honda, Y., Ashida, H., Kitaoka, M., Kumagai, H., Yamamoto, K., and Katayama, T. (2012) 1,3-1,4-α-L-Fucosynthase that specifically introduces Lewis a/x antigens into type-1/2 chains. *J Biol Chem*. **287**, 16709-16719
26. Ward, R.E., Niñonuevo, M., Mills, D.A., Lebrilla, C.B., and German, J.B. (2007) *In vitro* fermentability of human milk oligosaccharides by several strains of bifidobacteria. *Mol Nutr Food Res.* **51**, 1398-1405
27. Fukuda, S., Toh, H., Hase, K., Oshima, K., Nakanishi, Y., Yoshimura, K., Tobe, T., Clarke, J.M., Topping, D.L., Suzuki, T., Taylor, T.D., Itoh, K., Kikuchi, J., Morita, H., Hattori, M., and Ohno, H. (2011) Bifidobacteria can protect from enteropathogenic infection through production of acetate. *Nature* **469**, 543-547
28. Ito, T., Katayama, T., Hattie, M., Sakurama, H., Wada, J., Suzuki, R., Ashida, H., Wakagi, T., Yamamoto, K., Stubbs, K.A., and Fushinobu, S. (2013) Crystal structures of a glycoside hydrolase family 20 lacto-*N*-biosidase from *Bifidobacterium bifidum*. *J Biol Chem.* **288**, 11795-11806
29. Honda, Y., Nishimoto, M., Katayama, T., and Kitaoka, M. (2013) Characterization of the cytosolic β-*N*-acetylglucosaminidase from *Bifidobacterium longum* subsp. *longum*. *J Appl Glycosci*. *In press*.
30. Yoshida-Moriguchi, T., Yu, L., Stalnaker, S. H., Davis, S., Kunz, S., Madson, M., Oldstone, M.B., Schachter, H., Wells, L., and Campbell, K.P. (2010) *O*-mannosyl phosphorylation of α-dystroglycan is required for laminin binding. *Science* **327**, 88-92
31. Nishimoto, M. and Kitaoka, M. (2007). Practical preparation of lacto-***N***-biose I, the candidate of the bifidus factor in human milk. *Biosci Biotechnol Biochem.* **71**, 2101-2104
32. Inaba, T., Ohgushi, T., Iga, Y., and Hasegawa, E. (1984) Synthesis of 4-methylcoumarin-7-yloxy tetra-*N*-acetyl-β-chitotetraoside, a novel synthetic substrate for the fluorometric assay of lysozyme. *Chem Pharm Bull.* **32**, 1597-1603
33. Matsumura, H., Takeuchi, A., and Kano, Y. (1997) Construction of *Escherichia coli-Bifidobacterium longum* shuttle vector transforming *B. longum* 105-A and 108-A. *Biosci Biotech Biochem.* **61**, 1211-1212
34. Hirayama, Y., Sakanaka, M., Fukuma, H., Murayama, H., Kano, Y., Fukiya, S., and Yokota, A. (2012) Development of a double-crossover markerless gene deletion system in *Bifidobacterium longum*: functional analysis of the α-galactosidase gene for raffinose

assimilation. *Appl Environ Microbiol.* **78**, 4984-4949

35. Punta, M., Coggill, P.C., Eberhardt, R.Y., Mistry, J., Tate, J., Boursnell, C., Pang, N., Forslund, K., Ceric, G., Clements, J., Heger, A., Holm, L., Sonnhammer, E.L.L., Eddy, S.R., Bateman, A., and Finn, R.D. (2012) The Pfam protein families database. *Nucleic Acids Res.* **40**, D290-D301
36. Petersen, T.N., Brunak, S., von Heijne, G., and Nielsen, H. (2011) SignalP 4.0: discriminating signal peptides from transmembrane regions. *Nature Methods* **8**, 785-786
37. Sano, M., Hayakawa, K., and Kato, I. (1992) An enzyme releasing lacto-*N*-biose from oligosaccharides. *Proc Natl Acad Sci USA*. **89**, 8512-8516.
38. Hiruma, T., Togayachi, A., Okamura, K., Sato, T., Kikuchi, N., Kwon, Y.-D., Nakamura, A., Fujimura, K., Gotoh, M., Tachibana, K., Ishizuka, Y., Noce, T., Nakanishi, H., and Narimatsu H. (2004) A novel human β1,3-*N*-Acetylgalactosaminyltransferase that synthesizes a unique carbohydrate structure, GalNAcβ1-3GlcNAc. *J Biol Chem.* **279**, 14087-14095
39. Stevens, E., Carss, K.J., Cirak, S., Foley, A.R., Torelli, S., Willer, T., Tambunan, D.E., Yau, S., Brodd, L., Sewry, C.A., Feng, L., Haliloglu, G., Orhan, D., Dobyns, W.B., Enns, G.M., Manning, M., Krause, A., Salih, M.A., Walsh, C.A., Hurles, M., Campbell, K.P., Manzini, M.C; UK10K Consortium, Stemple, D., Lin, Y.Y., and Muntoni, F. (2013) Mutations in *B3GALNT2* cause congenital muscular dystrophy and hypoglycosylation of α-dystroglycan. *Am J Hum Genet.* **92**, 354-365
40. Woodworth, A., Fiete, D., and Baenziger, J.U. (2002) Spatial and temporal regulation of tenascin-R glycosylation in the cerebellum. *J Biol Chem.* **277**, 50941-50947
41. Wuhrer, M., Koeleman, C.A., Deelder, A.M., and Hokke, C.H. (2006) Repeats of LacdiNAc and fucosylated LacdiNAc on *N*-glycans of the human parasite *Schistosoma mansoni*. *FEBS J.* **273**, 347-361
42. Sasaki, N., Shinomi, M., Hirano, K., Ui-Tei, K., and Nishihara, S. (2011) LacdiNAc (GalNAcβ1-4GlcNAc) contributes to self-renewal of mouse embryoic stem cells by regulating leukemia inhibitory factor/STAT3 signaling. *Stem Cells* **29**, 641-650
43. Ju, T. and Cummings, R.D. (2002) A unique molecular chaperon Cosmc required for activity of the mammalian core 1 β3-galactosyltransferase. *Proc Natl Acad Sci USA*. **99**, 16613-16618.
44. Ashida, H., Hong, Y., Murakami, Y., Shishioh, N., Sugimoto, N., Kim, Y.U., Maeda, Y.,

and Kinoshita, T. (2005) Mammalian PIG-X and Yeast Pbn1p are the essential components of glycosylphosphatidylinositol-mannosyltransferase I. *Mol Biol Cell* **16**, 1439-1448

45. Anderson, K., Li, S.C., and Li, Y.T. (2000) Diphenylamine-aniline-phosphoric acid reagent, a versatile spray reagent for revealing glycoconjugates on thin-layer chromatography plates. *Anal Biochem.* **287**, 337-339

CHAPTER 2

α-L-Fucosidase from *Bacteroides thetaiotaomicron*

α-L-Fucosyl residues are frequently found at the non-reducing ends of glycoconjugates and play fundamental roles in various biological processes (1). For the examination of the biological activities of the fucose-containing glycoconjugates, α-L-fucosidase serves as a powerful tool because it can selectively remove the fucosyl residues without damaging the compounds. Currently, α-L-fucosidases occur in glycoside hydrolase (GH) families 29 and 95 (2). GH95 enzymes show strict substrate specificity to the terminal Fucα1-2Gal linkage and hydrolyze the linkage *via* an inverting mechanism (3,4), while GH29 enzymes show relatively relaxed substrate specificities with the hydrolysis proceeding *via* a retaining mechanism (5,6).

Ashida *et al*. recently isolated a GH29 enzyme from *Bifidobacterium bifidum* and found that the enzyme (*Bb*AfcB) acts exclusively on the terminal α-(1→3/4)-fucosidic linkages (7). Phylogenetic analysis revealed that *Bb*AfcB is distantly related to the well-studied GH29 enzymes from humans and *Thermotoga maritima* (6,8) and constitutes a different clade together with the enzymes from *Streptomyces* sp. and *Arabidopsis thaliana* (9,10) (Fig. 1a). These results suggested that GH29 can be divided into two subfamilies: one contains α-L-fucosidases with relaxed substrate specificities that can act on *p*-nitorophenyl-α-L-fucopyranoside (*p*NP-Fuc) (referred to as GH29-A) (EC 3.2.1.51), whereas the members of the other subfamily specifically hydrolyze α-L-(1→3/4)-fucosidic linkages and essentially do not act on *p*NP-Fuc (GH29-B) (EC 3.2.1.111) (7,9,10). The recent report describing α-L-fucosidases from *Lactobacillus casei* indicated that they are classified as belonging to the GH29-A subfamily (Fig. 1a) (11).

To explore the validity of this subfamily classification and to obtain a better understanding of the structural basis that underlies this classification, the author determined the substrate specificities of two structure-solved, but uncharacterized GH29 α-L-fucosidases from *Bacteroides thetaiotaomicron* VPI-5482*, i.e.*, the proteins with locus tag BT_2970 (GH29-A) and BT_2192 (GH29-B) (Fig. 1a) (12).

EXPERIMENTAL PROCEDURES

Chemicals−Lewis a and x ($Le^{a/x}$) trisaccharides [Galβ1-3/4(Fucα1-4/3)GlcNAc], $Le^{b/y}$

tetrasaccharides [Fucα1-2Galβ1-3/4(Fucα1-4/3)GlcNAc] and 6-fucosyl-*N*-acetylgllucosamine (F1-6Gn, Fucα1-6GlcNAc) disaccharide were purchased from Dextra Laboratories (Reading, UK). 3-fucosyl-*N*-acetylgllucosamine (F1-3Gn, Fucα1-3GlcNAc) and 4-fucosyl-*N*-acetylgllucosamine (F1-4Gn, Fucα1-4GlcNAc) disaccharides were from Carbosynth (Compton, UK). 2'-Fucosyllactose (2'-FL, Fucα1-2Galβ1-4Glc) and *p*-nitrophenyl-α-L-fucopyranoside (*p*NP-Fuc) were from Sigma (St.Louis, MO, USA). 3-Fucosyllactose [3-FL, Galβ1-4(Fucα1-3)Glc] was purchased from Dextra Laboratories, and further purified using Bio-Gel P2 gel filtration chromatography (Bio-Rad, CA, USA). L-Fucose dehydrogenase was purchased from Kikkoman (Noda, Japan). Other reagents of analytical grade were obtained from commercial sources.

Bacterial strains and growth conditions−The bacterial strain used in this chapter was *Bacteroides thetaiotaomicron* VPI-5482 that was obtained from the Japan Collection of Microorganisms (JCM), RIKEN Bioresource Center, Japan. The strain was anaerobically grown at 37°C in GAM medium (Nissui, Tokyo, Japan) with Anaeropack (Mitrubishi Chemical, Japan).

Expression and purification of BT_2192 and BT_2970−The gene products of the locus tags BT_2192 and BT_2970 were expressed in *Escherichia coli* BL21 Δ*lacZ* (DE3) (7). The N-terminal signal sequences, the presence of which was predicted using the Signal P 4.0 server (13), were eliminated in the vector construction. The genes were amplified by PCR involving KOD polymerase (Toyobo, Japan) using the genomic DNA of *B. thetaiotaomicron* VPI-5482 as a template. The sequences of the primers used were 5'-ccatatgcaagaagcaaagaaggaaatt-3' and 5'-ccctcgagtgttaaagcatctcgataaat -3' (for BT_2970), and 5'-ccatatgcaacaagcaccagctccttgc-3' and 5'-ccctcgagtaatttgaaaaccggtgactg-3' (for BT_2192). The amplified fragments were inserted into pET23b vector (Novagen, Madison, WI) to generate C-terminally histidine-tagged proteins. The PCR-generated fragments were sequenced to ensure that no base change other than those intended had occurred. The recombinant strains were cultured in lysogeny broth media containing 100 μg/ml ampicillin at 18°C until the optical density at 600 nm reached 0.5. Isopropyl-β-D-1-thiogalactopyranoside was then added to a final concentration of 0.1 mM to induce protein expression. Following further incubation for 15 h, the cells were harvested and disrupted by sonication. After

centrifugation, the supernatants were applied to a Ni-NTA agarose column (Qiagen, Hilden, Germany), and the proteins were eluted according to the manufacturer's instructions. The fractions were combined, concentrated using an Amicon Ultra 30 K (Millipore, MA, USA) and loaded onto a Superdex 200 10/300 GL gel filtration column (GE Healthcare Bio-Sciences, Uppsala, Sweden). The elution was carried out using a 20 mM tris(hydroxymethyl)aminomethane-HCl buffer (Tris-HCl) (pH 8.0) containing 150 mM NaCl. The molecular masses of the proteins were determined using the same column. Thyroglobulin (669 kDa), ferritin (443 kDa), aldolase (158 kDa), conalbumin (75 kDa) and ovalbumin (43 kDa) were used as the standards. The protein concentrations were determined using a BCA protein assay kit (Thermo Fisher Scientific, IL, USA) with bovine serum albumin as a standard.

Enzyme assay−The hydrolytic activity was determined using *p*NP-Fuc and fucosyl oligosaccharides as the substrates. The reaction mixture contained 100 mM 2-(*N*-morpholino)ethanesulfonic acid (MES) buffer (pH 6.0), 1 mM of each substrate, and the enzymes (for the *p*NP-Fuc hydrolysis, 20 μM of BT_2192 and 280 nM of BT_2970; for the natural fucosylated substrates, 690 nM of BT_2192 and 15 μM of BT_2970). For the *p*NP-Fuc hydrolysis, the reaction was carried out for an appropriate time at 37°C and terminated by the addition of 1 M sodium carbonate. The amount of the liberated *p*NP was determined by measuring the absorbance at 405 nm. For the fucosyl oligosaccharide hydrolysis, the reaction was carried out for an appropriate time at 37°C and terminated by heating. The amount of released Fuc was determined using a fucose dehydrogenase-coupled method (3,4,14). One unit of the enzyme activity was determined as the amount of enzyme required to produce 1 μmol of pNP or Fuc under the specified conditions.

The physicochemical properties of BT_2192 and BT_2970 were determined by using 3-FL and *p*NP-Fuc as the substrates, respectively. The optimal temperature was examined by incubating the reaction mixture containing 100 mM MES buffer (pH 6.0) at various temperatures for a short period of time (< 1 min) to prevent damage to the enzymes. The optimal pH value was determined using the following buffers (50 mM): citrate-NaOH (pH 4.0–5.0), MES (pH 5.0–6.5), and 3-(*N*-morpholino)propanesulfonic acid (MOPS) (pH 6.5–8.0). The temperature and pH stabilities were determined by measuring the residual activities after incubating the enzyme in 100 mM MES (pH 6.0) for 30 min at various

temperatures and after dialyzing the enzyme overnight against various 100 mM buffers at 4°C, respectively. The effect of the divalent cations on the activity was examined by adding 1 mM $CoCl_2$, $CaCl_2$, $MnCl_2$, $MgCl_2$, $CuCl_2$, and $ZnCl_2$ to the reaction mixture.

RESULTS AND DISCUSSION

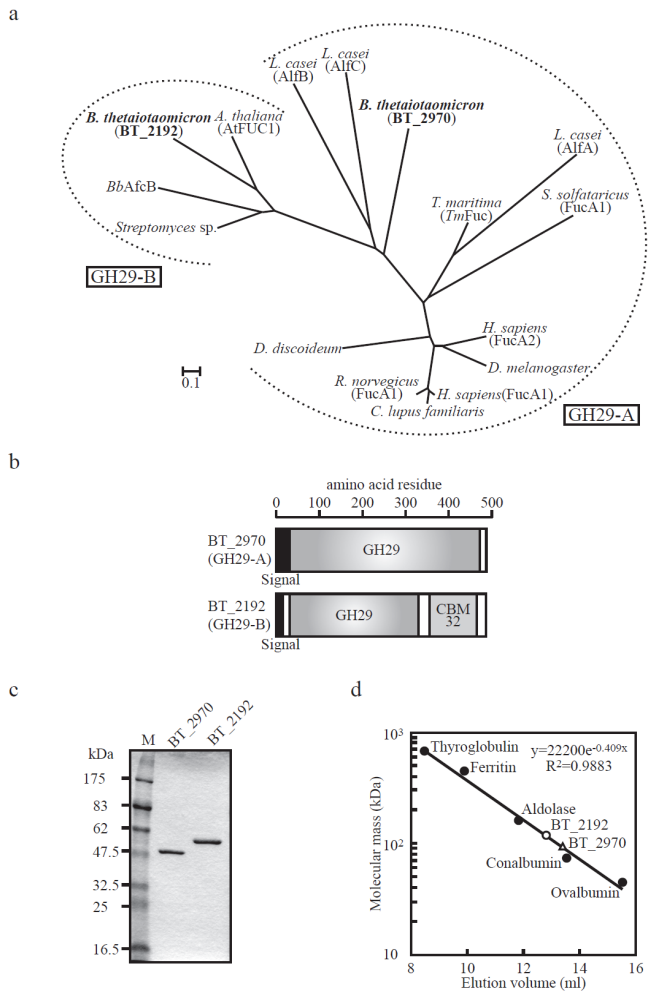

Figure 1. Subfamily classification of GH29 based on substrate specificity and phylogenetic analysis. (a) The tree was constructed using the ClustalW program with a neighbor-joining method (http://clustalw.ddbj.nig.ac.jp/top-j.html). (b) The domain organization of BT_2970 and BT_2192 was examined by the Pfam database (15). GH29, glycoside hydrolase family 29 domain; CBM32, carbohydrate-binding module 32 domain. (c) Results of the SDS-polyacrylamide gel electrophoresis of the purified recombinant proteins. (d) Gel filtration analysis using Superdex 200 10/300 GE column. The markers (closed circles) used were: thyroglobulin (669 kDa), ferritin (440 kDa), aldolase (158 kDa), conalbumin (75 kDa) and ovalbumin (43 kDa). The elution volumes of BT_2970 and BT_2192 are indicated by an open triangle and an open circle, respectively.

The domain organizations of the two enzymes are shown in Fig. 1b. Both proteins possess the GH29 catalytic domains, which are almost identical in their size but share only 32% identity in amino acid sequence (15). The GH29 domain of BT_2192 is followed by a carbohydrate-binding module 32. Both enzymes are predicted to be secretory proteins as they possess signal peptides (14). The author expressed these proteins with C-terminal histidine-tags in *Escherichia coli* BL21 Δ*lacZ* (DE3) (7,16). The signal sequences were removed in both cases. Expression and purification of the proteins were completed using a commercially-available kit according to the manufacturer's instructions (Qiagen, MD, USA). The purified proteins gave single bands on SDS-polyacrylamide gel electrophoresis (Fig. 1c). Gel filtration analysis indicated that both enzymes form dimers in solution (Fig. 1d).

Table 1 Substrate specificities of BT_2970 and BT_2192

Substrate[a]	Structure	Relative activity (%)[b]	
		BT_2970 (GH29-A)	BT_2192 (GH29-B)
*p*NP-Fuc		100	0.025
F1-3Gn	Fucα1-3GlcNAc	5.3	0
F1-4Gn	Fucα1-4GlcNAc	0.81	0
F1-6Gn	Fucα1-6GlcNAc	0	0
2′-FL	Fucα1-2Galβ1-4Glc	0	0.067
3-FL	Galβ1-4(Fucα1-3)Glc	0	100
Le^a	Galβ1-3(Fucα1-4)GlcNAc	0	120
Le^b	Fucα1-2Galβ1-3(Fucα1-4)GlcNAc	0	43
Le^x	Galβ1-4(Fucα1-3)GlcNAc	0	150
Le^y	Fucα1-2Galβ1-4(Fucα1-3)GlcNAc	0	57

Assays were performed in 100 mM MES buffer (pH 6.0) at 37°C. Activities were measured as previously described (3,7).
[a] The substrate was used at a concentration of 1.0 mM.
[b] The activities on *p*NP-Fuc and 3-FL were taken as 100% for BT_2970 and BT_2192, respectively.

The physicochemical properties of BT_2970 and BT_2192 were determined by using *p*NP-Fuc and 3-fucosyllactose (3-FL), respectively, as substrates. Both enzymes were most active at pH 6.0 in MES buffer and were stable in the pH range of 4.0 to 9.0. The optimal temperature for activity of BT_2970 and BT_2192 were 37°C and 50°C, respectively. Both enzymes were stable below 37°C for 30 min. The divalent cations, Co^{2+}, Ca^{2+}, Mg^{2+} and Mn^{2+} (1 mM), and the chelating agent, EDTA, did not affect enzyme activity. The k_{cat} and K_m values of BT_2970 for *p*NP-Fuc were calculated to be 1.3 s^{-1} and 1.5 mM, respectively. The kinetic parameters of BT_2192 could not be calculated because no saturation curve was obtained in the concentrations between 0.6-20 mM 3-FL. The specific activity of BT_2970 on *p*NP-Fuc (1 mM) was 0.60 U/mg, while that of BT_2192 on 3-FL (1 mM) was 0.79 U/mg. The observed specific activities were relatively lower than for the other glycosidases (4). However, the k_{cat} values of the GH29 members were generally between 1−10 /s (6,8,11).

Next, the author examined the substrate specificities using various substrates at a fixed concentration (1 mM) (Table 1). BT_2970 hydrolyzed F1-3Gn and F1-4Gn with considerably lower activities as compared to *p*NP-Fuc (5.3 and 0.81%, respectively). No activity was detected for the other substrates tested. In contrast, BT_2192 effectively hydrolyzed 3-FL and Lewis antigens, but was essentially inactive on *p*NP-Fuc. These results were consistent with the predicted substrate specificities based on phylogenetic clustering (Fig. 1a). Interestingly, BT_2192 was inert on F1-3/4Gn disaccharides although the linkages to be hydrolyzed are identical to those present in the Lewis a/x trisaccharides. *Bb*AfcB (GH29-B) also effectively hydrolyzed the Lewis trisaccharides, but did not act on F1-3/4Gn disaccharides (described in CHAPTER 3). This indicated that BT_2192 requires the presence of a branched Gal residue to exert its activity and suggested that the enzyme has a subsite to accommodate the Gal residue.

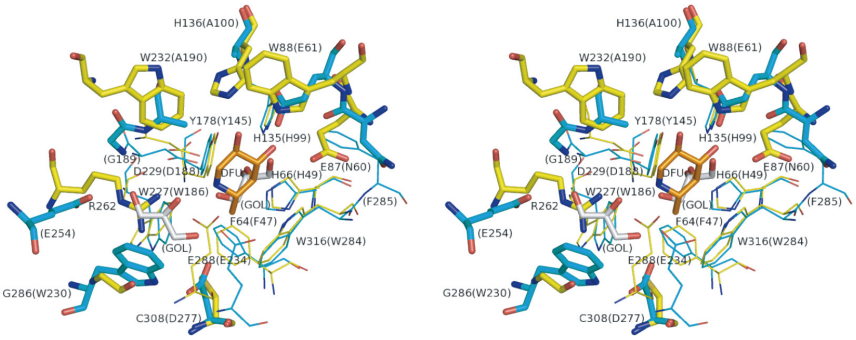

Figure 2. Comparison of the active site structures of BT_2970 (yellow, deoxyfuconojirimicin (DFU)-complexed) and BT_2192 (cyan) (stereoview). DFU and glycerol (GOL) are shown in orange and white, respectively. The numbers of the residues are shown (parenthesized for BT_2192).

The author then compared the active-site structures of BT_2970 D229N in complex with *p*NP-Fuc (PDB code 2WVU) (12) and BT_2192 (PDB code 3EYP, no ligand) (Fig. 2). Of the residues that are hydrogen-bonded with the Fuc moiety in BT_2970, E87, W88 and H136 are replaced with Asn (N60), Glu (E61) and Ala (A100), respectively, in BT_2192. Consequently, BT_2192 should lack two hydrogen bonds with the Fuc. In addition, R262 of BT_2970 forms a hydrogen bond with the nitro group of *p*NP, which could facilitate the departure of the leaving group. BT_2192 does not possess the corresponding Arg residue. The two additional hydrogen bonds with the Fuc and one additional hydrogen bond with *p*NP could therefore explain why BT_2970 shows considerably higher activity towards *p*NP-Fuc than BT_2192. However, to compensate for the missing Arg residue, BT_2192 successfully creates enough space to accommodate one sugar ring, next to the Fuc-binding site (Fig. 2). The pocket is mainly formed by the side chains of W230, E254 and D277, the residues of which are frequently employed to create sugar binding pockets, and by the main chain of G189-A190. The BT_2192 crystal contains a glycerol molecule (GOL) at the site. It is therefore likely that, in BT_2192, a branched Gal residue of 3-FL and Lewis antigens is bound to this pocket. The binding could be critical to fix the substrates at the active site as BT_2192 does not act on F1-3/4Gn. In BT_2970, the side chain of R262 should cause a steric hindrance with the branched Gal, which would explain the ability of the enzyme to act on F1-3/4Gn disaccharides but not on Lewis a/x trisaccharides. R262 of BT_2970 (GH29-A) and G189, A190, W230 and D277 of BT_2192 (GH29-B) are highly conserved in the respective subfamilies. These findings suggest that these residues are the key determinants that confer distinct substrate specificities to GH29-A and GH29-B members, although the author does not

have a clear explanation as to why the GH29-A enzymes show varied linkage preferences among its members (11).

This chapter affirms the validity of the two subfamily classification of GH29 and identifies candidate residues responsible for differentiating between subfamilies. Considering that BT_2192 as well as *Bb*AfcB are secretory enzymes produced by gut microbes, GH29-B might have evolved to efficiently act on human-related glycans such as Lewis antigens present in intestines. In this context, it should be mentioned that β-galactosidases are unable to liberate Gal from Lewis antigens without prior digestion by GH29-B enzymes (7,16,17).

REFERENCES

1. Becker, D.J. and Lowe, J.B. (2003) Fucose: biosynthesis and biological function in mammals. *Glycobiology* **13**, 41R-53R
2. Cantarel, B.L., Coutinho, P.M., Rancurel, C., Bernard, T., Lombard, V., and Henrissat, B. (2009) The Carbohydrate-Active EnZymes database (CAZy): an expert resource for Glycogenomics. *Nucleic Acids Res*. **37**, D233-D238
3. Katayama, T., Sakuma, A., Kimura, T., Makimura, Y., Hiratake, J., Sakata, K., Yamanoi, T., Kumagai, H., and Yamamoto, K. (2004) Molecular cloning and characterization of *Bifidobacterium bifidum* 1,2-α-L-fucosidase (AfcA), a novel inverting glycosidase (glycoside hydrolase family 95). *J Bacteriol*. **186,** 4885-4893
4. Nagae, M., Tsuchiya, A., Katayama, T., Yamamoto, K., Wakatsuki, S., and Kato, R. (2007) Structural basis of the catalytic reaction mechanism of novel 1,2-α-L-fucosidase from *Bifidobacterium bifidum*. *J Biol Chem*. **282**, 18497-18509
5. McCarter, J.D. and Withers, S.G. (1994) Mechanisms of enzymatic glycoside hydrolysis. *Curr Opin Struct Biol*. **4,** 885-892
6. Sulzenbacher, G., Bignon, C., Nishimura, T., Tarling, C.A., Withers, S.G., Henrissat, B., and Bourne, Y. (2004) Crystal structure of *Thermotoga maritime* α-L-fucosidase. Insights into the catalytic mechanism and the molecular basis for fucosidosis. *J Biol Chem*. **279**, 13119-13128
7. Ashida, H, Miyake, A., Kiyohara, M., Wada, J., Yoshida, E., Kumagai, H., Katayama, T., and Yamamoto, K. (2009) Two distinct α-L-fucosidases from *Bifidobacterium bifidum* are essential for the utilization of fucosylated milk oligosaccharides and glycoconjugates.

Glycobiology **19**, 1010-1017

8. Liu, S.W., Chen, C.S., Chang, S.S., Mong, K.K., Lin, C.H., Chang, C.W., Tang, C.Y., and Li, Y.K. (2009) Identification of essential residues of human α-L-fucosidase and tests of its mechanism. *Biochemistry* **48**, 110-120
9. Sano, M., Hayakawa, K., and Kato, I. (1992) Purification and characterization of α-L-fucosidase from *Streptomyces* species. *J Biol Chem*. **267**, 1522-1527
10. Zeleny, R., Leonard, R., Dorfner, G., Dalik, T., Kolarich, D., and Altmann, F. (2006) Molecular cloning and characterization of a plant α1,3/4-fucosidase based on sequence tags from almond fucosidase I. *Phytochemistry* **67**, 641-648
11. Rodríguez-Díaz, J., Monedero, V., and Yebra, M.J. (2011) Utilization of natural fucosylated oligosaccharides by three novel α-L-fucosidases from a probiotic Lactobacillus casei strain. *Appl Environ Microbiol*. **77**, 703-705
12. Lammerts van Bueren, A., Ardèvol, A., Fayers-Kerr, J., Luo, B., Zhang, Y., Sollogoub, M., Blériot, Y., Rovira, C., and Davies, G.J. (2010) Analysis of the reaction coordinate of alpha-L-fucosidases: a combined structural and quantum mechanical approach. *J Am Chem Soc*. **132**, 1804-1806
13. Petersen, T.N., Brunak, S., von Heijne, G., and Nielsen, H. (2011) SignalP 4.0: discriminating signal peptides from transmembrane regions. *Nat Methods*. **29**, 785-786
14. Cohenford, M.A., Abraham, A., Abraham, J., and Dain, J.A. (1989) Colorimetric assay for free and bound L-fucose. *Anal Biochem*. **177**, 172-177
15. Finn, R.D., Mistry, J., Tate, J., Coggill, P., Heger, A., Pollington, J.E., Gavin, O.L., Gunesekaran, P., Ceric, G., Forslund, K., Holm, L., Sonnhammer, E.L., Eddy, S.R., and Bateman, A. (2010) The Pfam protein families database. *Nucleic Acids Res.* **38**, D211-D222
16. Yoshida, E., Sakurama, H., Kiyohara, M., Nakajima, M., Kitaoka, M., Ashida, H., Hirose, J., Katayama, T., Yamamoto, K., and Kumagai, H. (2012) *Bifidobacterium longum* subsp. *infantis* uses two different β-galactosidases for selectively degrading type-1 and type-2 human milk oligosaccharides. *Glycobiology* **22,** 361-368
17. Asakuma, S., Hatakeyama, E., Urashima, T., Yoshida, E., Katayama, T., Yamamoto, K., Kumagai, H., Ashida, H., Hirose, J., and Kitaoka, M. (2011) Physiology of consumption of human milk oligosaccharides by infant gut-associated bifidobacteria. *J Biol Chem*. **286**, 34583-34592

CHAPTER 3

Fucosynthase mutants derived from 1,3-1,4-α-L-fucosidase

α-L-Fucosyl residues attached at the non-reducing ends of glycoconjugates constitute histo-blood group antigens Lewis (Le) and ABO. The blood group antigens are involved in various important biological processes, and especially, Lewis a and x epitopes [Galβ1-3/4(Fucα1-4/3)GlcNAc-, $Le^{a/x}$] play fundamental roles in mammalian cell-to-cell communications at the developmental stages and at the sites of inflammations (1-5). In mouse embryogenesis, the stage-specific synthesis of Le^x antigen has been observed and this transient expression is thought to be involved in the embryo compaction (2). Regulated expression of Le^x epitope is also found in the brain and postulated to be important for the development of the central nervous system. In addition, recent studies show that Le antigens modulate host-pathogen interactions (6,7). *Helicobacter pylori* shows phase-variable expression of Le antigens in its lipopolysaccharides (LPS), and the antigens act as adhesion pedestals between the organism and the host epithelial cells. The bacterium also utilizes the Le^x epitope of LPS to suppress immune responses through the dendritic cell-specific intercellular adhesion molecule-3-grabbing non-integrin (8). The $Le^{a/x}$ antigen-containing oligosaccharides are therefore indispensable tools for functional glycomics studies and for pharmaceutical applications.

The synthesis of oligosaccharides with defined structures requires the precise control of regio- and stereo specificity at the glycosidic bond. In this context, enzymatic synthesis has several advantages over chemical synthesis, because it enables the perfect control of anomeric configurations and provides relatively high regiospecificity without the requirement of laborious protection/deprotection steps. Enzymatic synthesis of oligosaccharides usually employs glycosyltransferases and glycosidases (9,10). Glycosyltransferases generally have strict regio- and acceptor specificity, and are therefore good catalysts for defined oligosaccharide syntheses. Efficient preparations of Le^x- and H-antigen oligosaccharides using α-1,3- and α-1,2-fucosyltransferases from *Helicobacter pylori* have been reported (11-13). However, as described in the literature (11), the use of glycosyltransferases requires an expensive sugar nucleotide or a complex system for nucleotide recycling. Moreover, the expression of glycosyltransferases is generally difficult to handle. In contrast, glycosidase-catalyzed transglycosylation has been efficiently used as a method for oligosaccharide

synthesis, because of the simplicity and versatility of the reactions (9,10). Notably, a new class of enzymes, glycosynthases, has been developed in the last decade (14-17). Glycosynthase is a mutant glycosidase that is devoid of hydrolysis, but is able to perform the transglycosylation reaction when a suitably activated donor (generally, glycosyl fluoride, and in a few cases, glycosyl azide) (18,19) is used as a substrate. Use of glycosidases and their mutants has thus become a promising option for the synthesis of oligosaccharides (10,20,21). However, as the regioselectivity and acceptor specificity of glycosidase-catalyzed transglycosylation are usually not that high, the reaction products are frequently obtained as mixtures of several oligosaccharides with varied linkages and sometimes varied lengths. These drawbacks become apparent in the synthesis of fucosyl oligosaccharides using α-L-fucosidases (22-25) and α-L-fucosynthases (18) (details are described later) that belong to the glycoside hydrolase family 29 (GH29) (http://www.cazy.org) (26). Such a result prevents the use of these enzymes in the synthesis of oligosaccharides with defined structures. Thus, in view of the requirement of strict glycosidic bond formation, it is crucial to find glycosidases that provide strict specificity, both in linkage and in leaving groups that become acceptors for transglycosylation.

In previous studies, Katayama *et al*. have isolated two α-L-fucosidases from *Bifidobacterium bifidum* and revealed that the enzymes have strict substrate specificities. One is 1,2-α-L-fucosidase (*Bb*AfcA) that belongs to GH95 (27,28), and the other is 1,3-1,4-α-L-fucosidase (*Bb*AfcB) belonging to GH29 (29). The high substrate specificities of the two α-L-fucosidases prompted the author to examine the possible use of these enzymes in the defined synthesis of fucosyl oligosaccharides. In a recent paper, Wada *et al*. introduced the glycosynthase technology into *Bb*AfcA (an inverting enzyme) and succeeded in generating 1,2-α-L-fucosynthase, which synthesized 2'-fucosyllactose (Fucα1-2Galβ1-4Glc, 2'-FL) exclusively when β-L-fucopyranosyl fluoride (FucF) and lactose (Lac) were used as a donor and an acceptor, respectively (30). No by-products were formed in that reaction.

In this chapter, to expand the possibility of glycosynthase technology, the author converted *Bb*AfcB to 1,3-1,4-α-L-fucosynthase and characterized the enzyme. The results indicated that the synthase should serve as a valuable tool to specifically introduce Le^a and Le^x epitopes into the type-1 (Galβ1-3GlcNAc, lacto-*N*-biose I, LNB) and type-2 (Galβ1-4GlcNAc, *N*-acetyllactosamine, LacNAc) chains, respectively. Moreover, the crystal structures of AfcB from *B. longum* subsp. *infantis* (*Bi*AfcB, Blon_2336), a paralogue of

*Bb*AfcB, in complex with an inhibitor deoxyfuconojirimycin (DFJ) and with lacto-*N*-fucopentaose II [Galβ1-3(Fucα1-4)GlcNAcβ1-3Galβ1-4Glc, LNFP II] (comprising the Le^a antigen), were determined. The structures revealed how the enzyme exerts its strict regio- and acceptor-specificity through an induced-fit motion of catalytically important residues.

EXPERIMENTAL PROCEDURES

Chemicals−2'-FL, LacNAc, Fucα1-6GlcNAc disaccharide, Le^a and Le^x trisaccharides were purchased from Dextra Laboratories (Reading, UK). Lacto-*N*-tetraose (Galβ1-3GlcNAcβ1-3Galβ1-4Glc, LNT) and lactodifucotetraose [Fucα1-2Galβ1-4(Fucα1-3)Glc, LDFT] were from Isosep (Tullinge, Sweden). LNFP II and Fucα1-3/4GlcNAc disaccharides were from Carbosynth (Compton, UK). *N,N'*-Diacetylchitobiose, DFJ and *p*-nitrophenyl-α-L-fucopyranoside (*p*NP-Fuc) were from Seikagaku Kogyo (Tokyo, Japan), Toronto Research Chemicals (North York, ON, Canada) and Sigma (St. Louis, MO, USA), respectively. LNB (31), galacto-*N*-biose (Galβ1-3GalNAc, GNB) (32), 2-acetoamide-2-deoxy-4-*O*-(β-glucosyl)-glucose (Glcβ1-4GlcNAc, GlcGlcNAc) (33) and FucF (30) were synthesized as described previously. 3-Fucosyllactose [Galβ1-4(Fucα1-3)Glc, 3-FL] was purchased from Dextra Laboratories, and further purified using Bio-Gel P2 gel filtration chromatography (Bio-Rad, CA, USA). L-Fucose dehydrogenase was purchased from Kikkoman (Noda, Japan). Other reagents of analytical grade were obtained from commercial sources.

Construction of* Bb*AfcB mutants−The mutants of *Bb*AfcB (D703A, D703C, D703G, D703S, W742A, E746A, D763A, D766A, D778A and D807A) were constructed using the QuikChange site-directed mutagenesis method (Stratagene, CA, USA) with the plasmid pET23b-*afcB* as the template (29). The following primers and their complementary primers were used: 5'-gaggtctggttcgcgggtgcccaaggc-3' (D703A), 5'-aggtctggttctgcggtgcccaaggc-3' (D703C), 5'- gaggtctggttcggcggtgcccaaggc-3' (D703G), 5'-gaggtctggttcagcggtgcccaaggc-3' (D703S), 5'-acgatgcccgagcggtgggcaacg-3' (W742A), 5'-ggtgggcaacgcggacggctggg-3' (E746A), 5'-ggcatacaacgccggcgtggaca-3' (D763A), 5'-cgacggcgtggccaaggtgtcgc-3' (D766A), 5'-gatggcccccgccggtaagcttg-3' (D778A), and 5'-ggccgaagtcgccgccaagaacc-3' (D807A). The entire sequence used for later manipulation was sequenced to check that no base change other than those designed had occurred. The resulting plasmids were used to transform *Escherichia*

coli BL21 Δ*lacZ* (DE3) (29).

Expression and purification of* Bb*AfcB variants−The recombinant strains were cultured in lysogeny broth media containing 100 μg/ml ampicillin at 18°C until the optical density at 600 nm reached 0.5. Isopropyl-β-D-1-thiogalactopyranoside (IPTG) was then added to a final concentration of 0.1 mM to induce protein expression. Following further incubation for 15 h, the cells were harvested and disrupted by sonication. After centrifugation, the supernatant was applied to a Ni-NTA agarose column (Qiagen, Hilden, Germany), and the protein was eluted according to the manufacturer's instructions. The fractions were combined, concentrated using an Amicon Ultra 50 K (Millipore, MA, USA) and loaded onto a Superdex 200 10/300 GL gel filtration column (GE Healthcare Bio-Sciences, Uppsala, Sweden). The elution was carried out using a 20 mM tris(hydroxymethyl)aminomethane-HCl buffer (Tris-HCl) (pH 8.0) containing 150 mM NaCl. The purified protein was extensively dialyzed against a 50 mM 4-(2-hydroxyethyl)-1-piperazineethanesulfonic acid (HEPES) buffer (pH 7.0). Protein concentrations were determined using a BCA protein assay kit (Thermo Fisher Scientific, IL, USA) with bovine serum albumin as a standard.

Enzyme assay−The hydrolytic activities of *Bb*AfcB variants were determined using 3-FL and *p*NP-Fuc as the substrates. The reaction mixture contained 100 mM 3-(*N*-morpholino)propanesulfonic acid (MOPS) buffer (pH 6.5), 1 mM substrate and the enzyme (for 3-FL hydrolysis: 14 nM of the wild-type (WT) and D766A, 12 μM of D703 mutants, 17 μM of W742A and E746A, 44 nM of D763A and D778A and 890 nM of D807A; for *p*NP-Fuc hydrolysis: 17 μM of WT and the mutants). The reaction was carried out for an appropriate time, in which the linearity of the reaction rate was observed, at 30°C, *i.e.* in the 3-FL hydrolysis: ~15 min for WT, W742A, D807A, D763A, D766A and D778A mutants, ~880 min for D703 mutants and ~240 min for E746A mutant; in the *p*NP-Fuc hydrolysis: ~150 min for WT and all mutants except for W742A, and ~500 min for W742A. The reaction was terminated by heating (for 3-FL hydrolysis) or by the addition of 1 M sodium carbonate (for *p*NP-Fuc hydrolysis). The amount of released Fuc was determined using a fucose dehydrogenase-coupled method (34). The amount of the liberated *p*NP was determined by measuring the absorbance at 405 nm. One unit of enzyme activity was determined as the amount of enzyme required to produce 1 μmol of Fuc or *p*NP under the specified conditions.

The glycosynthase activities of *Bb*AfcB mutants were examined by incubating the reaction mixtures (50 μl) containing 100 mM MOPS buffer (pH 7.0), 20 mM FucF (donor), 100 mM LNB/LacNAc (acceptor) and the enzymes (17 μM). The reaction was performed for 10 min at 30°C and terminated by adding 5 μl of 30% trichloroacetic acid. The reaction products were analyzed by high-performance liquid chromatography (HPLC) equipped with a sugar-D column (4.6 × 250 mm, Nacalai Tesque, Kyoto, Japan). The elution was performed under a constant flow (1.0 mL/min) of 75 or 78% acetonitrile at 40°C and monitored at 214 nm or using a charged aerosol detector (CAD) (Corona CAD, Esa, USA). The amounts of the reaction products were estimated by a standard curve created using known concentrations of Le^a and Le^x trisaccharides.

The optimal pH for the glycosynthase reaction was determined using the *Bb*AfcB D703S mutant. The buffers (100 mM) used were: citrate-NaOH (pH 4.0–5.0), 2-(*N*-morpholino)ethanesulfonic acid (MES) (pH 5.0–6.5) and MOPS (pH 6.5–8.0). The acceptor specificity of the *Bb*AfcB D703S mutant was examined using 13 different substrates. The reaction was carried out in 100 mM MES buffer (pH 5.0) containing 40 mM FucF and 100 mM of each acceptor for 40 min at 30°C in the presence and absence of 17 μM D703S. The reaction products were analyzed by HPLC-CAD.

Synthesis, purification and structural analysis of the reaction products−For Le^a synthesis, the *Bb*AfcB D703S mutant (17 μM) was incubated in the reaction mixture (300 μl) consisting of 100 mM MES buffer (pH 5.0), 40 mM FucF (donor) and 200 mM LNB (acceptor) at 30°C for 40 min. Le^x trisaccharide and LNFP II were synthesized in a similar manner, except that 100 mM LacNAc and LNT were used as the acceptors, respectively. The reaction products were deionized with Amberlite MB-3, lyophilized and purified using an HPLC equipped with a sugar-D column. The elution was performed as described above. Peak fractions were collected, lyophilized and further purified by a TSKgel ODS-80TS column (4.6 × 250 mm, Tosoh, Japan) to remove the remaining acceptors (LNB/LacNAc/LNT). The elution was carried out using water at a flow rate of 0.5 ml/min and monitored by a refractive index detector (RID-10A, Shimadzu, Kyoto, Japan). ^{1}H- and ^{13}C Nuclear magnetic resonance (NMR) spectra were recorded on a Bruker Avance 500 spectrometer. Electrospray ionization-mass spectrometry (ESI-MS) was carried out in a positive mode using a Bruker APEX II 70e Fourier transformed ion-cyclotron resonance mass spectrometer.

X-ray crystallography of* Bi*AfcB−The gene (locus tag Blon_2336) was amplified by PCR using the genomic DNA of *B. longum* subsp. *infantis* ATCC15697 and a primer pair (5'-gcatatgaacaatcctgcagatgc-3' and 5'-ctcgagtcagatgcgcacggcagcc-3'). The amplified fragment was inserted into the *Nde*I and *Xho*I sites of pET-30b to generate a non-tagged protein (Novagen, NJ, USA). The resulting plasmid pET30b-*BiafcB* was used to transform *E. coli* BL21 Δ*lacZ* (DE3). The transformants were cultured in lysogeny broth media containing 30 μg/ml kanamycin at 18°C to an optical density at 600 nm of 0.5. IPTG was added to a final concentration of 0.1 mM to induce protein expression. Following further incubation for 20 h, the harvested cells were disrupted by sonication. The protein was purified using MonoQ 5/50 GL column chromatography (GE Healthcare Bio-Sciences) followed by a Superdex 200 10/300 GL gel-filtration chromatography step. The *Bi*AfcB D172A/E217A double mutant was constructed using the QuikChange site-directed mutagenesis method with the plasmid pET30b-*BiafcB* as the template. The following primers and their complementary primers were used: 5'-ccgtctggcttgctggcgccaatgg-3' (D172A); 5'-tgggccgggaacgcagccgggcatgtg-3' (E217A). Purification of the mutant protein was performed using a similar procedure as described for the WT protein. The proteins were crystallized using the hanging-drop vapour-diffusion method at 20°C. The crystal of *Bi*AfcB complexed with DFJ (WT-DFJ-EG) was obtained by mixing 1 μl of a protein solution [10 mg/ml in 10 mM HEPES buffer (pH 7.0) containing 40 mM DFJ] with 1 μl of a reservoir solution consisting of 0.1 M citrate buffer (pH 4.0) and 20% (w/v) polyethylene glycol (PEG) 6000. The crystal of *Bi*AfcB D172A/E217A complexed with LNFP II (D172A/E217A-LNFP II) was obtained by mixing 1 μl of a protein solution [10 mg/ml in 10 mM HEPES buffer (pH 7.0) containing 100 mM LNFP II] with 1 μl of a reservoir solution consisting of 0.1 M sodium citrate buffer (pH 5.5) and 20% PEG 3000. After cryoprotection with 20% ethylene glycol, the crystals were flash-cooled in a nitrogen stream at 100 K. Diffraction data were collected using beamline NW12A at the Photon Factory-Advanced Ring, KEK, Tsukuba (λ = 1.0 Å). Diffraction images were processed using HKL2000 (35). Molecular replacement was performed with MOLREP (36), using the ligand-free *Bi*AfcB structure (PDB code 3MO4) (37) as a search model. Model rebuilding and refinement were performed using Coot (38) and Refmac5 (39). Figures were prepared using PyMol (DeLano Scientific).

Automated docking–Automated docking analysis was performed as described previously (40). Ligand model preparation and automated docking were performed using the Sweet2 server (41) and AUTODOCK 4.0 (42), respectively. Rotatable ligand bonds (8 in Le^x trisaccharide) were defined using the AutoDockTools interface. Water molecules in the D172A/E217A-LNFP II complex structure were removed. After adding polar hydrogens, Gasteiger charges were calculated for the ligand and protein. Grid maps were prepared with 40 × 40 × 40 points covering the substrate-binding pocket with a point spacing of 0.375 Å. For the Lamarckian genetic algorithm search, the size of the initial random population was 150 individuals, the maximal number of energy evaluations was 2.5×10^6, the maximal number of generations was 27,000, the number of top individuals that survived into the next generation was 1, the rate of mutation was 0.02, the rate of crossover was 0.80 and the average of the worst energy was calculated over a window of 10 generations. After 256 docking runs, all structures generated for a single compound were assigned to clusters based on a tolerance of 2.0 Å for all atom root mean square deviations from the lowest energy structure.

RESULTS

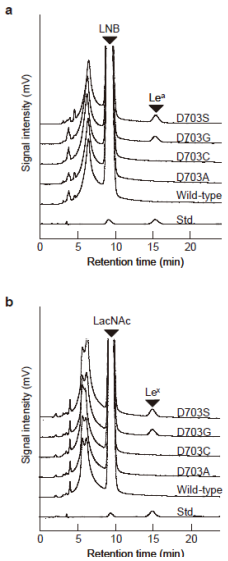

Supplemental Figure S1. Syntheses of Le^a (a) and Le^x (b) trisaccharides by the *Bb*AfcB D703 mutants. The WT enzyme and D703 mutants (17 µM) were incubated in the reaction mixtures (50 µl) consisting of 100 mM MOPS (pH 7.0), 20 mM FucF (donor) and 100 mM LNB (a) or LacNAc (b) (acceptor) for 10 min at 30°C. The reaction products were analyzed by HPLC-UV detection. Standard sugars (Std.) are: lacto-*N*-biose I (LNB), *N*-acetyllactosamine (LacNAc), Lewis a (Le^a) and Lewis x (Le^x).

Supplemental Table S1 Hydrolysis of 3-fucosyllactose (3-FL) and *p*NP-Fuc by *Bb*AfcB variants

Enzyme	Specific activity[a] (mU/mg)	
	3-FL	*p*NP-Fuc
WT	5,100	0.18
Nucleophile mutants		
D703A	0.032	n.d.[b]
D703C	0.11	n.d.
D703G	0.30	n.d.
D703S	0.067	n.d.
Acid/base mutant		
E746A	0.74	n.d.
Gal-binding site mutants		
W742A	2.8	0.043
D807A	64	0.080
Disordered loop mutants		
D763A	1,500	0.17
D766A	1,600	0.15
D778A	1,900	0.16

[a] Only the specific activities were determined because the kinetic parameters could not be calculated due to the linear increase of the initial velocity up to 20 mM of the substrate.
[b] not determined.

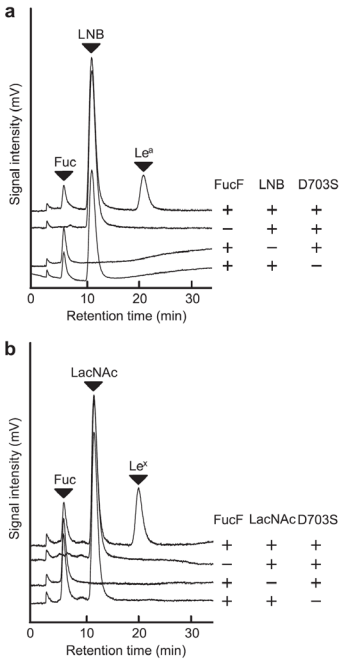

Figure 1. Specific syntheses of Le^a (a) and Le^x (b) trisaccharides by the *Bb*AfcB D703S mutant. (a) The reaction was carried out for 40 min at 30°C in 100 mM MES buffer (pH 5.0) containing 40 mM FucF (donor), 200 mM LNB (acceptor) and 17 μM of the *Bb*AfcB D703S mutant. For the control experiments, the substrate or enzyme was omitted from the reaction. (b) For the synthesis of Le^x, 100 mM LacNAc was used as the acceptor. The reaction products were analyzed by HPLC-CAD. The peaks of L-fucose (Fuc), lacto-*N*-biose I (LNB), *N*-acetyllactosamine (LacNAc), Lewis a (Le^a) and Lewis x (Le^x) are shown. Note that FucF is decomposed when terminating the reaction by trichloroacetic acid.

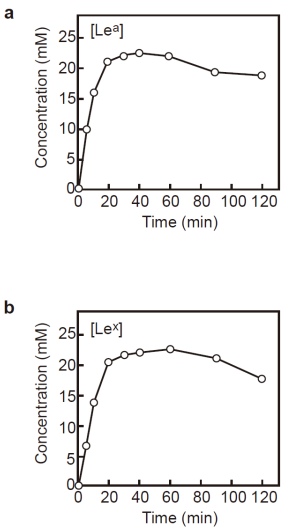

Supplemental Figure S2. Time courses of the Le^a (a) and Le^x (b) syntheses catalyzed by the *Bb*AfcB D703S mutant. (a) The reaction was carried out in 100 mM MES buffer (pH 5.0) containing 40 mM FucF and 200 mM LNB for 120 min at 30°C in the presence of the D703S mutant (17 μM). (b) A similar reaction was carried out for the synthesis of Le^x, except that 100 mM LacNAc was used. Aliquots were taken at the indicated times and analyzed by HPLC-CAD.

Conversion of 1,3-1,4-α-L-fucosidase to 1,3-1,4-α-L-fucosynthase—*Bb*AfcB belongs to GH29 (26). The members of this family hydrolyze α-L-fucosidic bonds *via* a retaining mechanism (43,44). The author replaced Asp703, which is assumed to be a nucleophile by sequence alignment with well-studied GH29 members (discussed later) (45), with alanine, cysteine, glycine and serine, and examined the hydrolytic activity of these mutants. Note that only the specific activities were determined because the kinetic parameters could not be calculated (Supplemental Table S1). The specific activities of D703A, D703C, D703G and D703S were found to decrease by 160,000-, 46,000-, 17,000- and 76,000-fold, respectively, as compared with that of the WT enzyme.

The glycosynthase activities of these mutants were then examined using 20 mM FucF and 100 mM LNB or LacNAc as the donor and the acceptor, respectively. Peaks corresponding to Le^a and Le^x trisaccharides appeared for the D703G/S mutants in the HPLC analysis of the reaction products, whereas no peak was observed for WT and the D703A/C mutants (Supplemental Fig. S1). In either case, D703S gave a slightly larger peak area than D703G, and hence, D703S was further analyzed.

The optimal pH for the synthase reaction was found to be 5.0 (data not shown). The synthase activity was observed only when the

reaction was carried out in the presence of FucF, LNB/LacNAc and the enzyme. No peaks other than the added substrates were detected when the donor (FucF), the acceptor (LNB/LacNAc) or the enzyme was omitted (Figs. 1a and 1b). Strikingly, no by-products other than the decomposed Fuc were detected in the reaction, as revealed by HPLC-CAD. Identification of the reaction products is described later.

The kinetic parameters of the reaction could not be calculated because of the rapid spontaneous decomposition of FucF. The half-life of FucF under the reaction conditions was determined to be 20 min (data not shown). In the time-course of the optimized reaction, the concentrations of the products Le^a and Le^x reached a maximum at ~40 and 60 min, respectively (Supplemental Fig. S2). The reaction efficiency was estimated to be 56% against the added FucF, when the reaction was carried out under the optimized conditions, *i.e.* in the presence of 40 mM FucF (donor), 200 mM LNB or 100 mM LacNAc (acceptor) and 17 μM of the enzyme. None of the *Bb*AfcB D703 variants used β-L-fucopyranosyl azide ($FucN_3$) as a donor (18) and was rescued by sodium azide (data not shown).

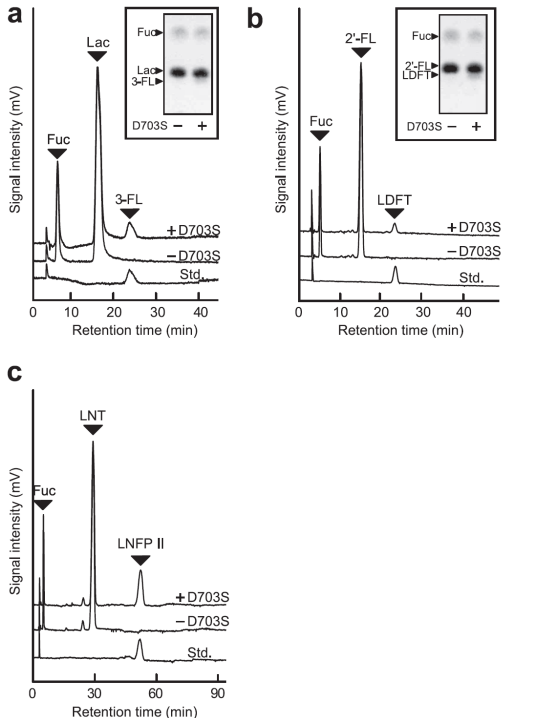

Figure 2. The acceptor specificity of the *Bb*AfcB D703S glycosynthase. The reaction was carried out in 100 mM MES buffer (pH 5.0) containing 40 mM FucF and 100 mM of each acceptor for 40 min at 30°C in the presence and absence of the D703S mutant (17 μM). The acceptors used were: (a) lactose (Lac), (b) 2'-fucosyllactose (2'-FL) and (c) lacto-*N*-tetraose (LNT). The reaction products were analyzed by HPLC-CAD. The peaks of L-fucose (Fuc), acceptor and standard sugars (Std.) are indicated. Inset in (a) and (b) are the results of the thin-layer chromatography (TLC) analysis of the reaction products. See also Table 1 and Supplemental Figs. S3−S7.

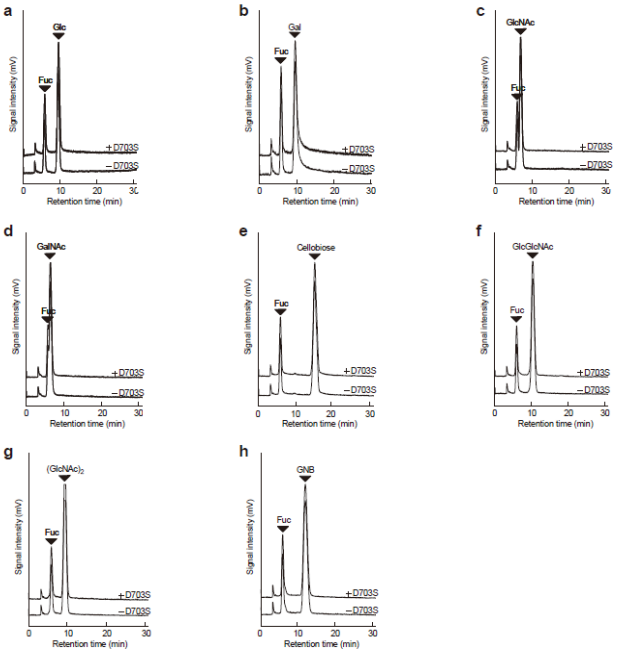

Supplemental Figure S3. The acceptor specificity of the *Bb*AfcB D703S glycosynthase. The reaction was carried out in 100 mM MES buffer (pH 5.0) containing 40 mM FucF and 100 mM of each acceptor for 40 min at 30°C in the presence and absence of the enzyme (17 μM). The reaction products were analyzed by HPLC-CAD. The acceptors used were: Glc (a), Gal (b), GlcNAc (c), GalNAc (d), cellobiose (e), 2-acetoamide-2-deoxy-4-*O*-(β-glucosyl)-glucose (GlcGlcNAc) (f), *N*,*N*'-diacetylchitobiose [$(GlcNAc)_2$] (g) and galacto-*N*-biose (GNB) (h). The peaks of Fuc and acceptor are indicated.

Table 1 Acceptor specificity of 1,3-1,4-α-L-fucosynthase (*Bb*AfcB D703S)

Substrates		Synthesized compounds		
Name	Structure	Name	Structure	Yield[a]
				%
Monosaccharides				
Glucose				0
Galactose				0
N-Acetylglucosamine				0
N-Acetylgalactosamine				0
Disaccharides				
Cellobiose	Glcβ1–4Glc			0
GlcGlcNAc[b]	Glcβ1–4GlcNAc			0
N,N′-Diacetylchitobiose	GlcNAcβ1–4GlcNAc			0
Lac	Galβ1–4Glc	3-FL	Galβ1–4 (Fucα1–3)Glc	13
LNB[b]	Galβ1–3GlcNAc	Le^a trisaccharide	Galβ1–3 (Fucα1–4)GlcNAc	47
LacNAc	Galβ1–4GlcNAc	Le^x trisaccharide	Galβ1–4 (Fucα1–3)GlcNAc	55
Galacto-*N*-biose[b]	Galβ1–3GalNAc			0
Tri- and tetrasaccharides				
2′-FL	Fucα1–2Galβ1–4Glc	Lactodifucotetraose	Fucα1–2Galβ1–4 (Fucα1–3)Glc	5.5
LNT	Galβ1–3GlcNAcβ1–3Galβ1–4Glc	LNFP II	Galβ1–3 (Fucα1–4)GlcNAcβ1–3Galβ1–4Glc	41

The reaction was carried out in 100 mM MES buffer (pH 5.0) containing 40 mM FucF (donor) and 100 mM of each acceptor for 40 min at 30°C in the presence and absence of 17 μM D703S. The reaction products were analyzed by HPLC-CAD (Fig. 2 and Supplemental Fig. S3).

[a]These substrates were prepared as described previously (31-33).

[b]The product yield against the added FucF.

Acceptor specificity−The acceptor specificity of *Bb*AfcB D703S was examined using various mono- and oligosaccharides at a fixed concentration (100 mM) (Table 1, Fig. 2 and Supplemental Fig. S3). In addition to LNB and LacNAc, the enzyme recognized Lac, 2'-FL and LNT as acceptors, and specifically produced 3-FL, LDFT and LNFP II in yields of 13, 5.5 and 41% against the added FucF, respectively. In contrast, the enzyme did not accept monosaccharides (Glc, Gal, GlcNAc and GalNAc), cellobiose, GlcGlcNAc, *N,N*'-diacetylchitobiose or GNB as a substrate.

Regio- and stereo-specificity−The author then analyzed the reaction products eluted from HPLC using ESI-MS and ^{1}H- and ^{13}C NMR spectroscopy. The MS spectra indicated that one fucosyl residue was attached to LNB and LacNAc (calculated for the sodium adduct $[M+Na]^+$ 552.19, observed 552.18, Supplemental Fig. S4). Both of the ^{1}H- and ^{13}C NMR spectra were identical to the spectra of the authentic Le^a and Le^x trisaccharides (Supplemental Figs. S5 and S6). In the case that LNT was used as an acceptor, only LNFP II, but not LNFP V [Galβ1-3GlcNAcβ1-3Galβ1-4(Fucα1-3)Glc] or lacto-*N*-difucohexaose II [Galβ1-3(Fucα1-4)GlcNAcβ1-3Galβ1-4(Fucα1-3)Glc, LNDFH II], was synthesized, as revealed by ^{1}H NMR analysis (Supplemental Fig. S7).

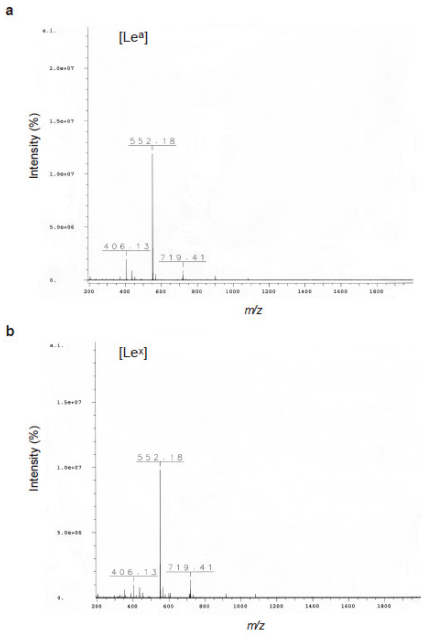

Supplemental Figure S4. ESI-MS analysis of the purified products (Le^a and Le^x). The syntheses of Le^a (a) and Le^x (b) trisaccharides were performed as described in the legend of Figure 1. The products were purified and subjected to ESI-MS analysis (calculated for the sodium adduct $[M+Na]^+$ 552.19, observed 552.18).

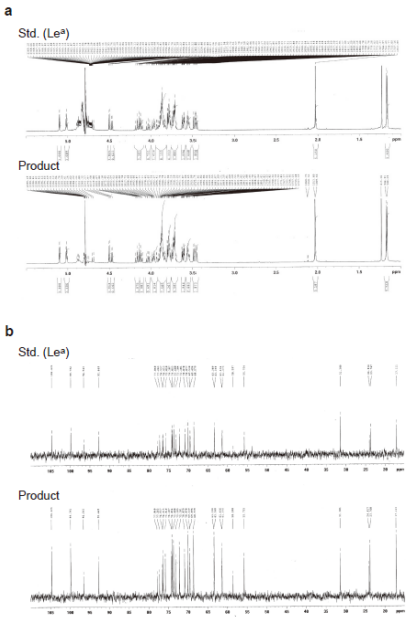

Supplemental Figure S5. NMR analysis of the purified product (Le^a). The ^1H (a) and ^{13}C (b) NMR spectra of the purified product (lower panels) were compared with those of the authentic Le^a (upper panels). The spectra were measured in D_2O using 2-methyl-2-propanol as the internal standard.

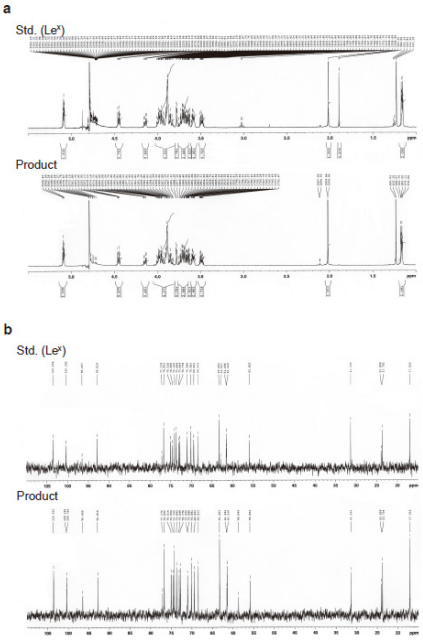

Supplemental Figure S6. NMR analysis of the purified product (Le^x). The ^1H (a) and ^{13}C (b) NMR spectra of the purified product (lower panels) were compared with those of the authentic Le^x (upper panels). The spectra were measured in D_2O using 2-methyl-2-propanol as the internal standard.

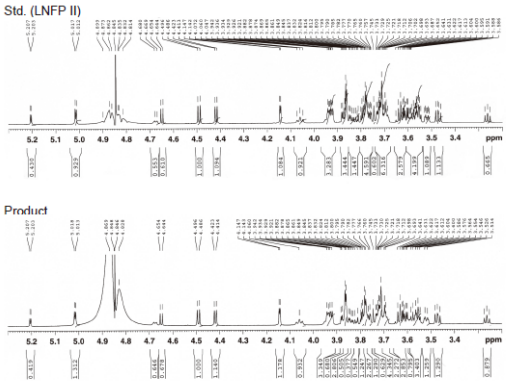

Supplemental Figure S7. ^1H NMR analysis of the purified product (LNFP II). The reaction was carried out in 100 mM MES buffer (pH 5.0) containing 40 mM FucF and 100 mM LNT at 30°C in the presence of 17 µM D703S. The spectra were obatined in D_2O using 2-methyl-2-propanol as the internal standard. Upper panel, authentic LNFP II; lower panel, purified product.

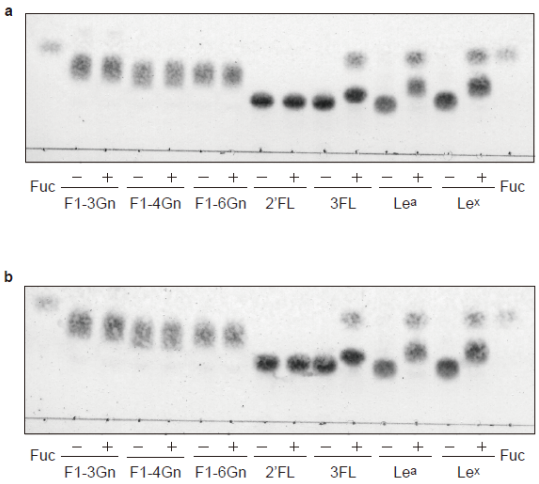

Supplemental Figure S8. Substrate specificities of *Bb*AfcB (a) and *Bi*AfcB (b). The reactions were carried out in 100 mM MOPS buffer (pH 6.5) containing 6 mM substrates at 30°C for 60 min in the presence and absence of the enzyme (*Bb*AfcB; 1.1 μM, *Bi*AfcB; 0.47 μM). The reaction products were analyzed by TLC (Silica Gel 60, Merck) using a solvent system of 1-butanol/acetic acid/water (2:1:1, by volume). The sugars were visualized as described previously (29). The substrates used were: Fucα1-3GlcNAc (F1-3Gn), Fucα1-4GlcNAc (F1-4Gn), Fucα1-6GlcNAc (F1-6Gn), 2'-fucosyllactose (2'-FL), 3-fucosyllactose (3-FL), Lewis a (Le^a) and Lewis x (Le^x).

Table 2 Crystallographic data collection and refinement statistics.

Data set	WT-DFJ-EG	D172A/E217A-LNFP II
Data collection		
Protein Data Bank code	3UES	3UET
Beamline	NW12A	NW12A
Space group	$P2_12_12_1$	$P2_12_12_1$
Unit cell (Å)	a = 64.0, b = 120.6, c = 142.5	a = 82.6, b = 106.0, c = 120.7
Matthews coefficient (Å^3/Da)	2.59	2.49
Solvent content (%)	52.5	50.6
Resolution (Å)	50.00-1.60 (1.66-1.60)	50.00-2.10 (2.14-2.10)
Total reflections	1,029,177	358,658
Unique reflections	146,170	60,403
Completeness (%)	99.9 (100.0)	96.4 (95.4)
Redundancy	7.0 (6.7)	5.9 (5.2)
Mean $I/\sigma(I)$	36.2 (4.1)	16.6 (2.6)
R_{sym} (%)	5.9 (33.5)	10.4 (47.4)
Refinement		
Resolution (Å)	25.91-1.60	32.05-2.10
No. of reflections	138,464	57,112
R-factor/R_{free} (%)	16.0/19.1	17.3/22.3
No. of atoms	8,320	7,683
r.m.s.d. from ideal values		
Bond lengths (Å)	0.029	0.020
Bond angles (°)	2.561	1.987
Ramachandran plot (%)		
Favored	98.0	97.1
Allowed	1.8	2.7
Outlier	0.2	0.2

r.m.s.d., root mean square deviation.
Values in parentheses are for the highest-resolution shell.

Crystallography of 1,3-1,4-α-L-fucosidase—To elucidate the structural basis underlying the unique substrate specificity of this synthase, the author tried to crystallize *Bb*AfcB and its variants; however, no crystal was obtained. *B. longum* subsp. *infantis* possesses the paralogue (locus_tag 2336) of *Bb*AfcB (46), and the author found that this paralogue (referred to as *Bi*AfcB) has an identical substrate specificity with *Bb*AfcB (Supplemental Fig. S8). The Pfam database (http://pfam.sanger ac.uk) suggested that *Bb*AfcB is a multi-modular enzyme whereas *Bi*AfcB possesses a simple domain organization. The structure of a ligand-free form of *Bi*AfcB has been recently determined (PDB code 3MO4) (37). The author obtained the crystals of *Bi*AfcB under the conditions different from those used by Sela *et al*. (37) and determined two complex structures of *Bi*AfcB; WT complexed with DFJ and ethylene glycol (WT-DFJ-EG, 1.6 Å resolution) and an inactive mutant complexed with LNFP II (D172A/E217A-LNFP II, 2.1 Å resolution). Asp172 and Glu217 are a nucleophile and a general acid/base, respectively (described later). Data collection and refinement statistics are shown in Table 2. *Bi*AfcB forms a

dimer in solution (data not shown), and all of the three *Bi*AfcB crystals contain homodimers in the asymmetric unit. Since the two chains (A and B) were almost identical in every case, the author describes the chain A of each structure. The DFJ and ethylene glycol (cryoprotectant) molecules in the WT-DFJ-EG structure, and the Fuc and Gal moieties in the D172A/E217A-LNFP II structure were clearly observed (Supplemental Fig. S9). However, the GlcNAc moiety in LNFP II was partially ambiguous, and the β1,3-linked Lac moiety at the reducing end was not visible. Therefore, the author included the Le^a trisaccharide structure [Galβ1-3(Fucα1-4)GlcNAc] in the model. The author also determined a complex structure of D172A/E217A with the Le^a trisaccharide, and the resulting electron density map was virtually identical to that of the D172A/E217A-LNFP II structure (data not shown).

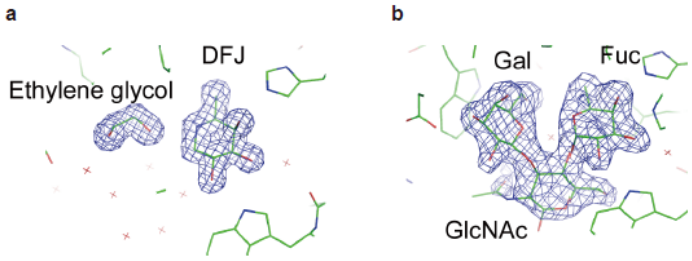

Supplemental Figure S9. |*Fo*| – |*Fc*| omit electron density maps of WT-DFJ-EG (a) and D172A/E217A-LNFP II (b) complex. The maps were contoured at 3 σ.

Figure 3 shows the comparison between the three *Bi*AfcB structures. Interestingly, upon ligand binding, *Bi*AfcB undergoes a large conformational change at two loop regions (173−182 and 215−220) (Fig. 3a), and to the author's surprise, the acid/base catalyst Glu217 is included in this induced-fit motion. In the substrate-free structure, the catalytic residues (Asp172 and Glu217) are not appropriately poised (separated by 20.8 Å) and a tyrosine molecule occupies subsite -1 (Fuc binding site) (Fig. 3b). In the WT-DFJ-EG structure, the loop (215−220) covers the catalytic pocket, so that Glu217 can be suitably poised to act as an acid/base. Consequently, the distance between the Oδ atom of Asp172 and the Oε atom of Glu217 becomes 5.8 Å, which is the typical length observed in retaining glycosidases (43). The Oδ atom of Asp172 is located at a distance of 3.1 Å from the C1 of the DFJ. Alanine replacement of each of these residues resulted in a ~20,000-fold decrease of the hydrolytic activity (data not shown). The DFJ and ethylene glycol molecules are tightly bound by many hydrogen bonds with the protein. In the D172A/E217A-LNFP II structure, Fuc and Gal moieties of LNFP II are extensively recognized through the formation of hydrogen-bonds,

whereas the GlcNAc moiety does not make any notable interactions with the protein. The Fuc makes direct hydrogen bonds with His36, Trp47, His85, His86 and Tyr131, and its C6 methyl group makes hydrophobic interaction with Phe34, Trp170 and Trp290. The Gal moiety forms hydrogen-bonds with the nitrogen atom of the main chain of Gly173 and the side chains of Glu237 and Asp283, and its hydrophobic β-face is stacked by Trp213 (Fig. 3c). The ethylene glycol in the WT-DFJ-EG complex occupies the Gal-binding site and interacts with the catalytic residues (Asp172 and Glu217) and the main chain of Gly173. A water-mediated hydrogen bond is also formed with the side chain of Glu237. However, its two hydroxyl groups do not overlap any of the Gal hydroxyl groups (Fig. 3b,c).

Sequence identity between *Bb*AfcB and *Bi*AfcB is modest (34%) in the alignment (495−998 for *Bb*AfcB and 4−472 for *Bi*AfcB), however the residues involved in substrate binding are essentially conserved to reflect the same substrate specificity (Supplemental Fig. S10). Asp172, Gly173, Trp213, Glu217 and Asp283 of *Bi*AfcB correspond to Asp703, Gly704, Trp742, Glu746 and Asp807 in *Bb*AfcB, respectively. *Bb*AfcB does not have a residue corresponding to Glu237 of *Bi*AfcB located in the disordered loop (236-254), but instead, three acid residues (Asp763, Asp766 and Asp778) are present in the corresponding region. The specific activities of W742A, E746A and D807A of *Bb*AfcB for the hydrolysis of 3-FL decreased by 1,800-, 6,900- and 80-folds, respectively, as compared with that of the WT enzyme (Supplemental Table S1). Alanine substitution for Asp763, Asp766 and Asp778 slightly lowered the enzyme activity.

DISCUSSION

A powerful tool to regiospecifically and stereospecifically install Fuc residues into glycoconjugates was developed. The *Bb*AfcB D703S mutant can introduce Le^a and Le^x epitopes into type-1 and type-2 chains at the non-reducing ends, respectively, without producing by-products. The yields were approximately 60% against the added FucF. The reaction efficiency of this glycosynthase may be slightly lower than those of typical glycosynthases (80% or more), and this could be due to the spontaneous decomposition of FucF during the reaction, as described above. Recently, Cobucci-Ponzano *et al*. demonstrated that some glycosynthases can accept glycosyl azide as a donor molecule (18,19). This finding is particularly valuable for the oligosaccharide synthesis using α-glycosynthase, because β-

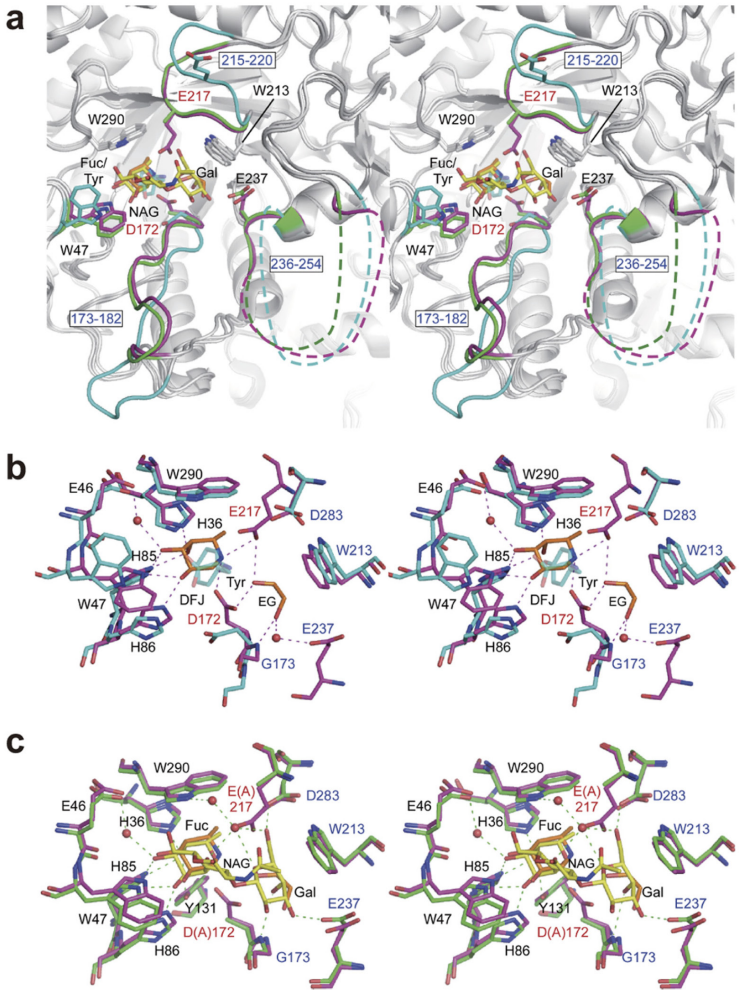

Figure 3. Induced-fit movement of *Bi*AfcB upon substrate binding (stereoviews). (a) Superimposed structures of the ligand-free form (cyan, PDB code 3MO4) (37), WT-DFJ-EG complex (protein in magenta, ligand in orange) and D172A/E217A-LNFP II complex (protein in green, ligand in yellow). The ligand-free structure contains a tyrosine molecule at the Fuc binding site (subsite -1). The side chain of Trp47 and two loop regions (173−182 and 215-220) are significantly displaced. Disordered regions of the 236−254 loop are shown as dotted lines. (b, c) The structure of the substrate-binding site. (b) Ligand-free (cyan) and WT-DFJ-EG complex (protein in magenta, ligand in orange). The tyrosine molecule bound to the ligand-free structure is shown transparently. Water molecules and hydrogen bonds in the WT-DFJ-EG complex are shown. (c) WT-DFJ-EG complex (protein in magenta, ligand in orange) and D172A/E217A-LNFP II complex (protein in green, ligand in yellow). Water molecules and hydrogen bonds in the LNFP II complex are shown. Ethylene glycol and GlcNAc are labeled as EG and NAG, respectively.

glycosyl azide is substantially stable as compared to β-glycosyl fluoride in aqueous solution. The author examined the availability of $FucN_3$ in the synthase reaction of *Bb*AfcB mutants, but no product was obtained in that reaction.

The glycosynthase exclusively recognized LNB, LacNAc and Lac disaccharide structures [Galβ1-3/4GlcNAc(Glc)] at the non-reducing ends, and did not recognize monosaccharides. Indeed, WT *Bb*AfcB did not hydrolyze Fucα1-3/4GlcNAc disaccharides (Supplemental Fig. S8), which had not been examined in the previous study of Ashida *et al*. (29). These results indicate that the presence of the branched Gal residue is critical for the catalytic activities of *Bb*AfcB and the glycosynthase mutant.

Structural basis for the substrate specificity of 1,3-1,4-α-L-fucosynthase–*Bi*AfcB was identified as a paralogue of *Bb*AfcB (46), and it showed the same substrate specificity as *Bb*AfcB (Supplemental Fig. S8). Structural analysis of *Bi*AfcB enabled the author to consider the mechanism of the unique enzymatic activity of 1,3-1,4-α-L-fucosidase (synthase). Binding of Fuc(F) and the Gal moiety of LNB/LacNAc would cause the induced-fit movement at the catalytic site. The ethylene glycol molecule in the WT-DFJ-EG complex may stabilize the induced-fit structure in the crystal. The Gal-binding site could be highly specific to Gal as the axial O4 hydroxyl group is recognized by the main chain (Gly173 in *Bi*AfcB, Gly704 in *Bb*AfcB), which is next to the nucleophile residue and is included in the mobile loop (Fig. 3c and Supplemental Fig. S10). The glycosynthase neither accepted cellobiose nor GlcGlcNAc (Table 1). The Gal O2 hydroxyl group is not recognized by any protein residues and is exposed to the solvent (Fig. 3c), which rationalizes that the enzyme used 2'-FL as the acceptor. The GlcNAc-binding site appears to be rather promiscuous. It is interesting to note that the faces of the GlcNAc sugar rings are inverted between the LNB and LacNAc disaccharides, and consequently, the geometric positions of the respective O4 and O3 hydroxyl groups of the GlcNAc residues become identical (Fig. 4). When automated docking analysis was performed using Le^x trisaccharide, the best docking result was found in the first-ranked cluster containing the majority of the 256 docking run conformations. The number of conformations in this cluster, lowest binding energy and mean binding energy were 81, -6.30 kcal/mol and -3.81 kcal/mol, respectively. In the predicted mode of Le^x-binding, the Fuc, Gal and GlcNAc moieties of the molecule overlap well with those of the Le^a trisaccharide observed in the D172A/E217A-LNFP II crystal, except for the hydroxylmethyl and *N*-acetyl groups of the GlcNAc (Fig. 4b). The O1 atoms of the inverted GlcNAc residues are exposed to the solvent in both cases, and rather protrude from the catalytic pocket. These results explain why this synthase accepts LNB, LacNAc and LNT almost equally (Table 1). The enzyme probably has no structural constraint at the reducing ends of

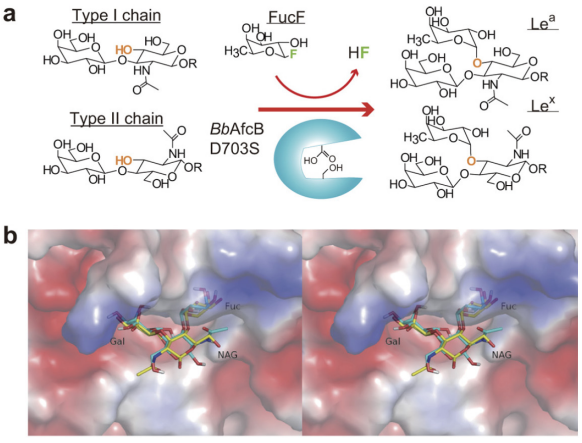

Figure 4. (a) Regio- and stereospecific installation of a Fuc residue into type-1/2 chains, catalyzed by the *Bb*AfcB D703S glycosynthase. (b) The predicted mode of binding of Le^x trisaccharide (cyan) and its comparison with the Le^a trisaccharide (yellow) observed in the D172A/E217A-LNFP II structure (electrostatic surface potential map) (stereoview).

the LNB/LacNAc disaccharides. Indeed, the Lac moiety is invisible in the D172A/E217A-LNFP II structure, and the rate of hydrolysis by *Bb*AfcB is the same between LNFP II (type-1) and LNFP III [Galβ1-4(Fucα1-3)GlcNAcβ1-3Galβ1-4Glc] (type-2) (29). GNB cannot be used in the synthase reaction, because the axial O4 hydroxyl group of the GalNAc moiety is not appropriately placed to make a glycosidic bond with Fuc. The GlcNAc-binding site can accept both GlcNAc and Glc, but the product yields in the synthetic reactions significantly differed between LNB and Lac (Table 1). The *N*-acetyl group of GlcNAc in the D172A/E217A-LNFP II structure does not form strong interactions with the protein, but the presence of the large *N*-acetyl group may stabilize the acceptor binding through a weak hydrophobic interaction with Trp47 or Trp213 (Fig. 3c). The enzyme synthesized LNFP II when LNT (Galβ1-3GlcNAcβ1-3Galβ1-4Glc) was included in the reaction mixture. LNT has two potential sites to be fucosylated by the enzyme, but in the analysis of the isolated product, the author only detected LNFP II. This is because the substitution of the O3 hydroxyl group of the penultimate Gal impaired the accommodation and/or constrained the induced-fit movement. Accordingly, when LNDFH II [Galβ1-3(Fucα1-4)GlcNAcβ1-3Galβ1-4(Fucα1-3)Glc] was incubated with the WT AfcBs, the Fucα1-4GlcNAc linkage was hydrolyzed about 100-fold faster than the Fucα1-3Glc linkage (data not shown).

The mutational study of *Bb*AfcB confirmed that Asp703 and Glu746 are the catalytic nucleophile and acid/base catalyst of the enzyme, respectively (Supplemental Table S1). The amino acid replacement at the Gal binding site (Trp742 and Asp807) resulted in a significant reduction (by 1800- and 80-folds, respectively) in the hydrolytic activity for 3-FL. It is interesting to note that the specific activities of the mutants decreased only by 2 to 4-folds for the *p*NP-Fuc hydrolysis (Supplemental Table S1), which agrees with the finding that these residues are involved in the interaction with the Gal moiety, and not in the Fuc binding. The presence of the branched Gal residue is important not only for the induced-fit movement but also for fixing the substrate at the catalytic site. In the D172A/E217A-LNFP II structure, Glu237 of *Bi*AfcB interacts with the Gal O3 hydroxyl group. *Bb*AfcB appears not to possess the corresponding residue, as the alanine substitutions at Asp763, Asp766 and Asp778 did not significantly affect hydrolytic activity. The sequence of the loop (236−254 in *Bi*AfcB and 758−773 in *Bb*AfcB) is not conserved between the two enzymes and the loop is disordered in the *Bi*AfcB structures (Fig. 3a and Supplemental Fig. S10). BT_2192, an another close homologue of *Bi*AfcB (see Fig. 5, described later), also does not possess the corresponding

residue in its sequence, but the side chain of Glu254 occupies the site in the structure (Supplemental Figs. S11 and S12). These results suggest an auxiliary role of this loop region in the substrate binding.

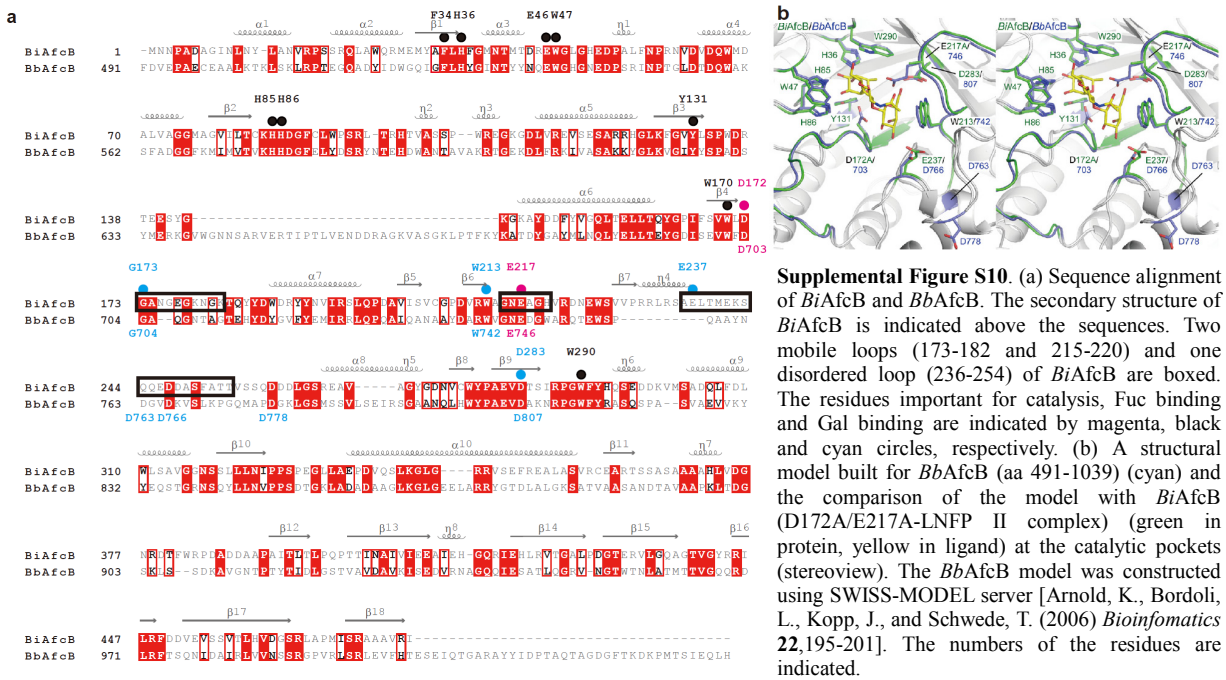

Supplemental Figure S10. (a) Sequence alignment of *Bi*AfcB and *Bb*AfcB. The secondary structure of *Bi*AfcB is indicated above the sequences. Two mobile loops (173-182 and 215-220) and one disordered loop (236-254) of *Bi*AfcB are boxed. The residues important for catalysis, Fuc binding and Gal binding are indicated by magenta, black and cyan circles, respectively. (b) A structural model built for *Bb*AfcB (aa 491-1039) (cyan) and the comparison of the model with *Bi*AfcB (D172A/E217A-LNFP II complex) (green in protein, yellow in ligand) at the catalytic pockets (stereoview). The *Bb*AfcB model was constructed using SWISS-MODEL server [Arnold, K., Bordoli, L., Kopp, J., and Schwede, T. (2006) *Bioinfomatics* **22**,195-201]. The numbers of the residues are indicated.

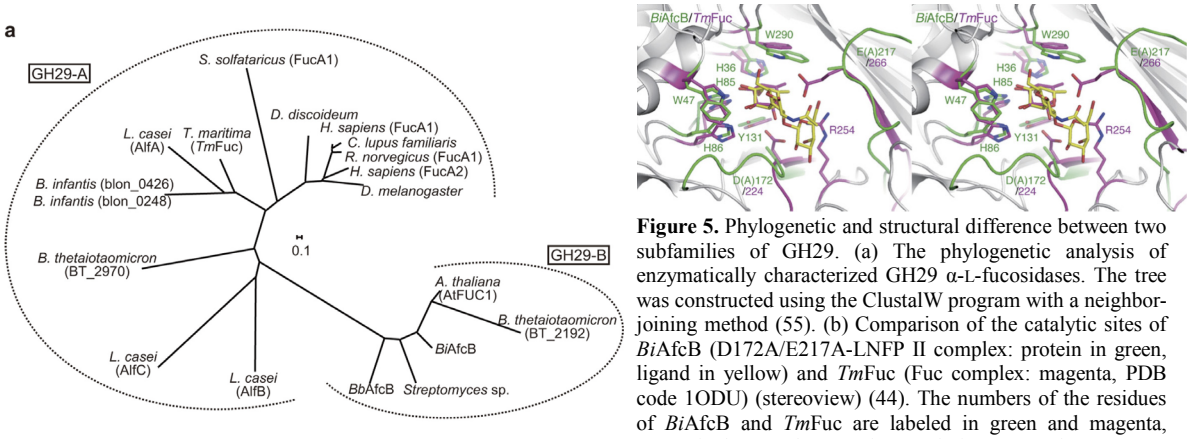

Figure 5. Phylogenetic and structural difference between two subfamilies of GH29. (a) The phylogenetic analysis of enzymatically characterized GH29 α-L-fucosidases. The tree was constructed using the ClustalW program with a neighbor-joining method (55). (b) Comparison of the catalytic sites of *Bi*AfcB (D172A/E217A-LNFP II complex: protein in green, ligand in yellow) and *Tm*Fuc (Fuc complex: magenta, PDB code 1ODU) (stereoview) (44). The numbers of the residues of *Bi*AfcB and *Tm*Fuc are labeled in green and magenta, respectively. See also Supplemental Figs. S11 and S12.

Comparison with other α-L-fucosidases−GH29 can be divided into two subfamilies by phylogenetic analysis (Fig. 5a), and this classification apparently correlates with the difference of the substrate specificities between the two groups (29). One subfamily (hereafter referred to as GH29-A) is comprised of enzymes that show relatively relaxed substrate specificity and act efficiently on a chromogenic substrate (*e.g.* *p*NP-Fuc), as do human and *Thermotoga maritima* (*Tm*Fuc) enzymes (EC 3.2.1.51) (44,47,48). In contrast, the members

of the other subfamily specifically hydrolyze the terminal α-(1,3/4)-fucosidic linkages and hardly act on *p*NP-Fuc (referred to as GH29-B) (EC 3.2.1.111) (49,50, unpublished results for BT_2192, the author and Dr. Katayama T. at Ishikawa Prefectural University). *Bb*AfcB and *Bi*AfcB are thus categorized into the GH29-B subfamily (29). The overall structure of *Bi*AfcB shows a resemblance to that of *Tm*Fuc (GH29-A) (PDB code 1ODU) (the root mean square deviation = 3.5 Å for 289 Cα atoms; Z score = 28.5; sequence identity = 24%). In particular, the structure of the Fuc-binding site (subsite -1) is similar between the two enzymes (Fig. 5b). The catalytic nucleophile Asp224 and the acid/base catalyst Glu266 of *Tm*Fuc overlap with Asp172 and Glu217 of *Bi*AfcB (by induced-fit movement), respectively (44, 45). *Tm*Fuc, however, does not have a Gal-binding site, and the side chain of Arg254 occupies the corresponding site and forms a hydrogen bond with the endocyclic oxygen atom of Fuc. This Arg residue is highly conserved in GH29-A enzymes (13 out of 14 members listed in Fig. 5a), while the Gal-binding residues (corresponding to G173, W213 and D283 of *Bi*AfcB) are invariable in the five characterized members of GH29-B. In addition, the constitution of the catalytic pocket is structurally conserved in the respective subfamilies (Supplemental Figs. 11 and 12) (51). The structural difference observed at that site may be therefore the basis that differentiates the substrate specificity between GH29-A and GH29-B enzymes. But it is interesting to note that, in both *Tm*Fuc (GH29-A) and *Bi*AfcB (GH29-B), two mobile loops (including or close to an acid/base residue) play critical roles in the catalytic processes (52) (Supplemental Fig. S11).

Transglycosylation activity of α-L-fucosidases from *Alcaligenes* sp., *Aspergillus niger*, *Penicillium multicolor* and *T. maritima* has been employed to produce fucosyl oligosaccharides using *p*NP-Fuc as a donor (22-25). Recently, the glycosynthase methodology was introduced in α-L-fucosidase from *Sulfolobus solfataricus* (*Ss*Fuc D242S) and *T. maritima* (*Tm*Fuc D224G) (18). These enzymes/mutants are efficient catalysts that attach an α-L-fucosyl residue(s) to various acceptor molecules; however, since they belong to the GH29-A subfamily, they intrinsically fail to control the regio-selectivity and acceptor specificity, even though they have some preference. For example, *Tm*Fuc synthesized a mixture of Fucα1-3Fucα-*p*NP and Fucα1-2Galβ-*p*NP as a result of transglycosylation when incubated with *p*NP-Fuc (donor) and *p*NP-β-Gal (acceptor) (25). The *Ss*Fuc glycosynthase mutant produced Fucα1-6Galβ-*p*NP, Fucα1-3Galβ-*p*NP, Fucα1-4Galβ-*p*NP and Fucα1-2(Fucα1-3)Galβ-*p*NP when incubated with $FucN_3$ and Galβ-*p*NP as the donor and the

acceptor, respectively (18).

The strict specificity exerted by the *Bb*AfcB D703S mutant is thus a quite unusual feature. The synthase should therefore serve as a powerful tool for introducing the Le^a and Le^x antigens into the type-1 and type-2 chains at the non-reducing ends of various glycoconjugates including glycoprotein and glycolipids, without attaching undesirable and unexpected α-L-fucosyl residues. Considering that 1,3-1,4-α-L-fucosynthase can recognize 2'-FL as the acceptor, the combination of this synthase with 1,2-α-L-fucosynthase, which Wada *et al*. have already developed (30), may afford the one-pot tailor-made synthesis of all-types of Le antigens including Le^b and Le^y. Mining glycosidases with strict specificity and exploiting those enzymes could be the closest approach to the specific synthesis of glycosides. In this sense, intestinal microorganisms including bifidobacteria represent good enzyme resources as they are found to possess various glycosidases specific to host glycans (46,53,54).

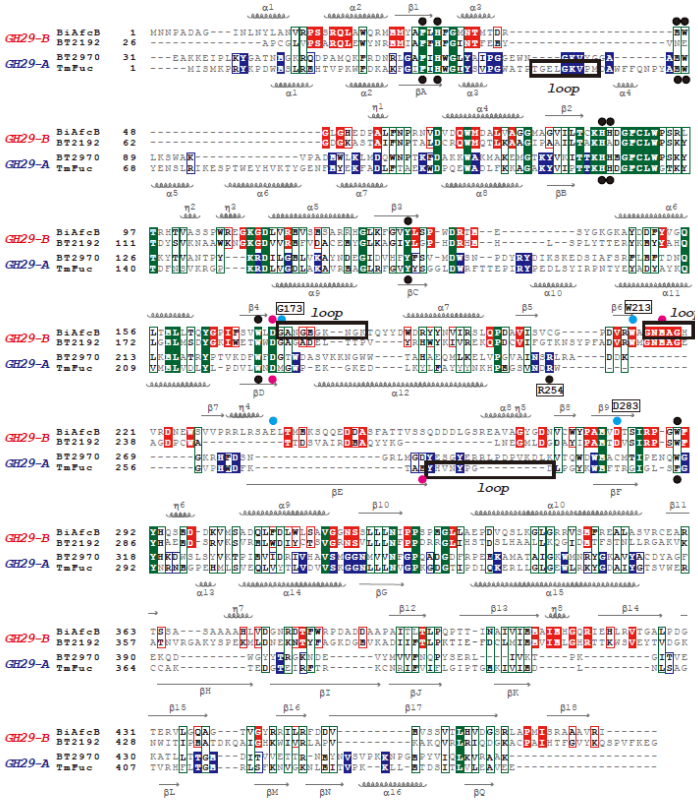

Supplemental Figure S11. Sequence alignment of enzymatically characterized, structure-solved GH29-A and GH29-B members. The secondary structures of *Bi*AfcB and *Tm*Fuc are indicated above and below the sequences. The residues conserved in GH29-A, GH29-B and the both are shown in blue, red and green, respctively. Two mobile loops (173-182 and 215-220 in *Bi*AfcB, 47-55 and 267-274 in *Tm*Fuc) are boxed. The residues important for catalysis (for *Bi*AfcB and *Tm*Fuc), Fuc-binding (for *Bi*AfcB and *Tm*Fuc) and Gal-binding (for *Bi*AfcB) are indicated by magenta, black and cyan circles, respectively. G173, W213 and D283 of *Bi*AfcB and R254 of *Tm*Fuc are indicated. See also Figure 5.

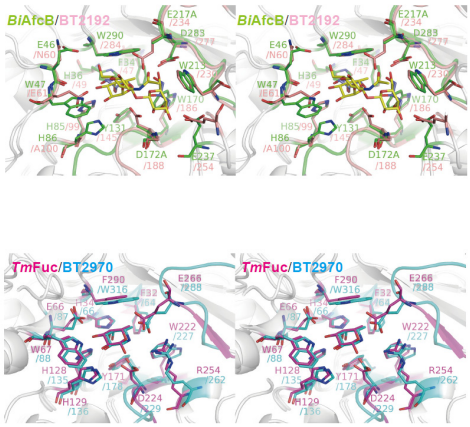

Supplemental Figure S12. Conservation of the active-site structures in the respective subfamilies. The enzymatically characterized members were used for comparison. (a) GH20-B: *Bi*AfcB (D172A/E217A-LPFP II complex: protein in green, ligand in yellow) vs. BT2192 (glycerol complex: protein in pink, ligand in violet, PDB code 3EYP), (b) GH29-A: *Tm*Fuc (Fuc complex: magenta, PDB code 1ODU) vs. BT2970 (DFJ complex: cyan, PDB code 2XIB). The numbers of the residues are indicated. See also Figure 5 and Supplemental Figure S11.

REFERENCES

1. Becker, D.J. and Lowe, J.B. (2003) Fucose: biosynthesis and biological function in mammals. *Glycobiology*. *Glycobiology* **13**, 41R-53R
2. Gooi, H.C., Feizi, T., Kapadia, A., Knowles, B.B., Solter, D., and Evans, M.J. (1981) Stage-specific embryonic antigen involves α 1 goes to 3 fucosylated type 2 blood group chains. *Nature* **292**, 156-158
3. Inoue, M., Sasagawa, T., Saito, J., Shimizu, H., Ueda, G., Tanizawa, O., and Nakayama, M. (1987) Expression of blood group antigens A, B, H, Lewis-a, and Lewis-b in fetal, normal, and malignant tissues of the uterine endometrium. *Cancer* **60**, 2985-2993
4. Phillips, M.L., Nudelman, E., Gaeta, F.C., Perez, M., Singhal, A.K., Hakomori, S., and Paulson, J.C. (1990) ELAM-1 mediates cell adhesion by recognition of a carbohydrate ligand, sialyl-Le^x. *Science* **250**, 1130-1132
5. Walz, G., Aruffo, A., Kolanus, W., Bevilacqua, M., and Seed, B. (1990) Recognition by ELAM-1 of the sialyl-Le^x determinant on myeloid and tumor cells. *Science* **250**, 1132-1135
6. Nilsson, C., Skoglund, A., Moran, A.P., Annuk, H., Engstrand, L., and Normark, S. (2006) An enzymatic ruler modulates Lewis antigen glycosylation of *Helicobacter pylori* LPS during persistent infection. *Proc Natl Acad Sci USA*. **103**, 2863-2868
7. Liu, T.W., Ho, C.W., Huang, H.H., Chang, S.M., Popat, S.D. , Wang, Y.T., Wu, M.S., Chen, Y.J., and Lin, C.H. (2009) Role for α-L-fucosidase in the control of *Helicobacter pylori*-infected gastric cancer cells. *Proc Natl Acad Sci USA*. **106**, 14581-14586
8. Bergman, M.P., Engering, A., Smits, H.H., van Vliet, S.J., van Bodegraven, A.A., Wirth, H.P., Kapsenberg, M.L., Vandenbroucke-Grauls, C.M., van Kooyk, Y., and Appelmelk, B.J. (2004) *Helicobacter pylori* modulates the T helper cell 1/T helper cell 2 balance through phase-variable interaction between lipopolysaccharide and DC-SIGN. *J Exp Med.* **200**, 979-990
9. Hancock, S.M., Vaughan, M.D., and Withers, S.G. (2006) Engineering of glycosidases and glycosyltransferases. *Curr Opin Chem Biol.* **10**, 509-519
10. Wang, L.X. and Huang, W. (2009) Enzymatic transglycosylation for glycoconjugate synthesis. *Curr. Opin. Chem. Biol.* **13**, 592-600
11. Wang, W., Hu, T., Frantom, P.A., Zheng, T., Gerwe, B., Del Amo D.S., Garret, S., Seidel,

R.D.III, and Wu, P. (2009) Chemoenzymatic synthesis of GDP-L-fucose and the Lewis X glycan derivatives. *Proc Natl Acad Sci USA.* **106**, 16096-16101

12. Dumon, C., Bosso, C., Utille, J.P., Heyraud, A., and Samain, E. (2006) Production of Lewis x tetrasaccharides by metabolically engineered *Escherichia coli*. *Chembiochem.* **7**, 359-365
13. Drouillard, S., Driguez, H., and Samain, E. (2006) Large-scale synthesis of H-antigen oligosaccharides by expressing *Helicobacter pylori* α1,2-fucosyltransferase in metabolically engineered *Escherichia coli* cells. *Angew Chem Int Ed Engl.* **45**, 1778-1780
14. Mackenzie, L.F., Wang, Q., Warren, R.A.J., and Withers, S.G. (1998) Glycosynthases: mutant glycosidases for oligosaccharide synthesis. *J Am Chem Soc*. **120**, 5583-5584
15. Malet, C. and Planas, A. (1998) From β-glucanase to β-glucansynthase: glycosyl transfer to α-glycosyl fluorides catalyzed by a mutant endoglucanase lacking its catalytic nucleophile. *FEBS Lett.* **440**, 208-212
16. Honda, Y. and Kitaoka, M. (2006) The first glycosynthase derived from an inverting glycoside hydrolase. *J Biol Chem.* **281**, 1426-1431
17. Cobucci-Ponzano, B., Strazzulli, A., Rossi, M., and Moracci, M. (2011) Glycosynthases in biocatalysis. *Adv Synth Catal.* **353**, 2284-2300
18. Cobucci-Ponzano, B., Conte, F., Bedini, E., Corsaro, M.M., Parrilli, M., Sulzenbacher, G., Lipski, A., Dal Piaz, F., Lepore, L., Rossi, M., and Moracci, M. (2009) β-Glycosyl azides as substrates for α-glycosynthases: preparation of efficient α-L-fucosynthases. *Chem Biol.* **16**, 1097-1108
19. Cobucci-Ponzano, B., Zorzetti, C., Strazzulli, A., Carillo, S., Bedini, E., Corsaro, M.M., Comfort, D.A., Kelly, R.M., Rossi, M., and Moracci, M. (2011) A novel α-D-galactosynthase from *Thermotoga maritime* converts β-D-galactopyranosyl azide to α-galacto-oligosaccharides. *Glycobiology* **21**, 448-456
20. Umekawa, M., Huang, W., Li, B., Fujita, K., Ashida, H., Wang, L.X., and Yamamoto, K. (2008) Mutants of *Mucor hiemalis* endo-β-*N*-acetylglucosaminidase show enhanced transglycosylation and glycosynthase-like activities. *J Biol Chem.* **283**, 4469-4479
21. Shaikh, F.A. and Withers, S.G. (2008) Teaching old enzymes new tricks: engineering and evolution of glycosidases and glycosyl transferases for improved glycoside synthesis. *Biochem Cell Biol*. **86**, 169-177
22. Ajisaka, K., Fujimoto, H., and Miyasato, M. (1998) An α-L-fucosidase from *Penicillium*

multicolor as a candidate enzyme for the synthesis of α(1→3)-linked fucosyl oligosaccharides by transglycosylation. *Carbohydr Res.* **309**, 125-129

23. Murata, T., Morimoto, S., Zeng, X., Watanabe, S., and Usui, T. (1999) Enzymatic synthesis of α-L-fucosyl-*N*-acetyllactosamines and 3'-*O*-α-L-fucosyllactose utilizingα-L-fucosidases. *Carbohydr Res.* **320**, 192-199
24. Farkas, E., Thiem, J., and Ajisaka, K. (2000) Enzymatic synthesis of fucose-containing disaccharides employing the partially purified α-L-fucosidase from *Penicillium multicolor*. *Carbohydr Res.* **328**, 293-299
25. Osanjo, G., Dion, M., Drone, J., Solleux, C., Tran, V., Rabiller, C., and Tellier, C. (2007) Directed evolution of the α-L-fucosidase from *Thermotoga maritima* into an α-L-transfucosidase. *Biochemistry* **46**, 1022-1033
26. Cantarel, B.L., Coutinho, P.M., Rancurel, C., Bernard, T., Lombard, V., and Henrissat, B. (2009) The Carbohydrate-Active EnZymes database (CAZy): an expert resource for Glycogenomics. *Nucleic Acids Res.* **37**, D233-D238
27. Katayama, T., Sakuma, A., Kimura, T., Makimura, Y., Hiratake, J., Sakata, K., Yamanoi, T., Kumagai, H., and Yamamoto, K. (2004) Molecular cloning and characterization of *Bifidobacterium bifidum* 1,2-α-L-fucosidase (AfcA), a novel inverting glycosidase (glycoside hydrolase family 95). *J Bacteriol.* **186**, 4885-4893
28. Nagae, M., Tsuchiya, A., Katayama, T., Yamamoto, K., Wakatsuki, S., and Kato, R. (2007) Structural basis of the catalytic reaction mechanism of novel 1,2-α-L-fucosidase from *Bifidobacterium bifidum*. *J Biol Chem.* **282**, 18497-18509
29. Ashida, H., Miyake, A., Kiyohara, M., Wada, J., Yoshida, E., Kumagai, H., Katayama, T., and Yamamoto, K. (2009) Two distinct α-L-fucosidases from *Bifidobacterium bifidum* are essential for the utilization of fucosylated milk oligosaccharides and glycoconjugates. *Glycobiology* **19**, 1010-1017
30. Wada, J., Honda, Y., Nagae, M., Kato, R., Wakatsuki, S., Katayama, T., Taniguchi, H., Kumagai, H., Kitaoka, M., and Yamamoto, K. (2008) 1,2-α-L-Fucosynthase: a glycosynthase derived from an inverting α-glycosidase with an unusual reaction mechanism. *FEBS Lett.* **582**, 3739-3743
31. Nishimoto, M. and Kitaoka, M. (2007) Practical preparation of lacto-*N*-biose I, a candidate for the bifidus factor in human milk. *Biosci Biotechnol Biochem.* **71**, 2101-2104

32. Nishimoto, M. and Kitaoka, M. (2009) One-pot enzymatic production of β-D-galactopyranosyl-(1→3)-2-acetamido-2-deoxy-F-galactose (galacto-*N*-biose) from sucrose and 2-acetamido-2-deoxy-D-galactose (*N*-acetylgalactosamine). *Carbohydr Res.* **344**, 2573-2576
33. Honda, Y., Kitaoka, M., and Hayashi, K. (2004) Reaction mechanism of chitobiose phosphorylase from *Vibrio proteolyticus*: identification of family 36 glycosyltransferase in *Vibrio*. *Biochem J.* **377**, 225-232
34. Cohenford, M.A., Abraham, A., Abraham, J., and Dain, J.A. (1989) Colorimetric assay for free and bound L-fucose. *Anal Biochem*. **177**, 172-177
35. Otwinowski, Z. and Minor, W. (1997) Processing of x-ray diffraction data collected in oscillation mode. *Methods Enzymol.* **276**, 307-326
36. Vagin, A., and Teplyakov, A. (1997) MOLREP: an automated program for molecular replacement. *J Appl Cryst.* **30**, 1022-1025
37. Sela, D.A., Garrido, D., Lerno, L., Wu, S., Tan, K., Eom, H.J., Joachimiak, A., Lebrilla, C.B., and Mills, D.A. (2012) *Bifidobacterium longum* subsp. *infantis* ATCC 15697 α-fucosidases are active on fucosylated human milk oligosaccharides. *Appl Environ Microbiol*. **78**, 795–803
38. Emsley, P., Lohkamp, B., Scott, W.G., and Cowtan, K. (2010) Features and development of Coot. *Acta Crystallogr. D Biol Crystallogr.* **66**, 486-501
39. Murshudov, G.N., Vagin, A.A., and Dodson, E.J. (1997) Refinement of macromolecular structures by the maximum-likelihood method. *Acta Crystallogr D Biol Crystallogr.* **53**, 240-255
40. Suzuki, R., Katayama, T., Kitaoka, M., Kumagai, H., Wakagi, T., Shoun, H., Ashida, H., Yamamoto, K., and Fushinobu, S. (2009) Crystallographic and mutational analyses of substrate recognition of endo-α-*N*-acetylgalactosaminidase from *Bifidobacterium longum*. *J Biochem*. **146**, 389-398
41. Bohne, A., Lang, E., and von der Lieth, C.W. (1999) SWEET—WWW-based rapid 3D construction of oligo- and polysaccharides. *Bioinformatics* **15**, 767-768
42. Morris, G.M., Goodsell, D.S., Halliday, R.S., Huey, R., Hart, W.E., Belew, R.K., and Olson, A.J. (1998) Automated docking using a Lamarckian genetic algorithm and an empirical binding free energy function. *J Comput Chem.* **19**, 1639-1662
43. McCarter, J.D. and Withers, S.G. (1994) Mechanisms of enzymatic glycoside hydrolysis.

Curr Opin Struct Biol. **4**, 885-892

44. Sulzenbacher, G., Bignon, C., Nishimura, T., Tarling, C. A., Withers, S. G., Henrissat, B., and Bourne, Y. (2004) Crystal structure of *Thermotoga maritime* α-L-fucosidase. Insights into the catalytic mechanism and the molecular basis for fucosidosis. *J Biol Chem.* **279**, 13119-13128
45. Tarling, C.A., He, S., Sulzenbacher, G., Bignon, C., Bourne, Y., Henrissat, B., and Withers, S.G. (2003) Identification of the catalytic nucleophile of the family 29 α-L-fucosidase from *Thermotoga maritime* through trapping of a covalent glycosyl-enzyme intermediate and mutagenesis. *J Biol Chem.* **278**, 47394-47399
46. Sela, D.A., Chapman, J., Adeuya, A., Kim, J.H., Chen, F., Whitehead, T.R., Lapidus, A., Rokhsar, D.S., Lebrilla, C.B., German, J.B., Price, N.P., Richardson, P.M., and Mills, D.A. (2008) The genome sequence of *Bifidobacterium longum* subsp.*infantis* reveals adaptations for milk utilization within the infant microbiome. *Proc Natl Acad Sci USA*. **105**, 18964-18969
47. Liu, S.W., Chen, C.S., Chang, S.S., Mong, K.K., Lin, C.H., Chang, C.W., Tang, C.Y., and Li, Y.K. (2009) Identification of essential residues of human α-L-fucosidase and tests of its mechanism. *Biochemistry* **48**, 110-120
48. Rodríguez-Díaz, J., Monedero, V., and Yebra, M.J. (2011) Utilization of natural fucosylated oligosaccharides by three novel α-L-fucosidases from a probiotic *Lactobacillus casei* strain. *Appl Environ Microbiol*. **77**, 703-705
49. Sano, M., Hayakawa, K., and Kato, I. (1992) Purification and characterization of α-L-fucosidase from *Streptomyces* species. *J Biol Chem.* **267**, 1522-1527.
50. Zeleny, R., Leonard, R., Dorfner, G., Dalik, T., Kolarich, D., and Altmann, F. (2006) Molecular cloning and characterization of a plant α1,3/4-fucosidase based on sequence tags from almond fucosidase I. *Phytochemistry* **67**, 641-648
51. Fisher, K.J. and Aronson, N.N.Jr. (1989) Isolation and sequence analysis of a cDNA encoding rat liver α-L-fucosidase. *Biochem J.* **264**, 695-701
52. Wu, H.J., Ho C.W., Ko, T.P., Popat, S.D., Lin, C.H., and Wang, A.H. (2010) Structural basis of α-fucosidase inhibition by iminocyclitols with K_i values in the micro- to picomolar range. *Angew Chem Int Ed Engl.* **49**, 337-340
53. Yoshida, E., Sakurama, H., Kiyohara, M., Nakajima, M., Kitaoka, M., Ashida, H., Hirose, J., Katayama, T., Yamamoto, K., and Kumagai, H. (2012) *Bifidobacterium longum*subsp.

Infantis uses two different β-galactosidases for selectively degrading type-1 and type-2 human milk oligosaccharides. *Glycobiology* **22**, 361-368

54. Asakuma, S., Hatakeyama, E., Urashima, T., Yoshida, E., Katayama, T., Yamamoto, K., Kumagai, H., Ashida, H., Hirose, J., and Kitaoka, M. (2011) Physiology of consumption of human milk oligosaccharides by infant gut-associated bifidobacteria. *J Biol Chem.* **286**, 34583-34592
55. Saitou, N. and Nei, M. (1987) The neighbor-joining method: a new method for reconstructing phylogenetic trees. *Mol Biol Evol.* **4**, 406-425

FOOTNOTES

The atomic coordinates and structure factors (code 3UES and 3UET) have been deposited in the Protein Data Bank, Research Collaboratory for Structural Bioinformatics, Rutgers University, New Brunswich, NJ (http://www.rcsb.org/).

CHAPTER 4

β-Glucuronidase from *Lactobacillus brevis* subsp. *coagulans*

Flavonoids have beneficial properties for human health, such as anticancer properties (1). They have been found as a component of traditional herbal medicine, and most of them exist naturally in conjugated form, primarily with sugar residues. Orally administered flavonoid glycosides are degraded into aglycones by intestinal microflora and are absorbed as aglycones (2,3). The intact flavonoid glycosides are usually not absorbed by the small intestine, and their aglycones often show an efficient drug action. Therefore, the intestinal microflora has been increasingly recognized as playing an important role in the degradation of flavonoid glycosides. However, all individuals possess their own characteristic microflora, and the bioconversion and bioavailability of flavonoid glycosides show a considerable interindividual variation (4,5). Therefore, the stable expression of drug action, regardless of the species of intestinal microflora, is required for the conversion of flavonoid glycosides into their aglycones after oral administration, more preferably in the small intestine.

Baicalin (baicalein 7-*O*-β-D-glucuronide) is one of the major flavonoids found in *Scutellaria baicalensis*, which is often included in traditional herbal medicines such as Bofu-Tsusho-San (BOF). Herbal medicines including baicalin are used for antibacterial (6), anti-inflammatory (7), and anticancer activities (8,9). Baicalein, the aglycone of baicalin, is absorbed more quickly and shows more effective properties than baicalin (10-12). However, it is not easy to obtain baicalein directly from *S. baicalensis* because of its low content (ca. 0.2%). Therefore, the bioconversion of baicalin to baicalein (Fig. 1a) is an attractive method, because baicalin is present in higher content in *S. baicalensis* (ca. 6–10%). Furthermore, the reaction occurring in the small intestine by the culture of probiotic lactic acid bacteria could be useful for enhancing the availability of baicalin as a precursor of baicalein.

β-Glucuronidases (EC 3.2.1.31, GUSs) can hydrolyze β-D-glucuronic bonds via a retaining mechanism and are often used to convert baicalin to baicalein. Most GUSs are known to occur in glycoside hydrolase (GH) family 2, while only a few occur in GH families 1 and 79 (EC 3.2.1.167) in the CAZy database (http://www.cazy.org) (13). The well-studied GUSs from *Escherichia coli* (*Ec*GUS2) and humans belong to GH family 2. These enzymes are involved in the enterohepatic recirculation of various compounds such as toxins, hormones, drugs, and carcinogens (14,15). On the other hand, the enzymes belonging to GH

families 1 (16,17) and 79 (18,19) show unique substrate specificities. For example, Klotho from *Mus musculus*, belonging to GH family 1, shows both of GUS and sialidase activities, and baicalin-β-glucuronidase (EC 3.2.1.167) from *S. baicalensis* (*Sb*GUS79), belonging to GH family 79, shows the strict substrate specificity for baicalin. Since bacterial enzymes can be often prepared more easily than other enzymes such as mammalian enzymes, bacterial GUSs are more promising. Bacterial GUSs were previously found in *E. coli* and closely related *Enterobacteriaceae* (20). Recently, however, *Lactobacillus gasseri* ADH (21) and *Lactobacillus brevis* RO1 (22) have been reported to have GUSs belonging to GH family 2.

Recently, the author has found that *L. brevis* subsp. *coagulans* can hydrolyze baicalin to baicalein. *L. brevis* subsp. *coagulans* is known for its potential benefits to human health (23), such that it is worth analyzing the function of *L. brevis* subsp. *coagulans* in flavonoid metabolism. In this chapter, the author aimed to identify and characterize the enzyme hydrolyzing baicalin from *L. brevis* subsp. *coagulans* (designated as *Lc*GUS30). First, the author purified and identified *Lc*GUS30 from *L. brevis* subsp. *coagulans*. Surprisingly, *Lc*GUS30 belongs to GH family 30. In addition, the author revealed the physicochemical properties and substrate specificity of *Lc*GUS30. These results indicated that *Lc*GUS30 and *L. brevis* subsp. *coagulans* could serve as valuable tools for the construction of a safe bioconversion system for baicalin and wogonin.

EXPERIMENTAL PROCEDURES

Bacterial strain, culture condition, and chemicals−*L. brevis* subsp. *coagulans* FERM BP-4693 was used in this chapter. *L. brevis* subsp. *coagulans* was cultivated at 37°C for 24 h in a Man-Rogosa-Sharpe (MRS) broth (Difco Laboratories Inc., MI, USA) with shaking (120 strokes/min). Phenolphthalein β-D-glucuronide (phenolphthalein-GlcA), 4-methylumbelliferyl-β-D-glucuronide hydrate (MU-GlcA), wogonoside (wogonin 7-*O*-β-D-glucuronide), estrone 3-(β-D-glucuronide) (estrone-GlcA), 4-nitrophenyl β-D-glucuronide (*p*NP-GlcA), and 4-methylumbelliferone (MU) were purchased from Sigma-Aldrich Co. Ltd. (MO, USA). Baicalin, baicalein, and estrone were purchased from Tokyo Chemical Industry Co., Ltd. (Tokyo, Japan). Phenolphthalein and *p*-nitrophenol (*p*NP) were purchased from Wako Pure Chemicals Industries, Ltd. (Osaka, Japan). Wogonin was from Nakalai Tesque, Inc. (Kyoto, Japan). All other chemicals used in this chapter were of analytical grade and

commercially available.

Purification of the native enzyme−All native enzyme purification procedures were carried out at 0–4°C, and 20 mM potassium phosphate buffer (KPB) (pH 6.5) was used as a standard buffer. *L. brevis* subsp. *coagulans* cells from 2.1-L culture medium (8.7 g wet weight cells) were suspended in 20 ml of the standard buffer and then disrupted for 5 min × 6 cycles by an ultrasonic oscillator with Insonator model 201M (Kubota, Tokyo, Japan). The lysate was centrifuged at 28,000 *g* for 15 min at 4°C and then subjected to ultracentrifugation at 100,000 *g* for 1 h at 4°C. Twenty milliliters of the obtained supernatant were used as the cell-free extracts. Purification was carried out as follows using a fast protein liquid chromatography (FPLC) system (GE Healthcare Biosciences UK Ltd., Buckinghamshire, UK). The activity in each fraction obtained during purification was measured under the condition of 20 mM citrate buffer (pH 5.0) containing 2.24 mM baicalin in a total volume of 1 ml at 37°C for 1 h with shaking (130 strokes/min).

Step 1: Mono Q 10/100 GL column chromatography

The cell-free extracts were loaded onto an 8-ml column of Mono Q 10/100 GL column (GE Healthcare Biosciences UK Ltd.) equilibrated with the standard buffer. After the column was washed with the standard buffer, the enzyme was eluted with a linear gradient of 0–1 M NaCl at 60 column volumes (CV). The active fractions were combined and concentrated by ultrafiltration using a Centriprep YM-10 filter (Merck Millipore Corp., MA, USA).

Step 2: HiLoad 26/600 Superdex 200 pg column chromatography

The enzyme solution was applied to a HiLoad 26/600 Superdex 200 pg column (GE Healthcare Biosciences UK Ltd.) equilibrated with the standard buffer, and the enzyme was eluted with the same buffer. The active fraction was concentrated by ultrafiltration using a Centriprep YM-10 filter.

Step 3: Mono Q 5/50 GL column chromatography

The enzyme solution was applied to a Mono Q 5/50 GL column (GE Healthcare Biosciences UK Ltd.) equilibrated with the standard buffer. After the column was washed with the standard buffer, the enzyme was eluted with a linear gradient of 0–0.3 M NaCl at 40 CV. The purified protein was extensively dialyzed against a 20 mM KPB (pH 6.5).

Analysis with sodium dodecyl sulfate-polyacrylamide gel electrophoresis−Sodium dodecyl sulfate-polyacrylamide gel electrophoresis (SDS-PAGE) was performed in a 10% concentration of polyacrylamide gel using the tris(hydroxymethyl)aminomethane (Tris)-glycine buffer system. The subunit molecular mass of the purified enzyme was estimated by comparison of the mobility with that of the standard protein.

Measurement of protein concentration−Protein concentrations were determined by a Bio-Rad Protein Assay Kit (Bio-Rad Co. Ltd., CA, USA). Bovine serum albumin was used as the protein standard.

NH_2-terminal amino acid sequencing−The active fractions of the final purification step were loaded onto a Sequi-Blot PVDF membrane (Bio-Rad Co. Ltd.). The N-terminal amino acid sequence of the immobilized enzyme was analyzed by automated Edman degradation with a PPSQ-33A protein sequencer (Shimadzu Co. Ltd., Kyoto, Japan).

Preparation of genomic DNA and extraction of plasmid DNA−For extraction of genomic DNA from *L. brevis* subsp. *coagulans*, the strain was cultivated at 37°C with shaking (120 strokes/min) for 2 days in 15 ml of MRS medium. Then cells were harvested by centrifugation at 1,700 *g* for 10 min, and the genomic DNA was extracted from the cells and purified by a DNeasy Blood & Tissue Kit (Qiagen Inc., Venlo, Netherlands). For extraction of plasmid DNA from *E. coli* transformant cells, a QIAprep Spin Miniprep Kit (Qiagen Inc.) was used.

Gene cloning of the native enzyme−The gene was amplified by PCR with the following primers (forward primer: 5'-GGGAAGCTTATGAAGAAGTTCCAACATGAA-3' and reverse primer: 5'-CCCGGATCCTTAATGCTGTCCAGGGGCGAC-3'). *Hind*III and *Bam*HI restriction sites were underlined. The PCR mixture consisted of 1 μl of the genomic DNA as a template, 0.2 μM of each primer, and 12.5 μl of PrimeSTAR™ Max Premix (Takara Bio inc., Shiga, Japan) in 10.5 μl of distilled water. PCR conditions were as follows: step 1: 98°C for 10 s; step 2: 98°C for 10 s; step 3: 55°C for 5 s; step 4: 72°C for 8 s; and 30 cycles from step 2 to step 4. The PCR product was phosphorylated with 1 mM of ATP and 1.0 U of T4 Polynucleotide Kinase (Takara Bio inc.) in 5 μl of T4 Polynucleotide Kinase Buffer at

37°C for 1 h. The pET-28a vector was digested with *Hind*III at 37°C for 1 h and blunt-ended with T4 DNA Polymerase (Takara Bio inc.) at 37°C for 5 min. Subsequently, the pET-28a was dephosphorylated with bacterial alkaline phosphatase (Takara Bio inc.). Then, the PCR product was ligated into pET-28a at 16°C for 3 h. The resulting vectors were sequenced and used as an expression vector. The cycle sequence was carried out using BigDye Terminator v3.1 Cycle Sequencing Kit (Applied Biosystems Inc., CA, USA). The base sequence was determined using ChromasPro 1.4 (Technelysium Pty Ltd., Tewantin, Australia) and compared to the international Base Sequence database (GenBank/DDBJ/EMBL).

***Expression of the recombinant enzyme in* E. coli**−The expression vector was transformed into *E. coli* Rosetta 2 (DE3) by the reported method (24). Transformed *E. coli* cells were inoculated into 5 ml of lysogeny broth (LB) medium containing 15 μg/ml kanamycin. After cultivation at 37°C for 1 day with shaking (200 strokes/min), 0.2 ml of culture was transferred to 10 ml of the same fresh medium and cultivated at 20°C for 4 h with shaking (150 strokes/min) until optical density at 600 nm reached about 0.5. Then, the culture was added to 0.5 mM isopropyl-β-D-1-thiogalactopyranoside (IPTG) and incubated at 20°C for 1 day with shaking (150 strokes/min).

Purification of the recombinant enzyme−The cells were harvested by centrifugation at 1,700 *g* for 10 min at 4°C, and washed twice with 0.85% NaCl, and then, washed cells were obtained. The transformed *E. coli* Rosetta 2 (DE3) cells obtained from 500 ml culture broth were suspended in 15 ml of 20 mM KPB (pH 7.5) containing 0.5 M NaCl and 20 mM imidazole and disrupted for 5 min × 4 cycles by an ultrasonic oscillator with Insonator model 201M. The lysate was centrifuged at 12,000 *g* for 20 min. The supernatant was used as the cell-free extracts.

The cell-free extracts were applied to a Ni-Sepharose column (HisTrap HP 5 ml; GE Healthcare Biosciences UK Ltd.) equilibrated with 20 mM KPB (pH 7.5) containing 0.5 M NaCl and 20 mM imidazole. After the column was washed with the same buffer, the enzyme was eluted with a linear gradient of 0.02–0.5 M imidazole. The fractions containing purified enzyme were combined and concentrated by the ultrafiltration. The purified protein was extensively dialyzed against a 20 mM KPB (pH 6.5) and used for further characterization.

Enzyme activity assay−The activity measurements of the enzyme were performed using baicalin, wogonoside, estrone-GlcA, phenolphthalein-GlcA, MU-GlcA, and *p*NP-linked monosaccharides including *p*NP-GlcA as substrates. The standard assays were performed in 100 mM citrate buffer (pH 5.0) at 37°C for 5 min (for phenolphthalein-GlcA, MU-GlcA, and *p*NP-linked monosaccharides hydrolysis) or 30 min (for baicalin, wogonoside, and estron-GlcA hydrolysis). When phenolphthalein-GlcA, MU-GlcA, and *p*NP-linked monosaccharides were used as substrates, the reaction was stopped by adding 60 μl of 1 M Na_2CO_3 (for *p*NP-GlcA and MU-GlcA hydrolysis) or 1 M glycine−NaOH buffer (pH 10.4) (for phenolphthalein-GlcA hydrolysis). The amount of librated *p*NP and phenolphthalein was determined by measuring the absorbance at 405- and 540-nm wavelength, respectively, with UV-1700 UV-visible spectrophotometer (Shimadzu). The amount of librated MU was measured spectrofluorometrically with excitation at 360 nm and emission at 450 nm using Spectra MaxGenimi XPS (Molecular Devices Inc., CA, USA). When baicalin, wogonoside, and estrone-GlcA were used as substrates, the reaction mixtures were treated as follows. The same volume of dimethyl sulfoxide was added to the reaction mixture to extract aglycones. The reaction mixtures were centrifuged at 20,000 *g* for 10 min. After filtration with 0.45-μm hydrophilic filter (Merck Millipore Corp.), the treated reaction mixtures were analyzed by high-performance liquid chromatography (HPLC) using Shimadzu LC 10A System (Shimadzu) equipped with a 2.5C_{18}-MS-II column (3.0 ID × 100 mm; COSMOSIL; Nacalai Tesque, Inc.) at 35°C. Forty microliters of the filtered supernatant was injected to HPLC. The mobile phase for gradient elution contained Milli-Q water (eluent A) and methanol/0.1% formic acid (eluent B). The flow rate was 0.8 ml/min. The gradient schemes of the analysis are as follows: 0−5 min: linear gradient from 30 to 100% (*v*/*v*) of eluent B and 5−8 min: 100% of eluent B. The effluents were monitored with a PDA detector at an excitation wavelength of 254 nm (for baicalein and wogonin detection) or 284 nm (for estrone detection). The kinetic parameters were calculated by curve fitting the experimental data to the Michaelis–Menten equation, using KaleidaGraph 4.0 (Synergy Software Inc., PA, USA). In the case that no saturation was observed, only the k_{cat}/K_m value was determined at the low substrate concentration. One unit of the enzyme activity was determined as the amount of enzyme required to produce 1 μmol of the products at 37°C in 100 mM citrate buffer (pH 5.0).

The physicochemical properties of the recombinant enzyme were determined by using 1 mM *p*NP-GlcA. The optimal temperature was examined by incubating the reaction

mixture containing 100 mM citrate buffer (pH 4.5) at various temperatures for 1 min to prevent damage to the enzyme. The optimal pH value was determined at 37°C using the following buffers (100 mM): citrate−NaOH (pH 3.0−6.0), KPB (pH 6.0−7.5), and Tris−HCl (pH 7.5−9.0). The temperature and pH stabilities were determined at 37°C by measuring the residual activities after incubating the enzyme in 100 mM citrate buffer (pH 4.5) for 30 min at various temperatures and after dialyzing the enzyme overnight against various 100 mM buffers at 4°C, respectively.

Nucleotide sequence accession number−The nucleotide sequence of the enzyme has been deposited in DDBJ under accession number AB820700.

RESULTS

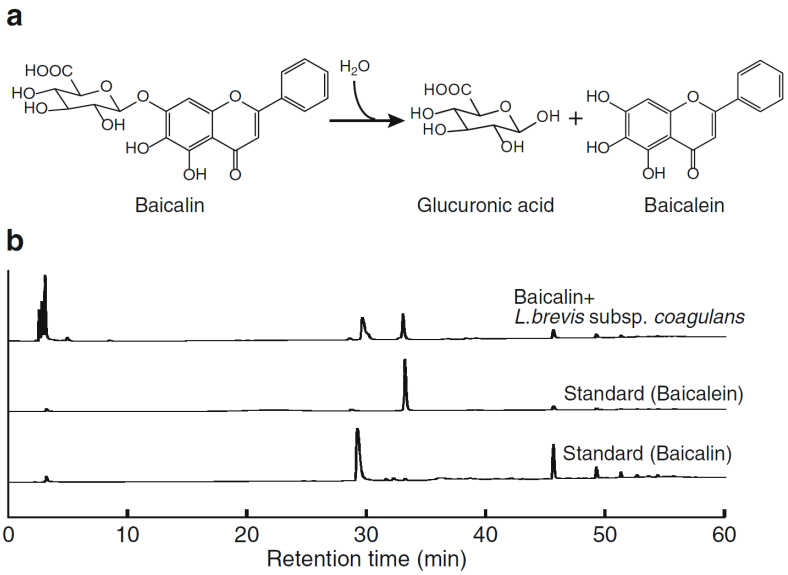

Figure 1. (a) Conversion of baicalin to baicalein catalyzed by β-D-glucuronidase. (b) HPLC analysis of the conversion of baicalin catalyzed by *L. brevis* subsp. *coagulans*.

Table 1 Summary of purification of native *Lc*GUS30

Purification step	Total protein (mg)	Total unit (U)	Specific activity (U/mg)	Fold	Yield (%)
Cell-free extracts	588	4.56	0.00411	1	100[a]
Mono Q 10/100 GL	61.6	18.0	0.117	28	390[a]
HiLoad 26/600 Superdex 200	0.184	0.245	1.33	320	5.4[a] (1.4)[b]
Mono Q 5/50 GL	0.00284	0.0215	7.57	1,800	0.47[a] (0.12)[b]

Native *Lc*GUS30 was purified from cell-free extracts of *L. brevis* subsp. *coagulans*. Purification was carried out by monitoring baicalin-hydrolyzing activity, as described under EXPERIMENTAL PROCEDURES.

[a] The yield of each step was calculated based on the cell-free extract sample.

[b] The yields of the steps calculated based on the Mono Q 10/100 GL sample were written in parentheses.

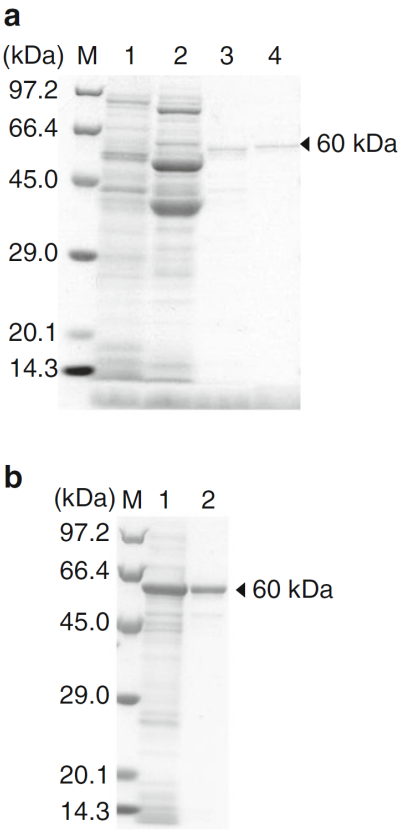

Figure 2. (a) SDS-PAGE analysis of fractions from the purification procedure. Lane M, molecular mass standards: from the top, phosphorylase b (97 kDa), bovine serum albumin (66 kDa), ovalbumin (45 kDa), carbonic anhydrase (30 kDa), trypsin inhibitor (20 kDa), and lysozyme (14 kDa). Lane 1, cell-free extracts. Lane 2, Mono Q 10/100 GL fraction. Lane 3, HiLoad 26/600 Superdex 200 fraction. Lane 4, Mono Q 5/50 GL fraction. The arrow indicates a 60-kDa protein applied to NH_2-terminal amino acid sequence analysis. (b) SDS-PAGE analysis of the recombinant *Lc*GUS30. Lane M, molecular mass standards. Lane 1, cell-free extracts of *E. coli* transformant. Lane 2, the purified recombinant *Lc*GUS30.

***Purification and identification of the enzyme (LcGUS30) converting baicalin to baicalein from* L. brevis *subsp.* coagulans**−The author found that *L. brevis* subsp. *coagulans* transforms baicalin to baicalein (Fig. 1b). The enzyme converting baicalin to baicalein was purified from *L. brevis* subsp. *coagulans* through three successive steps of separation by monitoring the baicalin hydrolytic activity. The purification process is summarized in Table 1. The purification increased the specific activity 1,800-fold, and the purification yield was found to be only 0.47%. The final preparation gave a single band on SDS-PAGE (Fig. 2a, lane 4), and its molecular mass was estimated to be 60 kDa. The k_{cat}, K_m, and k_{cat}/K_m values of this enzyme were as follows: for baicalin hydrolysis, 21.3 ± 3.2 s^{-1}, 1.52 ± 0.43 mM, and 14.0 ± 2.0 $mM^{-1}s^{-1}$ and for *p*NP-GlcA hydrolysis, 53.7 ± 1.5 s^{-1}, 0.154 ± 0.016 mM, and 348 ± 30 $mM^{-1}s^{-1}$, respectively.

Furthermore, the author determined the NH_2-terminal amino acid sequence of the purified enzyme, which revealed the following sequence: MKKFQHEFWTATSGD. A BLAST search (25) on this sequence indicated that this protein shows 100% sequence homology with an *O*-glycosyl hydrolase from *L. brevis* ATCC 367 (ABJ65276.1) (LVIS_2226), molecular weight of 56 kDa, length of 510 amino acids. Next, the author obtained the gene encoding this enzyme using the genomic DNA of *L. brevis* subsp. *coagulans* as a template and PCR primers based on LVIS_2226. The cloned gene consists of

Figure 3. Sequence alignment of *Lc*GUS30 and glucosylceramidase (GlcCerase). The alignment was created by ClustalW (http://clustalw.ddbj.nig.ac.jp/top-j.html). Residues important for catalysis are shown in closed circles. The residues interacting with the C6 hydroxyl group are shown in closed squares, while other residues involved in substrate binding are shown in closed triangles. Dotted box indicates "ERRC(M/L)" and "(S/A)(T/D)GR" sequence motifs.

1,533 bp and encodes a polypeptide of 56 kDa, which showed the same amino-acid sequence as LVIS_2226, with only a silent substitution (A1425G). Figure 3 shows the amino acid sequence of this enzyme. Surprisingly, domain analysis using Pfam (26) indicated that this enzyme belongs to GH family 30, which contains glucosylceramidase (GlcCerase, EC 3.2.1.45), β-1,6-glucanase (EC 3.2.1.75), β-xylosidase (EC 3.2.1.37), β-fucosidase (EC 3.2.1.38), β-glucosidase (EC 3.2.1.21), and endo-β-1,6-galactanase (EC 3.2.1.164), but does not contain GUS (13,27). This enzyme also shares much lower sequence homologies with *Ec*GUS2 (26% (18/69) identity), GUSs from *L. brevis* RO1 (*Lb*GUS2) (43% (15/35) identity), and *L. gasseri* ADH (*Lg*GUS2) (21% (8/39) identity), which belong to GH family 2, *Sb*GUS79 (belonging to GH family 79) (22% (30/134) identity), and Klotho from *M. musculus*, which belongs to GH family 1 (22% (19/86) identity).

***Expression and purification of the recombinant* Lc*GUS30 in* E. coli**−The author further investigated whether there is evidence that *Lc*GUS30 is GUS because *Lc*GUS30 shares much lower sequence homology with other GUSs that have been reported so far. To overexpress *Lc*GUS30 in *E. coli*, the *lcgus30* gene was inserted to the downstream of the IPTG-inducible T7 promoter and His_6-tag coding sequence on pET-28a vector (designated as pET28-*Lc*GUS30). *E. coli* Rosetta 2 (DE3)/pET28-*Lc*GUS30 cells were cultivated in LB medium supplemented with kanamycin and 1 mM IPTG as an inducer of T7 promoter. The SDS-PAGE analysis of the cell-free extracts prepared from the transformant showed that the recombinant *Lc*GUS30 was overexpressed abundantly compared to that from original *L. brevis* subsp. *coagulans* (Fig. 2a, lane 1 and Fig. 2b, lane 1). The recombinant *Lc*GUS30 was purified through a HisTrap HP from the cell-free extracts of *E. coli* Rosetta 2 (DE3)/pET28-*Lc*GUS30. The purified enzyme gave a single band on SDS-PAGE, and its molecular mass was estimated to be 60 kDa (Fig. 2b, lane 2). The k_{cat}, K_m, and k_{cat}/K_m values of the recombinant *Lc*GUS30 were as follows: for baicalin hydrolysis, 18.5 ± 0.6 s^{-1}, 1.74 ± 0.11 mM, and 10.6 ± 0.3 $mM^{-1}s^{-1}$ and for *p*NP-GlcA hydrolysis, 31.8 ± 0.7 s^{-1}, 0.156 ± 0.013 mM, and 204 ± 14 $mM^{-1}s^{-1}$, respectively. These values are similar to those of the native *Lc*GUS30. Therefore, the author ruled out the three possibilities that the author incorrectly cloned the enzyme converting baicalin to baicalein from *L. brevis* subsp. *coagulans*, that the author

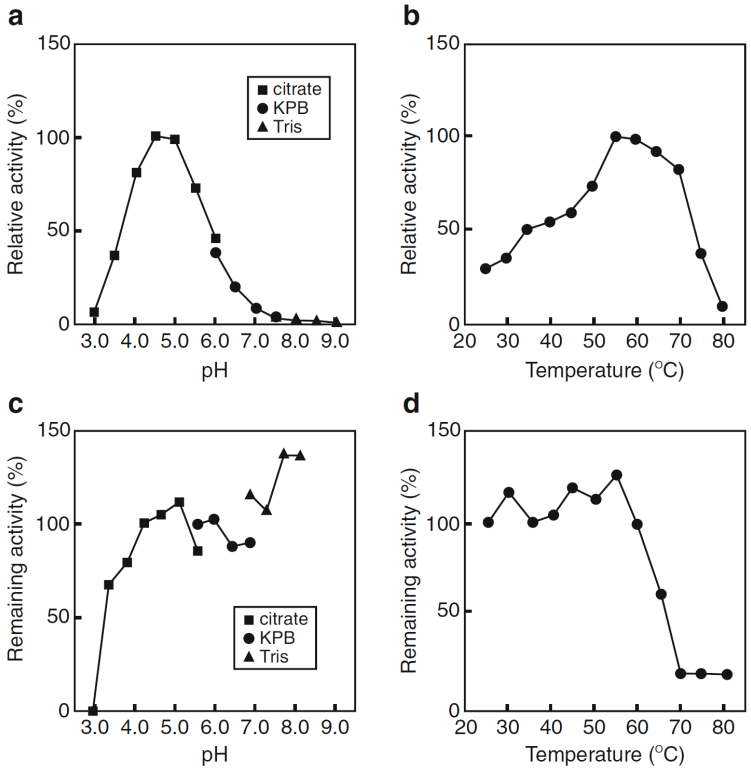

Figure 4. Physicochemical properties of the recombinant *Lc*GUS30. (a) Optimum pH value. The value at 100 mM citrate buffer (pH 4.5) was taken as 100%. The used buffers (100 mM) were citrate-NaOH buffer (closed square, pH 3.0–6.0), potassium phosphate buffer (KPB, closed circle, pH 6.0–7.5), and Tris-HCl buffer (closed triangles, pH 7.5–9.0). (b) Optimal temperature. The value at 55°C was taken as 100%. (c) pH stability. The values were determined by measuring the residual activities after dialyzing the enzyme overnight at 4°C. The value at 100 mM citrate buffer (pH 4.5) was taken as 100%. (d) Thermostability. The values were determined by measuring the residual activities after incubating the enzyme in 100 mM citrate buffer (pH 4.5) for 30 min at various temperatures. The value at 25°C was taken as 100%.

detected the activity of *Ec*GUS2 contaminated during the purification, and that N-terminal His_6-tag affects the enzyme properties.

The physicochemical property of the recombinant* Lc*GUS30−**The physicochemical property of the recombinant *Lc*GUS30 was determined using *p*NP-GlcA as a substrate. The optimum pH was 4.5 in citrate buffer (Fig. 4a). This enzyme showed below 50% of its maximal activity at pH above 6.0. The optimum temperature was at 55°C (Fig. 4b). The activity of *Lc*GUS30 was stable in the pH range between 4.5 and 9.0 (Fig. 4c) and was stable below 60°C for 30 min (Fig. 4d).

Substrate specificity of the recombinant* Lc*GUS30−**The author examined the substrate specificity of the recombinant *Lc*GUS30 using various substrates at a fixed concentration (0.5 mM) (Table 2). The used substrates were baicalin and wogonoside as flavonoid glucuronides, estrone-GlcA as a steroid glucuronide, and *p*NP-sugars, MU-GlcA, and phenolphthalein-GlcA as artificial substrates (Fig. 5). *Lc*GUS30 could hydrolyze only the substrates conjugated with glucuronic acid. No activity was detected for *p*NP-sugars except for *p*NP-GlcA, such as *p*NP-β-glucoside, *p*NP-β-xyloside, and *p*NP-β-L-fucoside, which are candidate substrates for the enzyme belonging to GH family 30. This indicated that *Lc*GUS30 is GUS that has strict glycon specificity. In contrast, *Lc*GUS30 enzyme did not show strict substrate specificity toward aglycones. However, among natural substrates, *Lc*GUS30 prefers baicalin rather than wogonoside and estrone-GlcA as a substrate.

To precisely evaluate the substrate specificity toward aglycones, the author determined the kinetic parameters for these substrates. *Lc*GUS30 showed the highest catalytic efficiency (k_{cat}/K_m value) on *p*NP-GlcA, which is 19-fold higher than that on baicalin. Compared with that toward baicalin, the catalytic efficiency toward MU-GlcA is 4-fold higher, that toward phenolphthalein-GlcA is almost comparable, and those toward wogonoside and estrone-GlcA are three- and four-fold lower, respectively. The difference between those toward baicalin and wogonoside is due to k_{cat} values. Interestingly, the K_m value toward estrone-GlcA was too high to determine, indicating the K_m value for estrone-GlcA is more than 5 mM. This value is the highest of all of used substrates. Therefore, the difference between the catalytic efficiencies toward baicalin and estrone-GlcA is due to the K_m value.

Table 2
Substrate specificity of the recombinant *Lc*GUS30

Substrate	Relative activity (%)[a]	Kinetic parameter		
		k_{cat} (s^{-1})	K_m (mM)	k_{cat}/K_m (mM^{-1} s^{-1})
Linked glucuronide				
Baicalin	100	18.5±0.6	1.74±0.11	10.6±0.3
Wogonoside	31	6.37±1.14	2.02±0.62	3.15±0.43
Estrone-β-GlcA[b]	31	n.d.	n.d.	2.58±0.12
pNP-β-GlcA	600	31.8±0.7	0.156±0.013	204±14
MU-β-GlcA	230	30.0±2.5	0.762±0.133	39.3±3.8
Phenolphthalein-β-GlcA	93	15.8±0.3	1.16±0.05	13.6±0.4
Other substrate				
pNP-α-glucopyranoside	–[c]			
pNP-β-glucopyranoside	–			
pNP-α-galactopyranoside	–			
pNP-β-galactopyranoside	–			
pNP-α-*N*-acetylglucosaminide	–			
pNP-β-*N*-acetylglucosaminide	–			
pNP-α-*N*-acetylgalactosaminide	–			
pNP-β-*N*-acetylgalactosaminide	–			
pNP-α-mannopyranoside	–			
pNP-β-mannopyranoside	–			
pNP-α-xylopyranoside	–			
pNP-β-xylopyranoside	–			
pNP-β-arabinofuranoside	–			
pNP-α-L-fucopyranoside	–			
pNP-β-L-fucopyranoside	–			

n.d. not determined.
[a] Assays were carried out in 100 mM citrate buffer (pH 5.0) including 0.5 mM of each substrate. The activity on baicalin was taken as 100%
[b] K_m value is too high to determine. Only the k_{cat}/K_m value was determined at the low substrate concentration
[c] Not detected

DISCUSSION

The GUSs from *Lactobacillus* species are thought to be useful for the construction of a safe bioconversion system of prodrugs such as baicalin, because *Lactobacillus* species are generally recognized as safe (GRAS) microorganisms. In this chapter, the author succeeded in the identification and cloning of the enzyme converting baicalin to baicalein from *L. brevis* subsp. *coagulans*, *Lc*GUS30. Surprisingly, the author revealed that *Lc*GUS30 is GUS belonging to GH family 30 and has strict glycon specificity. As mentioned above, GUSs are classified into GH families 1, 2, and 79, and therefore, the discovery of *Lc*GUS30 is the first finding of GUS belonging to GH family 30. So far, two GUSs from *Lactobacillus* (*Lg*GUS2 and *Lb*GUS2) have been reported and both of them belong to GH family 2 (21,22). It is noted that *Lc*GUS30 is not identical to *Lg*GUS2 and *Lb*GUS2 because *Lc*GUS30 shares low sequence homologies with them. In addition, the specific activity of *Lc*GUS30 (27.3 U/mg) toward *p*NP-GlcA is 20-fold higher than that of *Lb*GUS2 (1.28 U/mg, which was corrected based on the unit defined in this article) (22), and the physicochemical properties of *Lc*GUS30

differ so much from those of *Lg*GUS2, although the author could not compare with the specific activity of *Lg*GUS2, which has not been determined (21).

Three GUSs have been reported to convert baicalin to baicalein: *Lb*GUS2, *Sb*GUS79, and baicalin-β-glucuronidase from *S. viscidula* Bge, belonging to GH family 79 (*Sv*GUS79). Both *Sb*GUS79 and *Sv*GUS79 are highly specific for baicalin (18,19). This is in contrast to *Lc*GUS30. The activity of *Lc*GUS30 on baicalin is much lower than *Sb*GUS79 (k_{cat}/K_m value of 52.8 $\mu M^{-1}s^{-1}$) (18) but is similar to the value of *Sv*GUS79 (Specific activity of 9.3 U/mg, which was corrected based on the unit defined in this article) (19). A recent study applied the recombinant *Lb*GUS2 for the bioconversion of baicalin and wogonoside into their aglycones (22). The specific activities of *Lb*GUS2 on baicalin and wogonoside were ca. 0.8 and 1.3 U/mg, respectively (calculated based on the data when the concentration of baicalin and wogonoside was 0.15 and 0.125 mM, respectively (22)). In this chapter, the author demonstrated that, in addition to baicalin, *Lc*GUS30 can also convert wogonoside into wogonin. The specific activities of *Lc*GUS30 on baicalin and wogonoside were ca. 1.4 and 0.4 U/mg, respectively (predicted from each kinetic parameter when the concentration of baicalin and wogonoside were 0.15 and 0.125 mM). These values were comparable to those of *Lb*GUS2. Thus, the activity of *Lc*GUS30 on baicalin is comparable to those of other enzymes except for *Sb*GUS79; in addition, *Lc*GUS30 has the ability to convert wogonoside. Interestingly, *Lc*GUS30 could act on only baicalin contained in BOF, although BOF contains many glycosides such as paeoniflorin, sennoside A, and geniposide in addition to baicalin (data not shown). It is noted that the author established an expression and purification system of the recombinant *Lc*GUS30 in *E. coli*, which delivers high-level expression and simple purification (Fig. 2). These results indicated that the recombinant *Lc*GUS30

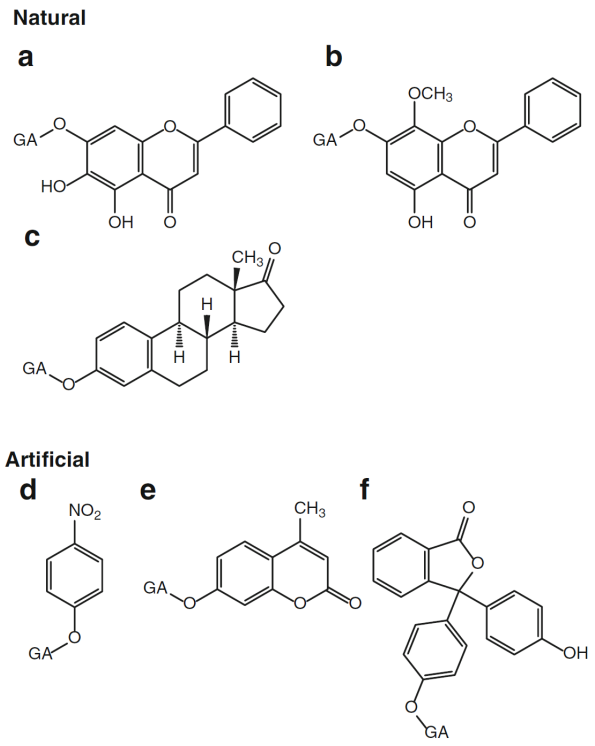

Figure 5. Structures of the following glucuronides: (a) baicalin, (b) wogonoside, (c) estrone-GlcA, (d) pNP-GlcA, (e) MU-GlcA, and (f) phenolphthalein-GlcA. GA indicates glucuronic acid.

should serve as a powerful tool for the construction of a safe bioconversion system for baicalin, wogonin, and traditional herbal medicines including them.

Despite their beneficial effects such as converting prodrugs, bacterial GUSs from human gut microbiota have detrimental effects, notably on the enterohepatic recirculation of various compounds such as steroid hormones, which contributes to a delayed elimination of them from the body (28,29). *Ec*GUS2 is one of the bacterial GUSs from human gut microbiota and is well known to be effective in the hydrolysis of steroid glucuronides. *Ec*GUS2 prefers steroid glucuronides, including estriol-3-glucuronide, rather than phenolphthalein-GlcA as a substrate (29), and its K_m value for the estriol-3-glucuronide is 0.2 mM (30,31). On the other hand, *Lc*GUS30 prefers baicalin and phenolphthalein-GlcA rather than estrone-GlcA as a substrate (Table 2). Interestingly, its K_m value for estrone-GlcA is more than 5 mM. This suggested that *Lc*GUS30 might have much less activity on steroid glucuronides than *Ec*GUS2 because both estriol and estrone have the same basic structure (steroid structure). Previous reports showed that the concentration of human endogenous steroid glucuronides in plasma is in in nanomolar order (32), suggesting that their concentration in the small intestine may be much lower than the K_m value for estrone-GlcA of *Lc*GUS30. This suggests that *Lc*GUS30 might not act on human endogenous glucuronides. In other words, *L. brevis* subsp. *coagulans* in the small intestine might act on only exogenous glucuronides but not on human endogenous glucuronides. It is noted that *L. brevis* subsp. *coagulans* has been reported to help maintain health (23). This suggested that *L. brevis* subsp. *coagulans* could be useful for enhancing the availability of baicalin and wogonoside as a precursor of baicalein and wogonin.

GH family 30 is now classified into eight subfamilies in the CAZy database (33). *Lc*GUS30 belongs to subfamily 3, because the 100%-identical LVIS_2226 is classified into subfamily 3. This subfamily currently contains 5 enzymes that have been characterized so far, which exhibit β-1,6-glucanase activity, interestingly all from fungi. However, *Lc*GUS30 does not share high sequence homologies (less than 31%) with any of these enzymes. *Lc*GUS30 was found to have 9 close homologs (>62% identity) using the BLAST search (25). Therefore, the author constructed a phylogenetic tree (Fig. 6a), and suggested that subfamily 3 can be further divided into two groups: β-1,6-glucanase and GUS groups .

GlcCerase (the *N*-nonyl-deoxynojirimycin (NND) complex structure, PDB code: 2v3e (34)) has the highest similarity (26% (118/454) identity) with *Lc*GUS30 among the GH

family 30 members whose structures have been determined so far. As shown in Fig. 3, the residues important for catalytic and substrate binding, except for the following residues, are completely conserved between GlcCerase and *Lc*GUS30, and the author deduced the candidate residues that confer the substrate specificity of *Lc*GUS30 based on GlcCerase structure. The difference between *Lc*GUS30 and GlcCerase occurs at the residues in close proximity to the C6 position of substrate sugar: S345 and N396 in GlcCerase (corresponding to T328 and S372 in *Lc*GUS30) form a hydrogen bond with the C6 hydroxyl group of the substrate sugar, where the structural difference between β-glucose (hydroxyl group) and β-glucuronic acid (carboxyl group) occurs. Interestingly, the BLAST search revealed that the amino acid sequences, "ERRC(M/L)" and "(S/A)(T/D)GR", located downstream of T328 and upstream of S372 in *Lc*GUS30, respectively, are completely conserved only in the close homologs (Fig. 6b). In the GlcCerase structure, the region corresponding to ERRC(M/L) and (S/A)(T/D)GR sequence motif of *Lc*GUS30 is located in the loop regions forming a hydrophobic patch that accepts C6 methylene group (located downstream of S345) and including N396 (interacting with the C6 hydroxyl group), respectively. In addition, as shown in Fig. 6c, the comparison with the GlcCerase and *Ec*GUS2 (the glucaro-δ-lactam inhibitor (GDL) complex structure, PDB code: 3k4d (35)) structures showed that the active site structure is similar with GlcCerase and *Ec*GUS2, and the side chains of S345 and N396 in GlcCerase overlap with K568 and R562 in *Ec*GUS2, respectively, both of which interact with the C6 carboxyl group of β-glucuronic acid. Therefore, the author proposes that the enzymes containing ERRC(M/L) and (S/A)(T/D)GR sequence motifs form a new group having GUS activity in subfamily 3, and especially, Arg residues within these motifs might be the candidate residues that confer the substrate specificity of this group. In addition, interestingly, *L. brevis* subsp. *coagulans* was isolated from traditional pickles called "Suguki" of Kyoto, Japan, and almost of these species are the bacteria coexisting with plants. Considering that glycosidases are often required for the degradation of the sugars to obtain energy, the author postulates that this new group might have evolved to be adapted to the glucuronides in plants such as flavonoid glucuronides. The presence of this new group in subfamily 3 of GH family 30 will promote deep understanding of this family.

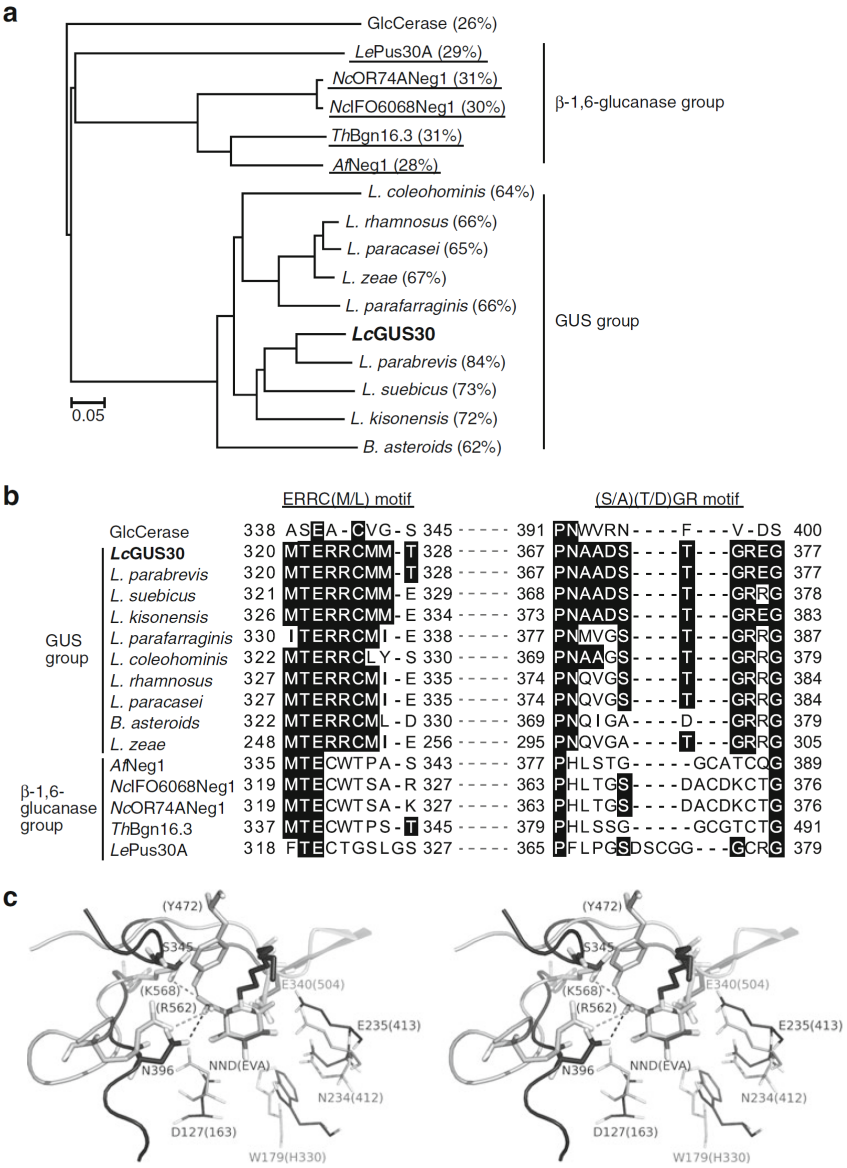

Figure 6. Classification of subfamily 3 in GH family 30. (a) The phylogenetic analysis. The phylogenetic tree was constructed using the ClustalW program with a neighbor-joining method (http://clustalw.ddbj.nig.ac.jp/top-j.html). The sequence identities of the enzymes with *Lc*GUS30 (shown in bold text) are shown in parenthesis. The characterized GH family 30 members, shown in underline, were β-1,6-glucanases from *Aspergillus fumigatus* (*Af*Neg1, 28% (121/431) identity), *Neurospora crassa* IFO6068 (*Nc*IFO6068Neg1, 30% (122/409) identity), *N. crassa* OR74A (*Nc*OR74ANeg1, 31% (126/409) identity), *Trichoderma harzianum* (*Th*Bgn16.3, 31% (123/392) identity), and *Lentinula edodes* (*Le*Pus30A, 29% (139/486) identity). The close homologs with *Lc*GUS30 were the enzymes from *Lactobacillus parabrevis* (84% (427/509) identity), *Lactobacillus suebicus* (isolated from apple and pear) (73% (374/510) identity), *Lactobacillus kisonensis* (isolated from sunki pickles) (72% (366/506) identity), *Lactobacillus parafarraginis* (isolated from shochu residue) (66% (337/508) identity), *Lactobacillus zeae* (isolated from wine) (67% (294/439) identity), *Lactobacillus coleohominis* (isolated from human sources) (64% (326/510) identity), *Lactobacillus rhamnosus* (isolated from human sources) (66% (337/508) identity), *Lactobacillus paracasei* (isolated from Estonian semi-hard cheese) (65% (332/508) identity), and *Bifidobacterium asteroids* PRL2011 (isolated from honeybee intestine) (62% (313/508) identity). Human GlcCerase was used as an outgroup. Scale bar represents the number of amino acid substitutions per site. (b) Partial sequence alignment involving in "ERRC(M/L)" and "(S/A)(T/D)GR" sequence motifs. Black boxes indicate the same amino acid residues as *Lc*GUS30. (c) Comparison of the active site structures of GlcCerase (black, the *N*-nonyl-deoxynojirimycin (NND) complex) and *Ec*GUS2 (light gray, the glucaro-δ-lactam inhibitor (GDL) complex) (stereoview). The numbers of the residues are shown (parenthesized for *Ec*GUS2).

REFERENCES

1. Middleton, E.Jr., Kandaswami, C., and Theoharides, T.C. (2000) The effects of plant flavonoids on mammalian cells: implications for inflammation, heart disease, and cancer. *Pharmacol Rev*. **52**, 673-751
2. Walle, T. (2004) Absorption and metabolism of flavonoids. *Free Radical Biology and Medicine* **36**, 829–837
3. Kobashi, K. and Akao, T. (1997) Relation of intestinal bacteria to pharmacological effect of glycosides. *Biosci Microflora* **16**, 1-7
4. Yim, J.S., Kim, Y.S., Moon, S.K., Cho, K.H., Bae, H.S., Kim, J. J., Park, E.K., and Kim, D.H. (2004) Metabolic activities of ginsenoside Rb1, baicalin, glycyrrhizin and geniposide to their bioactive compounds by human intestinal microflora. *Biol Pharm Bull*. **27**, 1580-1593
5. Simons, A.L., Renouf, M., Hendrich, S., and Murphy, P.A. (2005) Human gut microbial degradation of flavonoids: structure-function relationships. *J Agric Food Chem*. **53**, 4258-4263
6. Kubo, M., Kimura, Y., Odani, T., Tani, T., and Namba, K. (1981) Studies on *Scutellariae radix*. Part II: The antibacterial substance. *Planta Med*. **43**, 194-201
7. Shen, Y.C., Chiou, W.F., Chou, Y.C., and Chen, C.F. (2003) Mechanisms in mediating the anti-inflammatory effects of baicalin and baicalein in human leukocytes. *Eur J Pharmacol*. **465**, 171-181
8. Liu, J.J., Huang, T.S., Cheng, W.F., and Lu, F.J. (2003) Baicalein and baicalin are potent inhibitors of angiogenesis: Inhibition of endothelial cell proliferation, migration and differentiation. *Int J Cancer* **106**, 559-565
9. Ikemoto, S., Sugimura, K., Yoshida, N., Yasumoto, R., Wada, S., Yamamoto, K., and Kishimoto, T. (2000) Antitumor effects of *Scutellariae radix* and its components baicalein, baicalin, and wogonin on bladder cancer cell lines. *Urology* **55**, 951-955
10. Zhao, Y., Li, H., Gao, Z., Gong, Y., and Xu, H. (2006) Effects of flavonoids extracted from *Scutellaria baicalensis* Georgi on hemin-nitrite-H_2O_2 induced liver injury. *Eur J Pharmacol*. **536**, 192-199
11. Xing, J., Chen, X., and Zhong, D. (2005) Absorption and enterohepatic circulation of baicalin in rats. *Life Sci*. **78**, 140-146

12. Lai, M.Y., Hsiu, S.L., Tsai, S.Y., Hou, Y.C., and Chao, P.D. (2003) Comparison of metabolic pharmacokinetics of baicalin and baicalein in rats. *J Pharm Pharmacol*. **55**, 205-209
13. Cantarel, B.L., Coutinho, P.M., Rancurel, C., Bernard, T., Lombard, V., and Henrissat, B. (2009) The Carbohydrate-Active EnZymes database (CAZy): an expert resource for glycogenomics. *Nucleic Acids Res*. **37**, D233-D238
14. Adlercreutz, H., Martin, F., Pulkkinen, M., Dencker, H., Rimér, U., Sjöberg, N.O., and Tikkanen, M.J. (1976) Intestinal metabolism of estrogens. *J Clin Endocrinol Metab*. **43**, 497-505
15. Kuhn, J.G. (1998) Pharmacology of irinotecan. *Oncology* **12**, 39-42
16. Tohyama, O., Imura, A., Iwano, A., Freund, J.N., Henrissat, B., Fujimori, T., and Nabeshima, Y. (2004) Klotho is a novel β-glucuronidase capable of hydrolyzing steroid β-glucuronides. *J Biol Chem*. **279**, 9777-9784
17. Cha, S.K., Ortega, B., Kurosu, H., Rosenblatt, K.P., Kuro-O, M., and Huang, C.L. (2008) Removal of sialic acid involving Klotho causes cell-surface retention of TRPV5 channel via binding to galectin-1. *Proc Natl Acad Sci USA*. **105**, 9805-9810
18. Sasaki, K., Taura, F., Shoyama, Y., and Morimoto, S. (2000) Molecular characterization of a novel β-glucuronidase from *Scutellaria baicalensis* Georgi. *J Biol Chem*. **275**, 27466-27472
19. Zhang, C., Zhang, Y., Chen, J., and Liang, X. (2005) Purification and characterization of baicalin-β-D-glucuronidase hydrolyzing baicalin to baicalein from fresh roots of *Scutellaria viscidula* Bge. *Proc Biochem*. **40**, 1911-1915
20. Wilson, K.J., Hughes, S.G., and Jefferson, R.A. (1992) The *Escherichia coli* gus operon: induction and expression of the gus operon in *E. coli* and the occurrence and use of GUS in other bacteria. in *GUS protocols. Using the GUS gene as reporter of gene expression* (Gallagher, S.R., ed) pp. 7-22, Academic, San Diego
21. Russell, W.M. and Klaenhammer, T.R. (2001) Identification and cloning of *gusA*, encoding a new β-glucuronidase from *Lactobacillus gasseri* ADH. *Appl Environ Microbiol*. **67**, 1253-1261
22. Kim, H.S., Kim, J.Y., Park, M.S., Zheng, H., and Ji, G.E. (2009) Cloning and expression of β-glucuronidase from *Lactobacillus brevis* in *E. coli* and application in bioconversion of baicalin and wogonoside. *J Microbial Biotechnol*. **19**, 1650-1655

23. Kishi, A., Uno, K., Matsubara, Y., Okuda, C., and Kishida, T. (1996) Effect of the oral administration of *Lactobacillus brevis* subsp. *coagulans* on interferon-alpha producing capacity in humans. *J Am Coll Nutr*. **15**, 408-412
24. Inoue, H., Nojima, H., and Okayama, H. (1990) High efficiently transformation of *Escherichia coli* with plasmids. *Gene* **96**, 23-28
25. Altschul, S.F., Madden, T.L., Schäffer, A.A., and Zhang, J., Zhang, Z., Miller, W., and Lipman, D.J. (1997) Gapped BLAST and PSI-BLAST: a new generation of protein database search programs. *Nucleic Acids Res*. **25**, 3389-3402
26. Finn, R.D., Mistry, J., Tate, J., Coggill, P., Heger, A., Pollington, J.E., Gavin, O.L., Gunesekaran, P., Ceric, G., Forslund, K., Holm, L., Sonnhammer, E.L., Eddy, S.R., and Bateman, A. (2010) The Pfam protein families database. *Nucleic Acids Res.* **38**, D211-D222
27. St John, F.J., González, J.M., and Pozharski, E. (2010) Consolidation of glycosyl hydrolase family 30: a dual domain 4/7 hydrolase family consisting of two structurally distinct groups. *FEBS Lett*. **584**, 4435-41
28. Adlercreutz, H., Martin, F., Järvenpää, P., and Fotsis, T. (1979) Steroid absorption and enterohepatic recycling. *Contraception* **20**, 201-223
29. Graef, V., Furuya, E., and Nishikaze, O. (1977) Hydrolysis of steroid glucuronides with beta-glucuronidase preparations from bovine liver, *Helix pomatia*, and *E. coli*. *Clin Chem*. **23**, 532-535
30. Roy, A.B. (1970) Enzymological Aspects of Steroid Conjugation. in *Chemical and Biological Aspects of Steroid Conjunction* (Bernstein, S. and Soloman, S., eds) pp. 74-130, Springer, New York
31. Bowers, L.D. and Johnson, P.R. (1981) Characterization of immobilized β-glucuronidase in aqueous and mixed solvent systems. *Biochim Biophys Acta*. **661**, 100–105
32. Rémy-Martin, A., Prost, O., Nicollier, M., Burnod, J., and Adessi, G.L. (1983) Estrone sulfate concentrations in plasma of normal individuals, postmenopausal women with breast cancer, and men with cirrhosis. *Clin Chem*. **29**, 86-89
33. Aspeborg, H., Coutinho, P.M., Wang, Y., Brumer, H.3rd, and Henrissat, B. (2012) Evolution, substrate specificity and subfamily classification of glycoside hydrolase family 5 (GH5). *BMC Evol Biol*. **12**, 186
34. Brumshtein, B., Greenblatt, H.M., Butters, T.D., Shaaltiel, Y., Aviezer, D., Silman, I.,

Futerman, A.H., and Sussman, J.L. (2007) Crystal structures of complexes of *N*-butyl- and *N*-nonyl-deoxynojirimycin bound to acid β-glucosidase: insights into the mechanism of chemical chaperone action in Gaucher disease. *J Biol Chem*. **282**, 29052-29058

35. Wallace, B.D., Wang, H., Lane, K.T., Scott, J.E., Orans, J., Koo, J.S., Venkatesh, M., Jobin, C., Yeh, L.A., Mani, S., and Redinbo, M.R. (2010) Alleviating cancer drug toxicity by inhibiting a bacterial enzyme. *Science* **330**, 831-835

CHAPTER 5

Biohydrogenation of C_{20} polyunsaturated fatty acids by anaerobic bacteria

The polyunsaturated fatty acids (PUFAs) include many bioactive lipids that play an important role in the maintenance of biological functions in mammals (1,2). The vast majority of PUFAs has 2 or more *cis* double bonds that are separated from each other by a single methylene group (known as methylene-interrupted fatty acids). They include two major subgroups (the ω3 and ω6 PUFAs) that have different functions (1-3). Arachidonic acid [*cis*-5,*cis*-8,*cis*-11,*cis*-14-eicosatetraenoic acid (20:4, ω6), AA], which is the C_{20} PUFA of ω6 class and is made from linoleic acid [*cis*-9,*cis*-12-octadecadienoic acid (18:2, ω6), LA], is involved in many cellular signaling mechanisms, and is also the precursor for prostaglandin formation. On the other hand, eicosapentaenoic acid [*cis*-5,*cis*-8,*cis*-11,*cis*-14,*cis*-17-eicosapentaenoic acid (20:5, ω3), EPA], which is a C_{20} PUFAs of ω3 class and is made from α-linolenic acid [*cis*-9,*cis*-12,*cis*-15-octadecatrienoic acid (18:3, ω3)], have opposite effects to AA in addition to distinct biological role. Unlike methylene-interrupted fatty acids, rare isomers of PUFAs, which have at least two double bonds that are separated by a single carbon-carbon bond (known as conjugated fatty acids) (4-7) or 2 or more methylene groups [known as non-methylene-interrupted fatty acids (NMIFA)] (8-10), have been found in several materials including plant oil. These rare PUFAs have been also reported to show interesting physiological effects (9,11-15). Therefore, they have gained considerable attention, but natural sources rich in them are limited.

The partial hydrogenation of PUFAs is the process of converting PUFAs into the more saturated fatty acids and can produce NMIFAs from more readily available PUFAs. They can be mainly performed by chemical hydrogenation in industry and by microbial biohydrogenation in living organisms (16). Chemical partial hydrogenation is widely used to convert vegetable oils into foods such as margarine. The partial hydrogenation of vegetable oils produces various isomers of octadecenoic acid (18:1), depending on the reaction conditions. In contrast, microbial biohydrogenation can selectively produce the specific isomers (4-7). Thus, microbial biohydrogenation has several advantages over chemical hydrogenation.

Recently, some studies have found that many anaerobic bacteria, such as *Lactobacillus* species can produce conjugated linoleic acids from LA (4,17-20). Further, Kishino *et al*. have

revealed that lactic acid bacteria produce unique PUFAs from various C_{18} PUFAs through partial biohydrogenation (21-23). Thus, the biohydrogenation of C_{18} PUFAs has been widely studied. However, as far as the author knows, the biohydrogenation of other fatty acids, especially C_{20} PUFAs, has not been extensively studied so far.

These situations led the author to consider that anaerobic bacteria can produce novel PUFAs from C_{20} PUFAs through biohydrogenation. In this chapter, the author reports about the screening of anaerobic bacteria for the ability to transform C_{20} PUFAs through biohydrogenation. The author found that *Clostridium bifermentans* JCM 1386 can specifically convert AA and EPA into their partially saturated fatty acids with a *trans* double bond at ω7 position. The author further found that other C_{18} and C_{20} PUFAs were also converted in a similar manner. Thus, the author succeeded in the production of various C_{18} and C_{20} NMIFAs with a *trans* double bond at ω7 position through the biohydrogenation by *C. bifermentans* JCM 1386, leading to the development of novel potentially bioactive PUFAs.

EXPERIMENTAL PROCEDURES

Chemicals−LA and α-linolenic acid were purchased from Wako Pure Chemical (Osaka, Japan). γ-Linolenic acid (*cis*-6,*cis*-9,*cis*-12-18:3), dihomo-γ-linolenic acid [*cis*-8,*cis*-11,*cis*-14-eicosatrienoic acid (20:3)], AA, EPA, and methyl esters of LA and AA were purchased from Sigma (St. Louis, USA). Docosahexaenoic acid [*cis*-4,*cis*-7,*cis*-10,*cis*-13,*cis*-16,*cis*-19-docosahexaenoic acid (22:6), DHA] was purchased from Cayman Chemical (Mi, USA). All other chemicals used were of analytical grade and are commercially available.

Microorganism and cultivation−Anaerobic microorganisms preserved in laboratory of Fermentation Physiology and Applied Microbiology (AKU Culture Collection, Division of Applied Life Science, Faculty of Agriculture, Kyoto University, Kyoto, Japan) and those obtained from other culture collections (JCM, Japan Collection of Microorganisms, Saitama, Japan; and ATCC, American Type Culture Collection, VA, USA) were used for this chapter. The medium was GAM Broth (pH 7.0) (Nissui Pharmaceutical co., Ltd., Tokyo, Japan) supplemented with 0.03% (w/v) LA, AA or EPA. Each strain was inoculated into 15 mL of the medium in screw-capped tubes (16.5 × 215 mm) and then incubated in an anaerobic chamber (98% nitrogen and 2% hydrogen) at 37°C for 2-3 days. After the cultivation, the culture broth

was separated into supernatant and cells by centrifugation (8,000 *g*, 10 min), and the supernatant was used for lipid analysis.

Lipid analysis−Lipids were extracted from the supernatants with chloroform-methanol according to the procedure of Bligh-Dyer (24), and methylated with 4% methanolic-HCl at 50°C for 20 min. The resultant fatty acid methyl esters were extracted with *n*-hexane and analyzed by gas-liquid chromatography (GC) using a Shimadzu (Kyoto, Japan) GC-1700 gas chromatograph equipped with a flame ionization detector and a split injection system and fitted with a capillary column (ULBON HR-SS-10, 50 m × 0.25 mm I.D., Shinwa Kako, Kyoto, Japan). The column temperature was initially 180°C and was raised to 220°C at a rate of 2°C/min and maintained at that temperature for 20 min. The injector and detector were operated at 250°C. Helium was used as a carrier gas at 0.97 mL/min.

Isolation, derivatization, and identification of products−For the isolation of the newly synthesized fatty acid obtained from the 3-day culture broth of *C. bifermentans* JCM 1386 supplemented with 0.03% (w/v) AA (UK1), its methyl esters were purified by high-performance liquid chromatography (HPLC, monitored at 205 and 233 nm) using a Shimadzu LC-VP system fitted with a Cosmosil column 5C18-ARII (20 × 250 mm, Nacalai tesque, Kyoto, Japan). The mobile phase was acetonitrile-water (80:20, *v*/*v*) at a flow rate of 5.0 mL/min and the column temperature of 30°C. The fraction containing UK1 was further purified by HPLC on Inertsil ODS SQ5-1385 (4.6 × 250 mm, GL Science Inc., CA, USA) joined with Capcelpak C18 UG20 (4.6 × 250 mm, Shiseido, Tokyo, Japan). Acetonitrile-water (80:20, *v*/*v*) was used as the mobile phase at a flow rate of 1.2 mL/min. For the isolation of the newly synthesized fatty acid obtained from the 3-day culture broth of *C. bifermentans* JCM 1386 supplemented with 0.02% (w/v) EPA (UK2), its methyl esters were purified using a same procedure as described for UK1 except that the mobile phase used for the latter step was acetonitrile-water (80:20, *v*/*v*) at a flow rate of 1.0 mL/min.

The chemical structures of purified fatty acids were determined by mass spectroscopy (MS), proton nuclear magnetic resonance (^{1}H-NMR), ^{1}H-^{1}H-chemical shift correlation spectroscopy (COSY), two-dimensional nuclear Overhauser effect spectroscopy (NOESY), and ^{1}H clean-total correlation spectroscopy (TOCSY).

^{1}H-NMR, ^{1}H-^{1}H COSY, NOESY and TOCSY analyses−All NMR experiments were performed on a BrukerBiospin DX-750 (750 MHz for ^{1}H) and chemical shifts were assigned relative to the solvent signal (dichloromethane-d_2).

Preparation of pyrrolidide fatty acids−Pyrrolidide derivatives were prepared by direct treatment of the isolated methyl esters with pyrrolidine-acetic acid (10:1, *v*/*v*) in screw-cap tubes for 1 h at 115°C followed by extraction according to the method of Andersson and Holman (25). The organic extract was washed with water and dried over anhydrous Na_2SO_4, and then the solvent was removed by a vacuum in a rotary evaporator.

GC-MS analysis−GC-MS QP5050 (Shimadzu) with a GC-17A gas chromatograph was used for mass spectral analysis. The GC separation of the methyl ester and the pyrrolidide derivatives was performed on an ULBON HR-1 column (25m × 0.5 mm, Shinwa Kako) at 300°C. MS was used in the electron impact mode at 70 eV with a source temperature of 250°C. Split injection was employed with the injector port at 250°C.

MS-MS analysis−MS-MS analyses were performed on the free acids of the fatty acids with a JEOL-HX110A/HX110A tandem mass spectrometer. The ionization method was fast atom bombardment (FAB), and the acceleration voltage was 3 kV. Glycerol was used for the matrix.

RESULTS

Screening of anaerobic bacteria that have the ability to convert PUFAs−The ability of anaerobic bacteria to convert PUFAs conversion during cultivation was investigated. First, about 100 strains, which belonged to genera of *Megasphaera*, *Bifidobacterium*, *Lactobacillus*, *Propionibacterium*, *Clostridium*, *Bacteroides*, *Eubacterium*, and so on, were tested with LA as the substrate. The peaks of the PUFAs were identified by comparison with the retention time of the reference standards on GC analysis. Of these bacteria, 5 strains belonging to the genera of *Clostridium* and *Propionibacterium* were found to have the ability to convert LA to vaccenic acid (*trans*-11-18:1, VA) (Table 1). Figure 1a shows the GC chromatogram of methylated fatty acids produced by *C. bifermentans* JCM 1386. Next, the ability to transform

AA and EPA instead of LA was examined for these 5 strains (see Table 1). When *C. bifermentans* JCM 1386 was cultured with AA or EPA, newly generated fatty acids [UK1 from AA (Fig. 1b) and UK2 from EPA (Fig. 1c)] were detected on the GC chromatogram of methylated fatty acids. The same reactions were observed when *C. bifermentans* JCM 7832 was cultured with AA or EPA (Table 1). However, *C. sporogenes* JCM 7849, *C. sporogenes* JCM 7850, and *P. acnes* JCM 6473 couldn't convert AA and EPA. These indicated that two *C. bifermentans* strains, JCM 1386 and JCM 7832, could convert AA and EPA into unknown fatty acids, UK1 and UK2, respectively. As the concentration of both PUFAs added grew, *C. bifermentans* JCM1386 showed higher activity than *C. bifermentans* JCM 7832 (data not shown). *C. bifermentans* JCM1386 was used for further analyses.

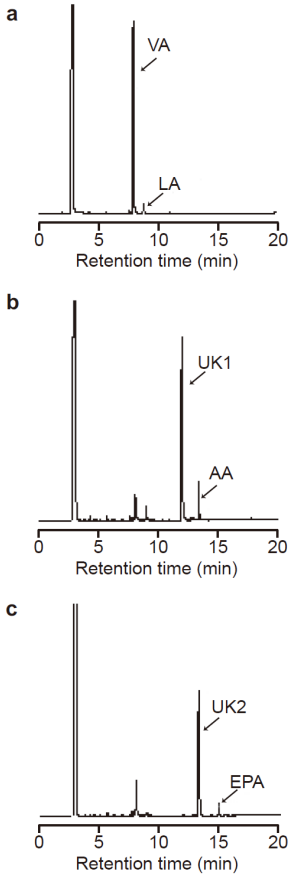

Figure 1. GC chromatograms of methyl esters of fatty acids produced by *C. bifermentans* JCM 1386. Cultivations were carried out in GAM medium with 0.03% (w/v) of linoleic acid (LA) (a), arachidonic acid (AA) (b), or eicosapentaenoic acid (EPA) (c) for 3 days. The lipid products were extracted from the supernatant and methylated as described in EXPERIMENTAL PROCEDURES. LA, AA and EPA are converted to vaccenic acid (VA), UK1 and UK2, respectively.

Table 1 Screening results for the ability of transforming polyunsaturated fatty acids

Strain	No.	Produced fatty acid (mg/mL culture broth)		
		VA from LA	UK1 from AA	UK2 from EPA
Clostridium bifermentans	JCM 1386	0.06	0.12	0.11
Clostridium bifermentans	JCM 7832	0.05	0.13	0.10
Clostridium sporogenes	JCM 7849	0.11	-	-
Clostridium sporogenes	JCM 7850	0.16	-	-
Propionibacterium acnes	JCM 6473	0.12	-	-

Cultivations were carried out in GAM medium with 0.03% (w/v) of linoleic acid (LA), arachidonic acid (AA) or eicosapentaenoic acid (EPA) for 3 days as described in EXPERIMENTAL PROCEDURES. -, not detected. VA, vaccenic acid.

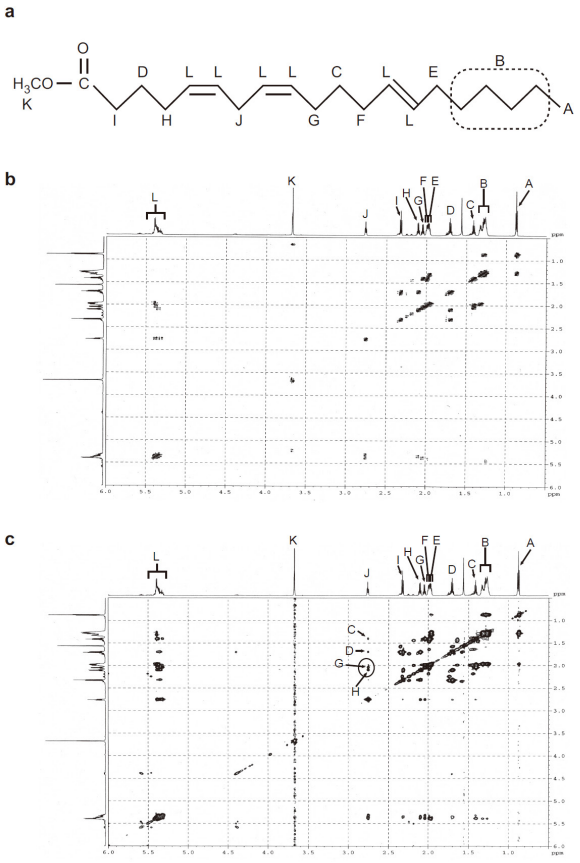

Figure 2. ^{1}H-NMR analysis of UK1 and structure of UK1 identified. (a) Structure of methyl ester of UK1. (b) ^{1}H-^{1}H-Chemical shift correlation spectroscopic (COSY) spectrum of the methyl ester of UK1. (c) ^{1}H Clean-total correlation spectroscopic (TOCSY) spectrum of the methyl ester of UK1.

Identification of the newly synthesized fatty acid obtained from AA−The mass spectrum of the isolated methyl ester of UK1 produced from AA exhibited a molecular weight of *m/z* 320, indicating that UK1 is C_{20} PUFA containing three double bonds. The molecular ion peak ($[M\text{-}Na]^{+}$, 343) obtained by FAB-MS analysis (FAB^{+}) of the methyl ester of UK1 was fragmented again by MS-MS [*m/z* (FAB^{+}, 8.00kV), 328(1), 314(2), 300(2), 299(3), 286(3), 285(4), 272(12), 258(1), 257(2), 232(3), 218(3), 217(28), 204(33), 190(1), 189(1), 164(35), 163(12), 150(3), 149(4), 124(5), 110(13), 109(68), 96(100), 82(6), and 81(40)]. The *m/z* 124, 150, 164, 190, 232, and 258 were derived from cleavage between single bonds 4-5, 6-7, 7-8, 9-10, 12-13, and 14-15, as numbered from the carboxyl group. The *m/z* 110, 150, 164, 204, 218, and 272 derived from the cleavage of single bonds between the α and β positions from the double bonds were detected. On the basis of the results of MS analyses, UK1 was identified as the geometrical isomers of 5, 8, and 13-20:3.

^{1}H-NMR analysis also suggested that UK1 is an isomer of 20:3 (see Fig. 2). The signal L intensity (5.36 ppm, *m*, 6H) indicates the existence of three double bonds in UK1. The sequence of the protons from the methyl end of the molecule was deduced A, B, E, L, L, J, L, L, G, C, F, L, L, H, D, and I or A, B, E, L, L, F, C, G, L, L, J, L, L, H, D, and I based on the signal pattern of interaction between adjacent protons observed by ^{1}H-^{1}H COSY analysis (see Fig. 2b). The sequence was confirmed as the latter one by the appearance of an interaction signal between J and H, but not J and E in TOCSY analysis (see Fig. 2c).

Furthermore, NOESY analysis identified that the geometric configurations of double bounds of Δ5 and Δ8 positions are in the *cis* configuration and Δ13 position is in the *trans* configuration (data not shown). On the basis of the results of the above spectral analyses, UK1 was identified as *cis*5,*cis*-8,*trans*-13-20:3 (see Fig. 2a).

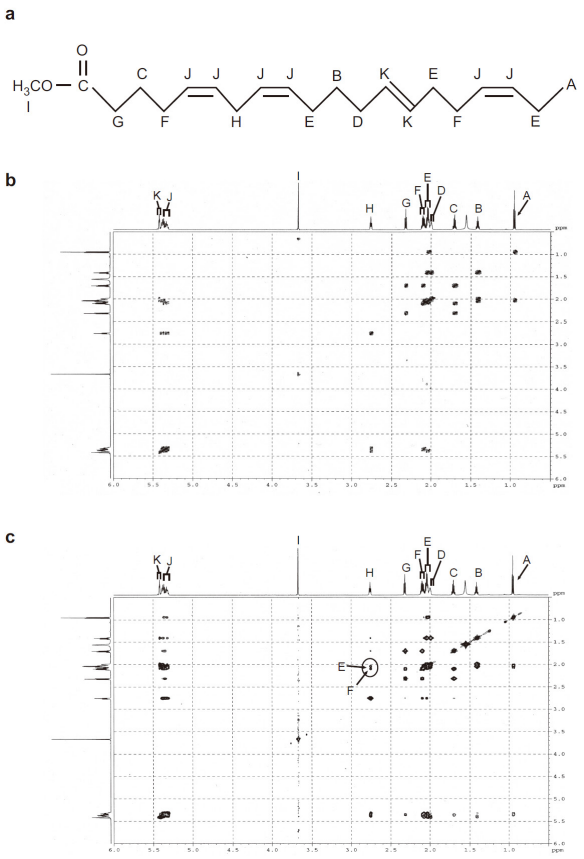

Figure 3. ^{1}H-NMR analysis of UK2 and structure of UK2 identified. (a) Structure of methyl ester of UK2. (b) ^{1}H-^{1}H-Chemical shift correlation spectroscopic (COSY) spectrum of the methyl ester of UK2. (c) ^{1}H Clean-total correlation spectroscopic (TOCSY) spectrum of the methyl ester of UK2.

Identification of the newly synthesized fatty acid obtained from EPA−The mass spectrum of the isolated methyl ester of UK2 exhibited a molecular weight of *m/z* 318. This result suggested that UK2 is C_{20} PUFAs containing four double bonds. The molecular ion peak ($[M+Na]^+$, 341) obtained by FAB-MS analysis (FAB^+) of the methyl ester of UK2 was fragmented again by MS-MS [*m/z* (FAB^+, 8.00kV), 326(4), 312(1), 311(1), 286(2), 272(6), 271(11), 258(1), 257(1), 232(2), 218(2), 217(22), 204(18), 190(1), 164(22), 150(2), 149(7), 124(5), 110(10), 109(57), 96(100), 82(4), 81(28)]. The *m/z* 124, 150, 164, 190, 232, 258, 286, and 312 were derived from the cleavage of single bonds 4-5, 6-7, 7-8, 9-10, 12-13, 14-15, 16-17, and 18-19 as numbered from carboxyl group. The *m/z* 110, 150, 164, 204, 218, 272, and 326 derived from the cleavage of single bonds between the α and β positions from the double bonds were detected. On the basis of the results of MS analyses, UK2 was identified as the geometrical isomers of 5,8,13,17-20:4. ^{1}H-NMR analysis also suggested that UK2 is an isomer of 20:4 (Fig. 3). The signals J (5.35 ppm, *m*, 6H) and K (5.42 ppm, *m*, 2H) indicate the existence of four double bonds in UK2. The sequence of the protons from the methyl end of the molecule

was deduced A, E, J, J, F, E, K, K, D, B, E, J, J, H, J, J, F, C, and G based on the integration of COSY and TOCSY analyses (see Fig. 3b,c). NOESY analysis was carried out to identify the geometric configurations of double bonds. The interaction signals appeared between F and H, H and E, and, F and E, suggesting that the three double bonds of Δ5, Δ8, and Δ17 position are all in *cis* configuration, whereas no interaction signal appeared between D and E, suggesting that the double bond of Δ13 position is in the *trans* configuration (data not shown). On the basis of the results of the above spectral analyses, UK2 was identified as *cis*5,*cis*-8,*trans*-13,*cis*-17-20:4 (see Fig. 3a).

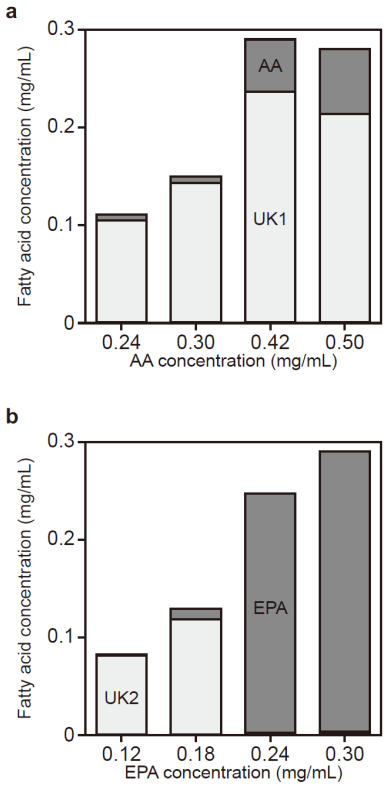

Figure 4. Effects of fatty acid concentration for medium on fatty acids transformation by *C. bifermentans* JCM 1386. (a) **A**rachidonic acid (AA) and (b) eicosapentaenoic acid (EPA). Cultivations were carried out with different concentrations of AA or EPA.

Effects of AA and EPA concentration in the medium on their transformation by* C. bifermentans *JCM 1386−Effects of AA and EPA concentration on their transformation by *C. bifermentans* JCM1386 were investigated (see Fig. 4). When various concentrations of AA were added to the media, the amount of UK1 production increased with increasing concentration of AA up to 0.42 mg/mL, giving a yield of 57% (0.24 mg/mL) with 82% purity against the added AA (0.42 mg/mL) (see Fig. 4a). When various concentrations of EPA were added to the medium, the amount of UK2 production increased with increasing concentration of EPA up to 0.18 mg/mL, giving a yield of 67% (0.12 mg/mL) with 92% purity against the added EPA (0.18 mg/mL) (see Fig. 4b). However, *C. bifermentans* JCM 1386 no longer produced UK2 when more than 0.24 mg/mL EPA was added.

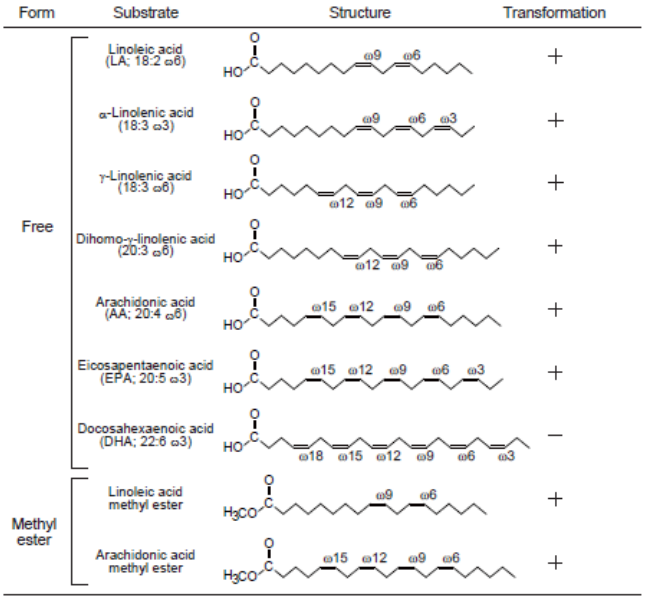

Figure 5. Transformation of polyunsaturated fatty acids by *C. bifermentans* JCM 1386

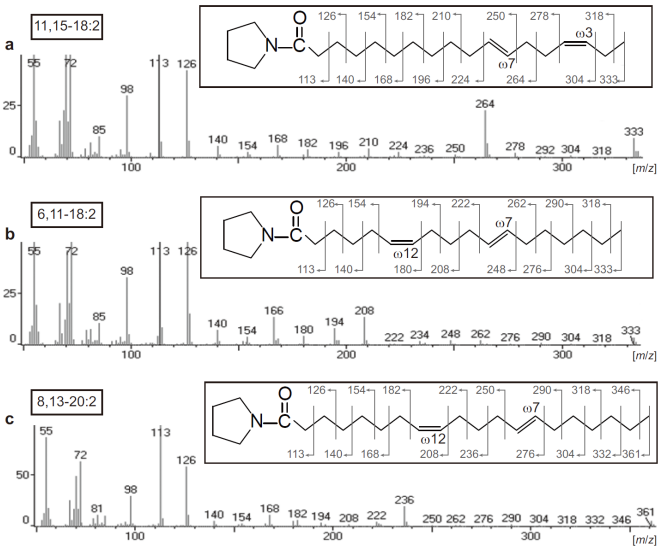

Figure 6. GC-MS spectra of pyrrolidide derivatives of the products from α-linolenic acid (a), γ-linolenic acid (b), and dihomo-γ-linolenic acid (c). The deduced structures are shown above the spectra.

Substrate specificity of polyunsaturated fatty acid transformation by* C. bifermentans *JCM 1386–To examine the substrate specificity of PUFAs transformation during the cultivation of *C. bifermentans* JCM 1386, free fatty acids of LA, α-linolenic acid, γ-linolenic acid, dihomo-γ-linolenic acid, AA, EPA, and DHA, and methyl esters of LA and AA were added to the medium (see Fig. 5). *C. bifermentans* JCM 1386 could convert LA, AA, EPA, α-linolenic acid, γ-linolenic acid, and dihomo-γ-linolenic acid. However, when DHA was added, no product was detected. The products from α-linolenic acid, γ-linolenic acid, and dihomo-γ-linolenic acid were analyzed by GC-MS (see Fig. 6). The spectrum of pyrrolidide derivative of the product from α-linolenic acid showed a molecular weight of *m/z* 333 and gaps of 26 amu between *m/z* 224 and 250, and between *m/z* 278 and 304, indicating that this is a C_{18} PUFA with double bonds at ω3 and ω7 positions (11,15-18:2) (see Fig. 6a). The pyrrolidide derivative of the product from γ-linolenic acid showed a molecular weight of *m/z* 333 and gaps of 26 amu between *m/z* 154 and 180, and between *m/z* 222 and 248, indicating that the product is a C_{18} PUFA with double bonds at ω7 and ω12 positions (6,11-18:2) (Fig. 6b). The pyrrolidide derivative of the product from

dihomo-γ-linolenic acid showed a molecular weight of *m/z* 361 and gaps of 26 amu between *m/z* 182 and 208, and between *m/z* 250 and 276, indicating that the product is a C_{20} PUFA with double bonds at *ω*7 and *ω*12 positions (8,13-20:2) (Fig. 6c). Thus, *C. bifermentans* JCM 1386 could eliminate one of the double bonds in each PUFA. Moreover, the methyl esters of LA and AA were also converted in a similar manner as their free fatty acids. These indicated that C_{18} and C_{20} PUFAs and these methyl esters with double bonds at *ω*6 and *ω*9 positions are converted into corresponding NMIFAs by *C. bifermentans* JCM 1386 (see Fig. 7). However, it was not clear whether the methyl ester transformation involves hydrolysis of methyl esters or direct conversion of methyl esters as an initial reaction.

DISCUSSION

The studies on PUFAs conversion by anaerobic bacteria have been done with the primary aim to improve the quality of the ruminant products such as milk or meat. In the course of these studies, numerous PUFA-transforming bacteria, such as *Butyrivibrio fibrisolvens* (4), *Lactobacillus plantarum* (20-23), and *Bifidobacterium breve* (19), have been isolated, and their metabolic pathways of C_{18} PUFAs, such as LA and α-linolenic acid, have been revealed. However, the ability to transform C_{20} and C_{22} PUFAs has not been studied in detail, although there have been several reports that EPA and DHA are hydrogenated in the rumen *in vivo* (26) and disappear during incubations *in vitro* with mixed ruminal microorganisms (27,28).

In this chapter, the author found that *C. bifermentans* JCM 1386 could specifically convert AA and EPA into *cis*-5,*cis*-8,*trans*-13-20:3 and *cis*-5,*cis*-8,*trans*-13,*cis*-17-20:4, respectively, which are NMIFAs with a *trans* double bond at ω7 position (see Figs. 4 and 7). This is the first report of the isolation of the bacterium transforming C_{20} PUFAs into corresponding NMIFAs. Considering that similar reactions were observed with LA (see Fig. 1a), this strain can specifically convert two *cis* double bonds at ω6 and ω9 positions in PUFAs into a *trans* double bond at ω7 position to generate the *trans* fatty acids regardless of the existence of double bonds at other positions. In addition, similar reactions were also observed of other C_{18} and C_{20} free PUFAs (α-linolenic acid, γ-linolenic acid, and dihomo-γ-linolenic acid) or the methyl esters of LA and AA (see Fig. 5). They might be converted into the corresponding NMIFAs with a *trans* double bond at ω7 position. However, *C. bifermentans*

JCM 1386 could not convert DHA, indicating that C_{22} PUFAs might not be a substrate for this strain. Thus, the author succeeded in the production of various C_{18} and C_{20} NMIFAs with a *trans* double bond at ω7 position through the biohydrogenation by *C. bifermentans* JCM 1386.

NMIFAs are a class of PUFAs that has received attention because of their unique structure and physiological activity, and they have often been found in plant oils. Pinolenic acid (*cis*-5,*cis*-9,*cis*-12-18:3) and columbinic acid (*trans*-5,*cis*-9,*cis*-12-18:3) are C_{18} NMIFAs that were found in *Pinus koraiensis* and *Aquilegia hybrida*, respectively (8,9). They are isomers of γ-linolenic acid and show various effects, such as the reduction of platelet aggregation by prostacyclin production, attenuation of the elevation of blood pressure, LDL-lowering and essential fatty acid activity (9,11,12). Podocarpic acid (*cis*-5,*cis*-11,*cis*-14-20:3) is a C_{20} NMIFA that was found in *Platycladus orientalis* oil (10). It has been reported to show a reduction in the AA concentration in the phosphatidylinositol fraction of rat liver (13), which functions in signal transduction, such as in the phospholipase C-signaling pathway (13,29). Considering that PUFAs often show an isomer-specific function, novel NMIFAs are expected to show novel interesting physiological effects. Interestingly, several natural plant oils have a high content of PUFAs with a double bond at ω7 position (30), and the biohydrogenation of PUFAs often produce PUFAs with a double bond at ω7 position, such as VA (6,7). These observations enable the author to consider that a double bond at ω7 position may become a key factor for a biological function. In this context, various C_{18} and C_{20} NMIFAs obtained in this chapter could be worthwhile. It is also noted that these NMIFAs were obtained in the high yield (approximately 60%) and purity (> 80%). Therefore, this chapter could serve to open up the development of novel methods in the preparation of theses rare possibly bioactive PUFAs.

Lipid metabolism by anaerobic bacteria is an attractive research area from the viewpoint of the role of the gut microbiota in relation to health of the host. Interestingly, obesity induced by a high-fat diet has been suggested as being associated with alterations of gut microbiota composition (31,32). Dietary fats are metabolized by gut microbiota as well as by the host. It is noted that the biohydrogenation of fatty acids might function as a detoxification mechanism in bacteria, and PUFAs especially are more toxic than saturated fatty acids (18,33). This suggests that the ability of the biohydrogenation of PUFAs might relate to the survival of gut bacteria when dietary intake of PUFAs is high. In addition, our

recent research suggested the possibility that lipid metabolism by gut microbiota affects the host's health by modifying fatty acid composition (23). Therefore, the evidence-based studies on the lipids metabolism by gut bacteria, including *C. bifermentans* (in this chapter) and *Lactobacillus* (21-23,34), should serve to maintain and improve human health.

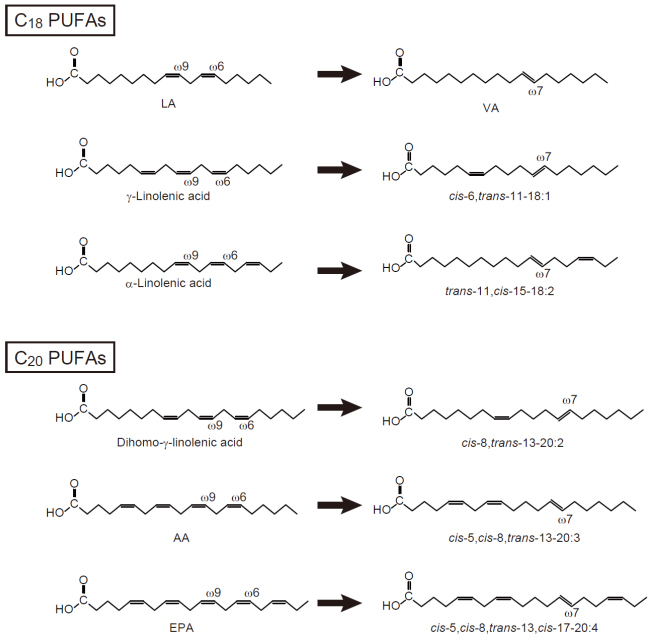

Figure 7. Pathway of polyunsaturated fatty acid transformation during cultivation of *C. bifermentans* JCM 1386. LA, linoleic acid. VA, vaccenic acid. AA, arachidonic acid. EPA, eicosapentaenoic acid.

REFERENCES

1. Benatti, P., Peluso, G., Nicolai, R., and Calvani, M. (2004) Polyunsaturated fatty acids: biochemical, nutritional and epigenetic properties. *J Am Coll Nutr*. **23**, 281-302
2. Spector, A.A. (1999) Essentiality of fatty acids. *Lipids* **34**, S1-S3
3. Lands, W.E. (2000) Stories about acyl chains. *Biochim Biophys Acta*. **1483**, 1-14
4. Kepler, C.R., Hirons, K.P., McNeill, J.J., and Tove, S.B. (1966) Intermediates and products of the biohydrogenation of linoleic acid by *Butyrinvibrio fibrisolvens*. *J Biol Chem*. **241**, 1350-1354
5. Wilde, P.F. and Dawson, R.M. (1966) The biohydrogenation of alpha-linolenic acid and oleic acid by rumen micro-organisms. *Biochem J*. **98**, 469-475
6. Harfoot, C.G. and Hazlewood, G.P. (1997) Lipid metabolism in the rumen. in *The Rumen Microbial Ecosystem* (Hobson, P.N. and Stewart, C.S., ed) pp. 382-426, Blackie Academic Progessional, London, UK.

7. Lawson, R.E., Moss, A.R., and Givens, D.I. (2001) The role of dairy products in supplying conjugated linoleic acid to man's diet: a review. *Nutr Res Rev*. **14**, 153-172
8. Wolff, R.L. and Bayard, C.C. (1995) Fatty acid composition of some pine seed oils. *J Am Oil Chem Soc*. **72**, 1043-1046
9. Houtsmuller, U.M. (1981) Columbinic acid, a new type of essential fatty acid. *Prog Lipid Res*. **20**, 889-896
10. Takagi, T. and Itabashi, Y. (1982) *cis*-5-Olefinic unusual fatty acids in seed lipids of gymnospermae and their distribution in triacylglycerols. *Lipids* **17**, 716-723
11. Sugano, M., Ikeda, I., Wakamatsu, K., and Oka, T. (1994) Influence of Korean pine (*Pinus koraiensis*)-seed oil containing *cis*-5,*cis*-9,*cis*-12-octadecatrienoic acid on polyunsaturated fatty acid metabolism, eicosanoid production and blood pressure of rats. *Br J Nutr*. **72**, 775-783
12. Lee, J.W., Lee, K.W., Lee, S.W., Kim, I.H., and Rhee, C. (2004) Selective increase in pinolenic acid (all-*cis*-5,9,12-18:3) in Korean pine nut oil by crystallization and its effect on LDL-receptor activity. *Lipids* **39**, 383-387
13. Berger, A. and German, J.B. (1991) Extensive incorporation of dietary delta-5,11,14 eicosatrienoate into the phosphatidylinositol pool. *Biochim Biophys Acta*. **1085**, 371-376
14. Pariza, M.W., Park, Y., and Cook, M.E. (2001) The biologically active isomers of conjugated linoleic acid. *Prog Lipid Res*. **40**, 283-298
15. Toomey, S., McMonagle, J., and Roche, H.M. (2006) Conjugated linoleic acid: a functional nutrient in the different pathophysiological components of the metabolic syndrome? *Curr Opin Clin Nutr Metab Care* **9**, 740-747
16. Menaa, F., Menaa, A., Tréton, J., and Menaa, B. (2013) Technological approaches to minimize industrial *trans* fatty acids in foods. *J Food Sci*. **78**, R377-R386
17. Mosley, E.E., Powell, G.L., Riley, M.B., and Jenkins, T.C. (2002) Microbial biohydrogenation of oleic acid to *trans* isomers *in vitro*. *J Lipid Res*. **43**, 290-296
18. Jiang, J., Björck, L., and Fondén, R. (1998) Production of conjugated linoleic acid by dairy starter cultures. *J Appl Microbiol*. **85**, 95-102
19. Coakley, M., Ross, R.P., Nordgren, M., Fitzgerald, G., Devery, R., and Stanton, C. (2003) Conjugated linoleic acid biosynthesis by human-derived Bifidobacterium species. *J Appl Microbiol*. **94**, 138-145

20. Ogawa, J., Kishino, S., Ando, A., Sugimoto, S., Mihara, K., and Shimizu, S. (2005) Production of conjugated fatty acids by lactic acid bacteria. *J Biosci Bioeng*. **100**, 355-364
21. Kishino, S., Ogawa, J., Yokozeki, K., and Shimizu, S. (2009) Metabolic diversity in biohydrogenation of polyunsaturated fatty acids by lactic acid bacteria involving conjugated fatty acid production. *Appl Microbiol Biotechnol*. **84**, 87-97
22. Kishino, S., Ogawa, J., Ando, A., Yokozeki, K., and Shimizu, S. (2010) Microbial production of conjugated gamma-linolenic acid from gamma-linolenic acid by *Lactobacillus plantarum* AKU 1009a. *J Appl Microbiol*. **108**, 2012-2018
23. Kishino, S., Takeuchi, M., Park, S.B., Hirata, A., Kitamura, N., Kunisawa, J., Kiyono, H., Iwamoto, R., Isobe, Y., Arita, M., Arai, H., Ueda, K., Shima, J., Takahashi, S., Yokozeki, K., Shimizu, S., and Ogawa, J. (2013) Polyunsaturated fatty acid saturation by gut lactic acid bacteria affecting host lipid composition. *Proc Natl Acad Sci USA*. **110**, 17808-17813
24. Bligh, E.G. and Dyer, W.J. (1959) A rapid method of total lipid extraction and purification. *Can J Biochem Physiol*. **37**, 911-917
25. Andersson, B.A. and Holman, R.T. (1974) Pyrrolidides for mass spectrometric determination of the position of the double bond in monounsaturated fatty acids. *Lipids* **9**, 185-190
26. Shingfield, K.J., Kairenius, P., Arölä, A., Paillard, D., Muetzel, S., Ahvenjärvi, S., Vanhatalo, A., Huhtanen, P., Toivonen, V., Griinari, J.M., and Wallace, R.J. (2012) Dietary fish oil supplements modify ruminal biohydrogenation, alter the flow of fatty acids at the omasum, and induce changes in the ruminal Butyrivibrio population in lactating cows. *J Nutr*. **142**, 1437-1448
27. Kairenius, P., Toivonen, V.K., and Shingfield, J. (2011) Identification and ruminal outflow of long-chain fatty acid biohydrogenation intermediates in cows fed diets containing fish oil. *Lipids* **46**, 587-606
28. AbuGhazaleh, A.A. and Jenkins, T.C. (2004) Disappearance of docosahexaenoic and eicosapentaenoic acids from cultures of mixed ruminal microorganisms. *J Dairy Sci*. **87**, 645-651
29. Rhee, S.G. (2001) Regulation of phosphoinositide-specific phospholipase C. *Annu Rev Biochem*. **70**, 281-312

30. Nguyen, H.T., Mishra, G., Whittle, E., Pidkowich, M.S., Bevan, S.A., Merlo, A.O., Walsh, T.A., and Shanklin, J. (2010) Metabolic engineering of seeds can achieve levels of omega-7 fatty acids comparable with the highest levels found in natural plant sources. *Plant Physiol*. **154**, 1897-1904
31. Bajzer, M. and Seeley, R.J. (2006) Physiology: obesity and gut flora. *Nature* **444**, 1009-1010
32. Turnbaugh, P.J., Bäckhed, F., Fulton, L., and Gordon, J.I. (2008) Diet-induced obesity is linked to marked but reversible alterations in the mouse distal gut microbiome. *Cell Host Microbe*. **3**, 213-223
33. Maia, M.R., Chaudhary, L.C., Bestwick, C.S., Richardson, A.J., McKain, N., Larson, T.R., Graham, I. A., and Wallace, R.J. (2010) Toxicity of unsaturated fatty acids to the biohydrogenating ruminal bacterium, *Butyrivibrio fibrisolvens*. *BMC Microbiol*. **10**, 52
34. Kishino, S., Park, S.B., Takeuchi, M., Yokozeki, K., Shimizu, S., and Ogawa, J. (2011) Novel multi-component enzyme machinery in lactic acid bacteria catalyzing C=C double bond migration useful for conjugated fatty acid synthesis. *Biochem Biophys Res Commun*. **416**, 188-193

SUMMARY

CHAPTER 1

Infant-gut associated bifidobacteria possess species-specific enzymatic sets to assimilate human milk oligosaccharides (HMOs), and lacto-*N*-biosidase (LNBase) is a key enzyme that degrades lacto-*N*-tetraose (LNT, Galβ1-3GlcNAcβ1-3Galβ1-4Glc), the main component of HMOs, to lacto-*N*-biose I (Galβ1-3GlcNAc) and lactose. LNBase activity in *Bifidobacterium bifidum* and some strains of *B. longum* subsp. *longum* (*B. longum*) have been previously identified. Subsequently, a glycoside hydrolase family 20 (GH20) LNBase was isolated from *B. bifidum*; however, the genome of the LNBase^{+}-strain of *B. longum* contains no GH20 LNBase homolog. Here, the author reveals that locus_tags BLLJ_1505 and BLLJ_1506 constitute LNBase from *B. longum* JCM1217. The gene products, designated LnbX and LnbY, respectively, showed no sequence similarity to previously characterized proteins. The purified enzyme, which consisted of LnbX only, hydrolyzed via a retaining mechanism the GlcNAcβ1-3Gal linkage in LNT, lacto-*N*-fucopentaose I (Fucα1-2Galβ1-3GlcNAcβ1-3Galβ1-4Glc), and sialyllacto-*N*-tetraose a (Neu5Acα2-3Galβ1-3GlcNAcβ1-3Galβ1-4Gal); the latter two are not hydrolyzed by GH20 LNBase. Among the chromogenic substrates examined, the enzyme acted on *p*-nitrophenyl (*p*NP)-β-lacto-*N*-bioside I (Galβ1-3GlcNAcβ-*p*NP) and GalNAcβ1-3GlcNAcβ-*p*NP. GalNAcβ1-3GlcNAcβ-linkage has been found in *O*-mannosyl glycans of α-dystroglycan. Therefore, the enzyme may serve as a new tool for examining glycan structures. *In vitro* refolding experiments revealed that LnbY and metal ions (Ca^{2+} and Mg^{2+}) are required for proper folding of LnbX. The LnbX and LnbY homologs have been found only in *B. bifidum*, *B. longum*, and a few gut microbes, suggesting that the proteins have evolved in specialized niches.

CHAPTER 2

Recent studies suggest that α-L-fucosidases of the glycoside hydrolase family 29 can be divided into two subfamilies based on substrate specificity and phylogenetic clustering. To explore the validity of this classification, the author enzymatically characterized two structure-solved α-L-fucosidases representing the respective subfamilies. Differences in

substrate specificities are then discussed in relationship to differences in the active-site structures between the two enzymes.

CHAPTER 3

α-L-Fucosyl residues attached at the non-reducing ends of glycoconjugates constitute histo-blood group antigens Lewis (Le) and ABO, and play fundamental roles in various biological processes. Therefore, establishing a method for synthesizing the antigens is important for functional glycomics studies. However, regiospecific synthesis of glycosyl linkages, especially α-L-fucosyl linkages, is quite difficult to control both by chemists and enzymologists. Here, the author generated an α-L-fucosynthase that specifically introduces Le^a and Le^x antigens into the type-1 and type-2 chains, respectively, *i.e.*, the enzyme specifically accepts the disaccharide structures (Galβ1-3/4GlcNAc) at the non-reducing ends and attaches a Fuc residue *via* an α-(1,4/3)-linkage to the GlcNAc. X-ray crystallographic studies revealed the structural basis of this strict regio- and acceptor-specificity, that includes the induced-fit movement of the catalytically important residues, and the difference between the active site structures of 1,3-1,4-α-L-fucosidase (EC 3.2.1.111) and α-L-fucosidase (EC 3.2.1.51) in the glycoside hydrolase family 29. The glycosynthase developed in this chapter should serve as a potentially powerful tool to specifically introduce the $Le^{a/x}$ epitopes onto labile glycoconjugates including glycoproteins. Mining glycosidases with strict specificity may represent the closest approach to the specific synthesis of glycosidic bonds.

CHAPTER 4

Baicalin (baicalein 7-*O*-β-D-glucuronide) is one of the major flavonoid glucuronides found in traditional herbal medicines. Because its aglycone, baicalein, is absorbed more quickly and shows more effective properties than baicalin, the conversion of baicalin into baicalein by β-glucuronidase (GUS) has drawn the attention of researchers. Recently, the author has found that *Lactobacillus brevis* subsp. *coagulans* can convert baicalin to baicalein. Therefore, the author aimed to identify and characterize the converting enzyme from *L. brevis* subsp. *coagulans*. First, the author purified this enzyme from the cell-free extracts of *L. brevis* subsp. *coagulans* and cloned its gene. Surprisingly, this enzyme was found to be a GUS

belonging to glycoside hydrolase (GH) family 30 (designated as *Lc*GUS30), and its amino acid sequence has little similarity with any GUS belonging to GH families 1, 2, and 79 that have been reported so far. The author then established a high-level expression and simple purification system of the recombinant *Lc*GUS30 in *Escherichia coli*. The detailed analysis of the substrate specificity revealed that *Lc*GUS30 has strict specificity toward glycon but not toward aglycones. Interestingly, *Lc*GUS30 prefers baicalin rather than estrone 3-(β-D-glucuronide), one of the human endogenous steroid hormones. These results indicated that *L. brevis* subsp. *coagulans* and *Lc*GUS30 should serve as powerful tools for the construction of a safe bioconversion system for baicalin. In addition, the author proposes that this novel type of GUS forms a new group in subfamily 3 of GH family 30.

CHAPTER 5

The polyunsaturated fatty acids (PUFAs) include many bioactive lipids. The microbial metabolism of C_{18} PUFAs is known to produce their bioactive isomers, such as conjugated fatty acids and hydroxy fatty acids, but there is little information on that of C_{20} PUFAs. In this chapter, the author aimed to obtain anaerobic bacteria for the ability to produce novel PUFA from C_{20} PUFAs. Through the screening of about 100 strains of anaerobic bacteria, *Clostridium bifermentans* JCM 1386 was selected as a strain with the ability to saturate PUFAs during anaerobic cultivation. This strain specifically converted arachidonic acid (*cis*-5,*cis*-8,*cis*-11,*cis*-14-eicosatetraenoic acid) and eicosapentaenoic acid (*cis*-5,*cis*-8,*cis*-11,*cis*-14,*cis*-17-eicosapentaenoic acid) into *cis*-5,*cis*-8,*trans*-13-eicosatrienoic acid and *cis*-5,*cis*-8,*trans*-13,*cis*-17-eicosatetraenoic acid, giving yields of 57% and 67% against the added PUFAs, respectively. This is the first report of the isolation of a bacterium transforming C_{20} PUFAs into corresponding non-methylene-interrupted fatty acids. The author further investigated the substrate specificity of the biohydrogenation by this strain and revealed that it can specifically convert two *cis* double bonds at ω6 and ω9 positions in various C_{18} and C_{20} PUFAs into a *trans* double bond at ω7 position. This chapter should serve to open up the development of novel potentially bioactive PUFAs.

LIST OF PUBLICATIONS

1. **Sakurama, H.**, Kiyohara, M., Wada, J., Honda, Y., Yamaguchi, M., Fukiya, S., Yokota, A., Ashida, H., Kumagai, H., Kitaoka, M., Yamamoto, K., and Katayama, T. (2013) Lacto-*N*-biosidase encoded by a novel gene of *Bifidobacterium longum* subsp. *longum* shows unique substrate specificity and requires a designated chaperon for its active expression. *J Biol Chem.* **288**, 25194-25206
2. **Sakurama, H.**, Tsutsumi, E., Ashida, H., Katayama, T., Yamamoto, K., and Kumagai, H. (2012) Difference in the substrate specificities and active-site structures of two α-L-fucosidases (glycoside hydrolase family 29) from *Bacteroides thetaiotaomicron*. *Biosci Biotechnol Biochem.* **76**, 1022-1024
3. **Sakurama, H.**, Fushinobu, S., Hidaka, M., Yoshida, E., Honda, Y., Ashida, H., Kitaoka, M., Kumagai, H., Yamamoto, K., and Katayama, T. (2012) 1,3-1,4-α-L-Fucosynthase that specifically introduces Lewis a/x antigens into type-1/2 chains. *J Biol Chem*. **287,** 16709-16719
4. **Sakurama, H.**, Kishino, S., Uchibori, Y., Yonejima, Y., Ashida, H., Kita, K., Takahashi, S., and Ogawa, J. β-Glucuronidase from *Lactobacillus brevis* useful for baicalin hydrolysis belongs to glycoside hydrolase family 30. *Appl Microbiol Biotechnol*. *in press*
5. **Sakurama, H.**, Kishino, S., Mihara, K., Kita, K., Takahashi, S., Shimizu, S., and Ogawa, J. Biohydrogenation of C_{20} polyunsaturated fatty acids by anaerobic bacteria. *J Lipid Res.* (submitted on 2013/11/5)

RELATED PAPERS

1. Ito, T., Katayama, T., Hattie, M., **Sakurama, H.**, Wada, J., Suzuki, R., Ashida, H., Wakagi, T., Yamamoto, K., Stubbs, K.A., and Fushinobu, S. (2013) Crystal structures of a glycoside hydrolase family 20 lacto-*N*-biosidase from *Bifidobacterium bifidum*. *J Biol Chem.* **288**, 11795-11806
2. Koyanagi, T., Nakagawa, A., **Sakurama, H.**, Yamamoto, K., Sakurai, N., Takagi, Y., Minami, H., Katayama, T., and Kumagai, H. (2012) Eukaryotic-type aromatic amino acid decarboxylase from the root colonizer *Pseudomonas putida* is highly specific for 3,4-

dihydroxyphenyl-L-alanine, an allelochemical in the rhizosphere. *Microbiology* **158,** 2965-2974

3. Yoshida, E., **Sakurama, H.**, Kiyohara, M., Nakajima, M., Kitaoka, M., Ashida, H., Hirose, J., Katayama, T., Yamamoto, K., and Kumagai, H. (2012) *Bifidobacterium longum* subsp. *infantis* uses two different β-galactosidases for selectively degrading type-1 and type-2 human milk oligosaccharides. *Glycobiology* **22,** 361-368
4. **Sakurama, H.**, Takita, T., Mikami, B., Itoh, T., Yasukawa, K., and Inouye, K. (2009) Two crystal structures of lysyl-tRNA synthetase from *Bacillus stearothermophilus* in complex with lysyladenylate-like compounds: insights into the irreversible formation of the enzyme-bound adenylate of L-lysine hydroxamate. *J Biochem*. **145,** 555-563
5. Yano, S., Wang, W., Li, Q., Matsumoto, K., **Sakurama, H.**, Nakamura, T., Ogino, H., Kakiuchi, S., Hanibuchi, M., Nishioka, Y., Uehara, H., Mitsudomi, T., Yatabe, Y., Nakamura, T., and Sone, S. (2008) Hepatocyte growth factor induces gefitinib resistance of lung adenocarcinoma with epidermal growth factor receptor-activating mutations. *Cancer Res.* **68,** 9479-9487
6. Takita, T., Aono, T., **Sakurama, H.**, Itoh, T., Wada, T., Minoda, M., Yasukawa, K., and Inouye, K. (2008) Effects of introducing negative charges into the molecular surface of thermolysin by site-directed mutagenesis on its activity and stability. *Biochim Biophys Acta.* **1784,** 481-488
7. Inouye, K., Minoda, M., Takita, T., **Sakurama, H.**, Hashida, Y., Kusano, M., and Yasukawa, K. (2006) Extracellular production of recombinant thermolysin expressed in *Escherichia coli*, and its purification and enzymatic characterization. *Protein Expr Purif*. **46,** 248-255
8. 中村 隆弘, **櫻間 晴子**, 中村 敏一, 松本 邦夫 (2009) HGF 研究の進展と制癌剤開発. がん分子標的治療 Vol. **7**, pp 92-102, メディカルレビュー社 (In Japanese)

ACKNOWLEDGEMENTS

The author wishes to express her most sincere gratitude to Dr. Keiko Kita, Professor of Laboratory of Molecular Microbiology, Graduate School of Agriculture, Kyoto University, for her kind guidance, constant encouragement, and generous support throughout this study.

The author greatly appreciates to Dr. Satomi Takahashi, Professor of Laboratory of Industrial Microbiology, Graduate School of Agriculture, Kyoto University, for his helpful advices and warm encouragement throughout this study.

The author would like to express her sincere gratitude to Dr. Jun Ogawa, Professor of Laboratory of Fermentation Physiology and Applied Microbiology, Graduate School of Agriculture, Kyoto University, for his constructive instruction, extensive discussion, and tremendous supports throughout this study.

The author especially would like to express her heartful appreciation to Dr. Takane Katayama, Professor of Laboratory of Host-Microbe Interaction Research, Ishikawa Prefectural University, for his invaluable instruction and practical discussion that make her research of great achievement and her study unforgettable.

The author is greatly indebted to Dr. Shigenobu Kishino, Assistant Professor of Laboratory of Fermentation Physiology and Applied Microbiology, Kyoto University, for his constructive advice, practical discussion, and sincere encouragement.

The author is also greatly indebted to Dr. Masashi Kiyohara, Laboratory of Applied Microbiology, Ishikawa Prefectural University, Ms. Yoshie Uchibori, Research and Development Department, Nitto Pharmaceutical Industries, and Mr. Kousuke Mihara, Laboratory of Fermentation Physiology and Applied Microbiology, Kyoto University, for their significant contribution that make her research of great achievement.

The author would like to express a special appreciation to Dr. Hidehiko Kumagai, Professor emeritus of Kyoto University and President of Ishikawa University, and Dr. Sakayu

Shimizu, Professor emeritus of Kyoto University and Professor of Kyoto Gakuen University, Dr. Kenji Yamamoto, Professor emeritus of Kyoto University and Professor of Laboratory of Applied Microbiology, Ishikawa Prefectural University, for their considerable encouragement. The author would like to express thankful appreciation to Dr. Hisashi Ashida, Professor of the Faculty of Biology-Oriented Science and Technology, Kinki University, Dr. Motomitsu Kitaoka, National Food Research Institute, National Agriculture and Food Research Organization, Dr. Yuji Honda, Associate Professor of Ishikawa Prefectural University, Dr. Shinya Fushinobu, Professor of The University of Tokyo, Dr. Masafumi Hidaka, Assistant Professor of Tohoku University, for their valuable collaboration. The author is very grateful to Dr. Atsushi Yokota, Professor of Laboratory of Microbial physiology, Hokkaido University, Dr. Satoru Fukiya, Lecturer of Microbial physiology, Hokkaido University, Dr. Masanori Yamaguchi, Associate Professor of Department of Organic Chemistry, Wakayama University, and Dr. Yasunori Yonejima, Nitto Pharmaceutical Industries, for their technical cooperation in her experiments. The author thanks Dr. Jun Wada, Dr. Erina Yoshida, Ms. Yuko Mori, Ms. Kaori Morii, and Ms. Erika Tsutsumi, Laboratory of Applied Microbiology, Ishikawa Prefectural University, and the staff of the Photon Factory for the X-ray data collection for their technical assistance in her experiments. Acknowlegements are also made to Dr. Takashi Koyanagi, Associate Professor of Ishikawa Prefectural University, Dr. Akinori Ando, Assistant Professor of Research Unit for Physiological Chemistry, Kyoto University, and Dr. Makoto Hibi, Assistant Professor of Laboratory of Industrial Microbiology, Kyoto University, for their helpful collaboration and kind supports. The author wishes to express her deep appreciation to all the members of Laboratory of Molecular Microbiology, Laboratory of Industrial Microbiology, and Laboratory of Fermentation Physiology and Applied Microbiology, Graduate School of Agriculture, Kyoto University, and Laboratory of Applied Microbiology, Ishikawa Prefectural University.

The author would like to express special thanks of Dr. Toshiyuki Sakaki, Professor of Biotechnology Research Center, Engineering, Toyama Prefectural University, for his hearty continuous encouragement and supports. Finally, the author greatly thanks her parents for their constant support, encouragement, and sacrifice throughout her study.

Haruko Sakurama